

# Soil moisture – temperature interaction and feedback - strength in GCM's and RCM's under changing climate conditions

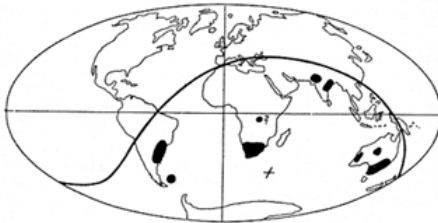
David Kohlfürst

January 2019



The **Wegener Center for Climate and Global Change** combines as an interdisciplinary, internationally oriented research institute the competences of the University of Graz in the research area “Climate, Environmental and Global Change”. It brings together, in a dedicated building close to the University central campus, research teams and scientists from fields such as geo- and climate physics, meteorology, economics, geography, and regional sciences. At the same time close links exist and are further developed with many cooperation partners, both nationally and internationally. The research interests extend from monitoring, analysis, modeling and prediction of climate and environmental change via climate impact research to the analysis of the human dimensions of these changes, i.e, the role of humans in causing and being effected by climate and environmental change as well as in adaptation and mitigation. (more informationen at [www.wegcenter.at](http://www.wegcenter.at))

The present report is the result of a Master thesis work completed in November 2018.



**Alfred Wegener** (1880-1930), after whom the Wegener Center is named, was founding holder of the University of Graz Geophysics Chair (1924-1930). In his work in the fields of geophysics, meteorology, and climatology he was a brilliant scientist and scholar, thinking and acting in an interdisciplinary way, far ahead of his time with this style. The way of his ground-breaking research on continental drift is a shining role model—his sketch on the relations of continents based on traces of an ice age about 300 million years ago (left) as basis for the Wegener Center Logo is thus a continuous encouragement to explore equally innovative ways: *paths emerge in that we walk them* (Motto of the Wegener Center).

## Wegener Center Verlag • Graz, Austria

© 2019 All Rights Reserved.

Selected use of individual figures, tables or parts of text is permitted for non-commercial purposes, provided this report is correctly and clearly cited as the source. Publisher contact for any interests beyond such use: [wegcenter@uni-graz.at](mailto:wegcenter@uni-graz.at).

ISBN 978-3-9504717-0-0

January 2019

Contact: David Kohlfürst, BSc MSc  
[david.kohlfuerst@edu.uni-graz.at](mailto:david.kohlfuerst@edu.uni-graz.at)

Wegener Center for Climate and Global Change  
University of Graz  
Brandhofgasse 5  
A-8010 Graz, Austria  
[www.wegcenter.at](http://www.wegcenter.at)



Wegener Zentrum für Klima und  
Globalen Wandel  
Karl-Franzens-Universität Graz



Masterarbeit  
zur Erlangung des akademischen Grades  
Master of Science  
an der Umwelt-, Regional- und  
Bildungswissenschaftlichen Fakultät der  
Universität Graz

**Soil moisture - temperature interaction  
and feedback-strength in GCM's and RCM's  
under changing climate conditions**

DAVID KOHLFÜRST

Graz, November 2018

Begutachter:  
Ass.-Prof. Mag. Dr. Douglas Maraun  
Mag. Dr. rer. nat. Heimo Truhetz



# Abstract

Earth's climate system is influenced and controlled by solar radiation factors as well as crucial feedback mechanisms and their components. One of these components is the total soil moisture content (Mrso), which plays an important role not only globally, but especially at the regional scale. In order to better understand impacts and changes of soil moisture, General Circulation Models (GCM) and Regional Climate Models (RCM) are used. In this thesis three aspects regarding Mrso and its impact on maximum near-surface air temperature (Tmax) as well as the soil moisture-air temperature coupling mechanism within Europe are discussed.

In the first step, it is shown how well the climate models can reproduce observations in summer season. To be more specific, the soil moisture-air temperature coupling as well as the zoning for various European regions will be discussed. Furthermore, we consider the relationship between the different climate model types to each other.

Next, we take the consideration of Mrso and Tmax as possible elements for the reduction of uncertainty in climate projections into account. The use of so-called *Emergent Constraints* is resorted to this approach. They represent a link between observed and projected values from the RCMs and GCMs and try to find a possible connection between them.

Additionally, an overview for a method to determine the strength of the soil moisture-air temperature coupling is given. This is done with the help of surface net radiation (Rn) and evapotranspiration (Evap) to get accurate results. This shows how differentiated the impact of the soil moisture-air temperature within the European summer season is. The approach to reflect possible changes for these feedback strengths are also taken into account.



# Zusammenfassung

Das Klimasystem der Erde wird von vielen Faktoren wie z.B. der Energie der Sonne sowie die damit verbundenen Rückkoppelungsschleifen beeinflusst und gesteuert. Einer dieser Faktoren stellt die Bodenfeuchte dar, die nicht nur global sondern vor allem regional eine große Rolle spielt. Um diese Veränderungen sowie deren Einfluss besser zu verstehen, wird auf globale Klimamodelle (GCM) sowie regionale Klimamodelle (RCM) zurückgegriffen. Vor diesem Hintergrund befasst sich diese Arbeit mit drei Hauptaspekten der Bodenfeuchte sowie im speziellen deren Auswirkungen auf die maximale Lufttemperatur und die Bodenfeuchte-Lufttemperatur Rückkoppelung im Allgemeinen.

Im ersten Schritt wird gezeigt, wie gut die Klimamodelle die Beobachtung im Sommer reproduzieren können. Insbesondere wird auf die Bodenfeuchte-Lufttemperatur-Rückkoppelung sowie die Einteilung der verschiedenen europäischen Regionen, die während der gesamten Arbeit verwendet werden, eingegangen. Zusätzlich wird die Beziehung zwischen den verschiedenen Klimamodelltypen zueinander näher diskutiert.

In einem weiteren Schritt betrachten wir die Bodenfeuchte und die maximale Lufttemperatur als mögliche Faktoren für die Reduktion der Unsicherheiten in Modellprojektionen. Die Verwendung sogenannter *Emergent Constraints* ist hierbei entscheidend. Dabei wird versucht, eine Verbindung zwischen beobachteten und projizierten Werten der RCMs und GCMs zu ermitteln. Dadurch können eventuelle Zusammenhänge abgeleitet werden die man zur Reduktion von Unsicherheiten in den Modellen benutzen kann.

Zusätzlich wird die Stärke der Bodenfeuchte-Lufttemperatur-Rückkoppelung innerhalb Europas für den Sommer ermittelt. Es wird dabei auf die Nettosolarstrahlung sowie die Evapotranspiration zurückgegriffen um ein möglichst genaues jedoch unverfälschtes Ergebnis zu bekommen. Es zeigt sich dabei, dass es zu großen Unterschieden innerhalb Europas während des Sommers kommt. Ebenfalls berücksichtigt werden mögliche Änderungen dieser Rückkoppelungsstärke im Zuge des sich ändernden Klimas.





# Acknowledgement

First of all, I just want to say "Thank you" to everyone who accompanied me during my studies and my life in general. Luckily I had the chance to write the thesis as a member of the ReLoClim group at the Wegener Center for Climate and Global Change, where besides working and engaging with inspiring people, I also got the opportunity to get an insight into scientific researches. That's why I would like to thank my supervisor Assoc. Prof. Dr. Douglas Maraun and my Co-supervisor Dr. Heimo Truhetz. Both of them always encouraged me, never let me down and supported me wherever they could with valuable input.

Further I would like to thank and acknowledge the E-OBS dataset from the EU-FP6 project ENSEMBLES (<http://ensembles-eu.metoffice.com>) and the data providers in the ECAD project (<http://www.ecad.eu>). Thanks to the World Climate Research Programme's Working Group on Coupled Modelling which are responsible for the CMIP and the EURO-CORDEX data as well as the ESGF for providing those data. Another thanks goes to the Max-Planck Institute for Meteorology in Hamburg for the software Climate Data Operators (cdo) as well as the R-Project for the availability of R software. My thanks also goes to the ECMWF for providing global atmospheric reanalysis data from ERA-Interim as well as to Michael Pock who created the  $\text{\LaTeX}$  template which was used to write this thesis.

Also a special thanks goes to the members at the Wegener Center for Climate and Global Change for making me feel welcome. This thesis would not be what it is without their knowledge, the skills that I acquired through them and of course the fun I had at the Institute. Especially worth mentioning here are my office colleagues Thomas Mendlik, Martin Jury and Emanuele Bevacqua. They did something that will always be a mystery to me. Every single day they were the most annoying but at the same time the funniest, most helpful and just most likeable colleagues one can imagine. And if I have a choice, I would always choose them again without any questions.

And at last, I would like to thank my family and my friends. I am so grateful for my parents, who always supported me either in a financial or emotional way throughout my years of study. And of course my brother who was always there if I needed help and encouraged me in times I felt uncertain about my path. Thanks also to my friends for the beautiful and funny time we spend together. Without you all, this work would not have been possible. Finally, a special thanks goes to my brother, Douglas and Heimo for proofreading this work.



# Contents

<b>Abstract</b>	<b>i</b>
<b>Zusammenfassung</b>	<b>iii</b>
<b>Acknowledgement</b>	<b>v</b>
<b>1 Introduction</b>	<b>1</b>
<b>2 Climate system</b>	<b>5</b>
2.1 Description of the climate system . . . . .	6
2.2 Feedbacks and land-atmosphere coupling . . . . .	8
<b>3 Modeling</b>	<b>11</b>
3.1 Types of climate models . . . . .	11
3.1.1 Generell Circulation Models . . . . .	12
3.1.2 Regional Climate Models . . . . .	15
3.1.3 Uncertainties in climate modeling . . . . .	18
3.2 Observations and reanalysis . . . . .	21
3.3 Datasets and Variables . . . . .	22
3.3.1 Variables . . . . .	22
3.3.2 Model data . . . . .	24
<b>4 Statistics</b>	<b>27</b>
4.1 Arithmetic mean, variance and standard deviation . . . . .	27
4.2 Trend analysis . . . . .	28
4.3 Measure of coherence . . . . .	28
4.4 Remapping . . . . .	29
<b>5 Results and Discussion</b>	<b>31</b>
5.1 Overview and verification of similarities between models and observations	31
5.1.1 Model comparison . . . . .	37
5.1.2 Model differences . . . . .	43

*Contents*

---

5.2	Uncertainty reduction through constraints . . . . .	50
5.2.1	Emergent constraints . . . . .	50
5.2.2	Long-term climate projections with trend values . . . . .	51
5.2.3	Interannual variability by variances . . . . .	56
5.3	Soil moisture-air temperature feedback strength . . . . .	61
5.3.1	Different strength approaches . . . . .	65
5.3.2	Projected feedback strength . . . . .	76
<b>6</b>	<b>Conclusion and Outlook</b>	<b>81</b>
	<b>Appendix</b>	<b>85</b>
	<b>List of Figures</b>	<b>89</b>
	<b>List of Tables</b>	<b>91</b>
	<b>Acronyms</b>	<b>93</b>
	<b>Bibliography</b>	<b>97</b>

# 1

## Introduction

Anthropogenetic climate change is one of the biggest problems to deal with because it is affecting mankind in different ways all over the world. For example water supply, potential disastrous natural phenomena like floodings or heat waves and a shifting agriculture are affected by a changing climate. The fact that the climate is changing both naturally and due to anthropogenetic influences is not new. The fact that greenhouse gases (GHG) have an impact on the climate is known since 1827 by French scientist Jean-Baptiste Fourier (Landsberg 1945; Houghton 2009). Therefore it is necessary to improve the knowledge about climate further and to prevent man-made changes which can harm humanity in short- and long-term periods (WMO 1979; White 1979).

Robust statements about present climate conditions through reliable observations are needed as urgently as trustworthy projections of future changes. To meet these requirements, atmospheric and soil-related variables are particularly suitable for this task due to the fact that many crucial feedback effects for humanity occur in near-surface areas. In addition to temperature and precipitation, soil moisture and the land-atmosphere feedback are key components, especially for the regional climate system (Seneviratne et al. 2006b). Soil moisture is a storage component that is involved in a number of feedback processes (Seneviratne and Stöckli 2008). According to Miralles et al. (2012) it is essential for the cooling process during evaporation and it also regulates the sensible heat flux. In addition, van Oldenborgh et al. (2013) and Jaeger (2011) found out that soil moisture mainly influences the maximum air temperature, especially during the summer season. Hence, the summer temperature variability is highly influenced by land-atmosphere coupling. This could be a key element in the increase in summer temperature variability in Europe (Seneviratne et al. 2006a). Although the soil moisture-air

temperature coupling mechanism exists everywhere, the sensitivity in some regions is stronger than in others. This can be explained by the variability of the amount of soil moisture which is not the same everywhere. As a result, the impact of temperature in this regions varies as well (Seneviratne et al. 2006b; van Oldenborgh et al. 2013).

Regions, where a relatively high sensitivity regarding climate processes with respect to land surface conditions exist can be detected with the correlation diagnostic tool from Seneviratne et al. (2006b). It highlights the patterns over Europe where the regional climate can be affected by evapotranspiration and, in turn, the sensible heat flux. This tool basically connects air temperature and evapotranspiration in order to allow conclusions about the soil moisture and its influence due to the lack of soil field measurements. The estimated results of the tool show the influence of soil moisture variations on the climate variability and the impact on temperature and precipitation due to the feedback mechanism. In Fig. 1.2 high and low estimated soil moisture-temperature coupling areas in the present and projected future values based on three different climate models are depicted. Currently, large parts of southern Europe show a strong coupling whereas the projections assume, that this condition will also affect areas further in the north (IPCC 2007; Seneviratne et al. 2010).

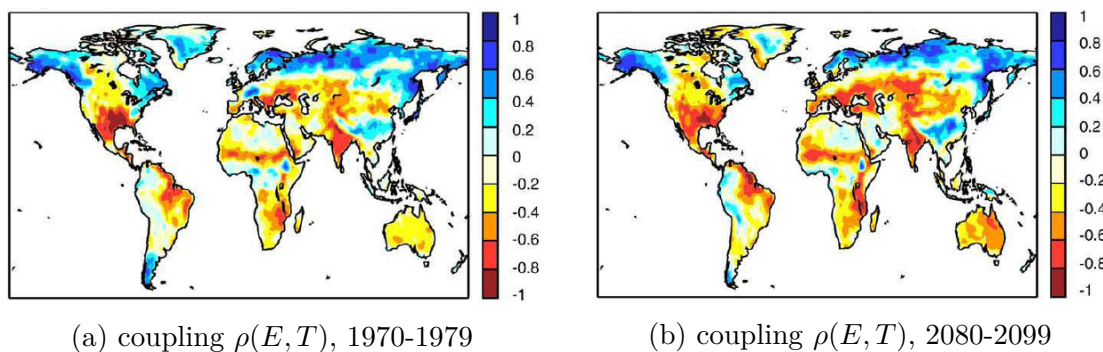


Fig. 1.2 Soil moisture-temperature coupling estimation based on the diagnose formula from *seneviratne2006b*. Fig. 1.1a depict the coupling strength from 1970-1989, while figure Fig. 1.1b shows it for 2080-2099. The closer the region is to  $\pm 1$ , the stronger or weaker is the land-air coupling factor (Seneviratne et al. 2006b).

This thesis deals mainly with this self-influencing process of the soil moisture-air temperature coupling and its impact over European regions. In order to achieve the feedback strength, the use of different climate models is indispensable. Within the EURO-CORDEX project, scientists investigate climatological aspects over Europe with a couple of regional high resolution models with a grid spacing of  $12.5 \text{ km} \times 12.5 \text{ km}$ . This is a considerable increase over the older model generation which had a spatial resolution between 100 km and 500 km (Jacob et al. 2014). In addition, this can help to further

---

consolidate current evidence in terms of projected changes and the feedback strength between the mentioned variables above. Currently, it is believed that in Central and Eastern European regions evapotranspiration will increase. This leads to the assumption that soil moisture could become a limiting factor in areas where it is currently not the case (Seneviratne et al. 2006a). As a result, some models show a reduction in cooling and an increase in air temperature but there are also some deviations between the different models (Seneviratne et al. 2010; IPCC 2007). A more detailed invest in the coupling interaction and the coupling strength for present and future events are planned. A coupling estimation tool already exists, however, the results vary greatly from model to model and cannot be validated by field measurements. In addition, the diagnostic tool is developed for global climate models and not for regional ones (Miralles et al. 2012).

This thesis engages in the study of the following aspects:

1. To deepen the knowledge of soil moisture related processes in connection with air temperature as well as long-term climate condition and model representation in the European region. Particular attention is paid to the self-reinforcing process of the soil moisture-air temperature feedback.
2. A validation of different model performances with regard to the soil moisture-air temperature feedback to get additional information about possible feedback changes.
3. An attempt to reduce uncertainties for model projections considering the current soil moisture-air temperature relationship.

Also, it can particularly help to better understand future developments of soil moisture changes in certain European regions. This would be important due to the fact, that for instance the occurrence of heat waves or precipitation events, in general, are also affected by soil moisture changes (Seneviratne et al. 2010; van den Hurk et al. 2012). Also, some forecasts are depending on the initial values of soil moisture (Koster et al. 2004). Particularly affected are those areas, where small changes suddenly cause soil moisture to be a limiting factor (Seneviratne et al. 2010). Eastern Europe could be such a region and is accordingly an area of interest for this thesis. There are indications that this region will be stronger affected by climate change than other areas and the reason could be a shift in soil moisture (Cubasch et al. 2013; Seneviratne et al. 2006a).

Chapter 2 provides a basic overview of the climate system and the importance of feedbacks and couplings, whereas Chapter 3 presents the different model types which are used in climate research. It also shows a more detailed explanation of the two relevant types within the thesis. Furthermore, this chapter contains information about the different uncertainty sources of climate modeling as well as descriptions about relevant

variables and specific climate model data. The different statistical methods that are used throughout the thesis are shown in Chapter 4. The results of the work are presented in Chapter 5, whereby it is divided into three larger subchapters. The first one contains the performances of the models in terms of soil moisture and air temperature compared to each other as well as to observations. The second subchapter describes the results of the *Emergent Constraints* approach to enable a reduction of the projected values. The focus of the last subchapter is particularly on the influence of the soil moisture-air temperature coupling in European regions. It shows the current feedback strengths over the different regions and possible future changes based on the projected model values. The analysis of soil moisture impacts on the climate as well as the discussion of the results can be found at the end of the work in Chapter 6. In addition, this chapter contains notes and thoughts on possible causes and improvements as well as new approaches for further works.



# 2

## Climate system

Climate is changing naturally since billions of years on earth. However, the events within the 20<sup>th</sup> century have changed our perspective on climate change as it is partly caused by humans. For instance, the impact of the anthropogenetic greenhouse gases (GHG) that have been released since the industrial revolution on the climate system creates several problems for flora and fauna (IPCC 2007). Those changes lead the Executive Committee of the World Meteorological Organization (WMO) to detain the first World Climate Conference in 1979. Over the following years, the WMO took the leading role in supporting science facilities to determine events which are connected to a changing climate as well as their interactions between environment and society (WMO 1979). With the monitoring of atmospheric carbon dioxide concentration by Keeling et al. (1984), a documentation of the increase in GHG was established. This was the evidence, that human activities have an influence on the chemical composition of the atmosphere (IPCC 2007). As a reaction to this, the Intergovernmental Panel on Climate Change (IPCC) was established by the WMO and the United Nations Environment Programme (UNEP) in 1988 to assess the gathered information on those topics (Agrawala 1998). For communication, the IPCC provides an Assessment Report which summarizes and concisely shows the most recent findings on climate change issues. This is done by providing the data by thousands of scientist throughout the world. All research results are under review to ensure a complete assessment of current climate facts.

Weather and climate is not the same. To a certain extent the term climate change also leads to a false interpretation. Therefore, the Fifth Assessment Report (AR5), published by the IPCC, defines the meaning of the term *climate* as follows (Cubasch et al. 2013):

*"Climate in a narrow sense is usually defined as the average weather, or more rigorously, as the statistical description in terms of the mean and variability of relevant quantities over a period of time ranging from months to thousands or millions of years. The relevant quantities are most often surface variables such as temperature, precipitation and wind. Classically the period for averaging these variables is 30 years, as defined by the World Meteorological Organization. Climate in a wider sense also includes not just the mean conditions, but also the associated statistics (frequency, magnitude, persistence, trends, etc.), often combining parameters to describe phenomena such as droughts."*

### 2.1 Description of the climate system

The global climate system is a theoretical construct that combines different interactive sub-systems. It basically consists of the hydro- and cryosphere (including solid, liquid and gaseous phase of water), the litho- and pedosphere (including the space from the earth crust to the land surface), the atmosphere and the biosphere. Those spheres interact and interpenetrate each other although the most obvious component which is associated with climate is the atmosphere. The whole system itself get its energy from the sun or more precisely by solar radiation as figure Fig. 2.1 shows. Based on their specific electromagnetic wavelength it is also called incoming shortwave radiation (SWR).

Approximately 50% of the SWR from the sun gets absorbed by Earth's surface, 30% is reflected back into space due to the albedo and 20% is absorbed in the atmosphere. According to the Stefan-Boltzmann law, the incident and the emitting radiation have to be in balance. Based on the surface temperature the biggest part of this emitting fluxes takes place in the infrared spectrum. This infrared radiation is also known as longwave radiation (LWR) and gets absorbed and emitted itself by GHG and clouds. To sum it up, both SWR and LWR have an emitting and an incident part. By changing the radiation balance, the surface temperature will change as well (Cubasch et al. 2013). According to the Fourth Assessment Report (AR4) from the IPCC (2007) there are some crucial ways to change the Earth's energy balance. For instance by altering the albedo which would change the reflectivity relating to solar radiation or by modifying the incident SWR and emitting LWR from Earth. A change in the GHG composition could be the cause of such effects. In such case, Earths climate will react directly, and also indirectly, to those changes through a couple of feedback mechanisms (Cubasch et al. 2013).

Nonetheless, these changes don't influence the climate immediately. As mentioned before, the climate system is a combination of sub-systems and changes in them occur at different scales, both time and spatial as well as different rates. Cubasch et al. (2013)

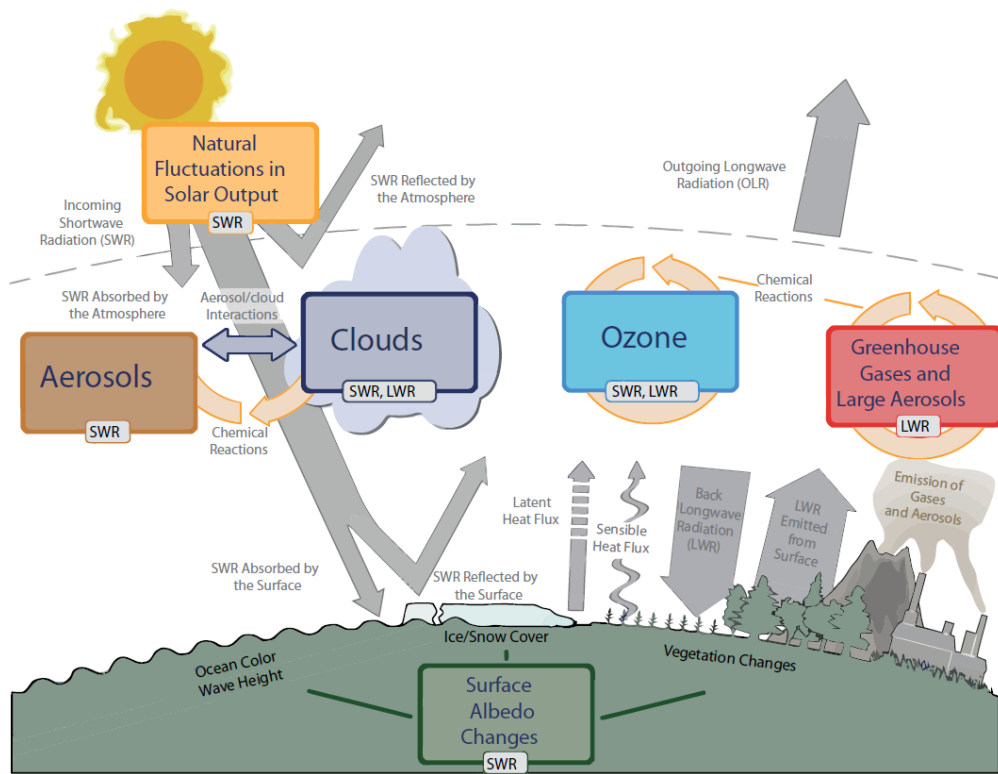


Fig. 2.1 Interaction between solar radiation and the atmosphere. Shown is the interaction of the incoming and outgoing radiation with the different components of the atmosphere which are acting as a *driver* of the global climate. Both the SWR as well as the LWR are reflected or absorbed and emitted several times within the atmosphere. In addition to the human component in the form of emitted GHG, the albedo, fluctuations of the solar output, O<sub>3</sub> and other aerosols are also influential factors for climate changes (Forster et al. 2007).

define it as follows:

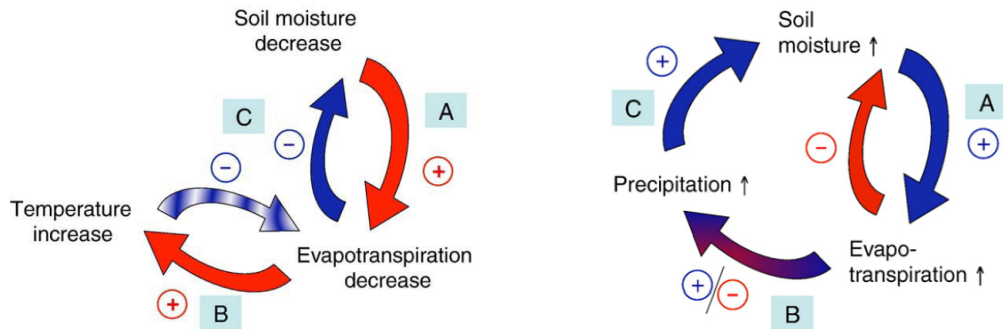
*"Climate change refers to a change in the state of the climate that can be identified (e.g., by using statistical tests) by changes in the mean and/or the variability of its properties, and that persists for an extended period, typically decades or longer."*

Therefore the Earth's climate system is changing continuously and dynamically as a result of external forces and internal dynamics (Robock 1978).

### 2.2 Feedbacks and land-atmosphere coupling

Internal feedbacks can alter the behavior of a system. A feedback loop describes a mechanism of mutual interactions between processes. The change of an initial process results in a change of a second process, which in turn affects the initial one again (Carter et al. 2001). Due to the mutual influence of the processes, the system deviates from a linear relationship to a non-linear relationship. In case of the global climate system, there are many feedback loops which can either dampen (negative feedback) or amplify (positive feedback) the impacts of a change by a climate forcing (Le Treut et al. 2007). Positive feedback loops lead to an instability while negative feedback loops stabilize the system. An important part here is to consider the timescale of those feedback mechanisms. Some of them operate within an hour, some of them develop over centuries or even longer. For example, the ice-albedo feedback reacts to the melting of land ice sheets which can take millennia. In contrast to this, the water vapor feedback could have an effect within days. Some other feedback loops which have an effect on the global climate are the the Bjerkenes, the cloud feedback or the land-atmosphere coupling. The processes contributing to the soil moisture-air temperature coupling are shown in Fig. 2.3 (IPCC 2013).

To avoid misunderstandings, besides the land-atmosphere feedback the term land-atmosphere coupling is often used for the same process within the scientific community (Seneviratne et al. 2006b; Goosse 2015). Fig. 2.3 depicts the two main parts of this land-atmosphere coupling. The left one (Fig. 2.2a) shows the impact of soil moisture on the near-surface air temperature and vice versa. As a result of this feedback, a decrease in soil moisture simultaneously leads to a reduction in evapotranspiration. And as a consequence of these reductions, atmospheric cooling effects which are a result of evapotranspiration, are also getting weaker because there is not enough soil moisture available. This in turn increases the near-surface air temperature ( $T_{\text{mean}}$ ). A higher  $T_{\text{mean}}$  normally leads to a further evaporative demand from the soil which results in an additional atmospheric cooling and also into a further decrease in soil moisture. But a dry or even dehydrated soil limits the evapotranspiration process and therefore cooling



(a) Soil moisture-temperature coupling      (b) Soil moisture-precipitation coupling

Fig. 2.3 Contributing processes for the soil moisture-land atmosphere coupling. The different steps within the loop on the left side represent one part of the soil moisture-air temperature coupling mechanism with the key variables total soil moisture content ( $M_{rso}$ ), maximum near-surface air temperature ( $T_{max}$ ) and evapotranspiration ( $Evap$ ). The figure on the right side is the second part of the whole feedback loop and includes Precipitation as well. The figure shows the relationship between the individual variables and their influential direction. A positive sign indicates an escalation and a minus sign indicates a deescalating interaction (Seneviratne et al. 2010).

is also restricted. This causes an increase in soil temperature and consequently also in sensible heating and higher  $T_{mean}$  values because more energy from radiation becomes accessible (Seneviratne et al. 2010; Goosse 2015). As Jaeger (2011) and Durre et al. (2000) have shown, this process can be one of the reasons for heat waves and extremely hot temperatures.

In contrast, another type of land-atmosphere coupling describes the connection between soil moisture and precipitation and is depicted in Fig. 2.2b. Note that the relationship between variables and their impact on regional and global climate has been an object of modeling studies since the second half of the 20<sup>th</sup> century (see e.g. Charney et al. (1977)) and is still not fully understood.

An increase in soil moisture leads to a rise in evapotranspiration. But this also induces a decrease in soil moisture itself because moisture gets removed from the ground during the process. The effect of the evapotranspiration on precipitation is the most uncertain and at the same time also the most difficult one to investigate because it is also scale-dependent. Due to atmospheric sub-processes such as the advection of air masses or changes in the atmospheric stability, a direct influence of evapotranspiration on the local precipitation is difficult to detect. Therefore, it is not clear if an interaction between these two variables have an amplifying or a weakening effect on each other according to Schär et al. (1999a) and Koster et al. (2004). The last part of this feedback loop is the relationship

between precipitation and soil moisture. In principle, a higher precipitation leads to higher soil moisture. But in the case of a very dry or saturated area, rainfall can only percolate to a certain amount due to the condition of the underground. The remaining part evaporates or will result in runoff which is not shown in Fig. 2.2b (Seneviratne et al. 2010).

# 3

## Modeling

Models are simplifications of real-world processes. As experiments in climate research are rarely feasible one has to use climate models to get information regarding reactions due to a specific forcing within the climate system (Flato et al. 2013). In this Chapter, a short introduction in modeling and validation of model data is given starting with an overview about two climate model types which will be used in Chapter 5 as well as an introduction of observational and reanalysis data.

### 3.1 Types of climate models

Climate models are basically mathematical simplifications and constructions of existing climate processes of the world. Each one of them has its own level of complexity and is used for specific reasons. The simplest model is called Energy balance model (EBM) as shown in Fig. 4.1. It can project temperature changes by calculating the energy budget based on global averages of incoming and outgoing shortwave radiation (SWR) and longwave radiation (LWR). The next higher level of complexity is the Box model. They expand EBMs by adding interactions and transfer functions among different sub-systems within the model environment. The Earth System Models of Intermediate Complexity (EMIC) contain relevant but often idealized components of the climate systems. They include for example the Earth's orography and zonal averages of the atmosphere but with a rather low resolution. However, they are valid as a gap-closer between an EBM and a General Circulation Model (GCM) (Claussen et al. 2002). Nowadays GCMs are the most complex climate models. Their main purpose is to support understanding the internal dynamics of physical components and reactions due to different climate forcing.

Additional to this, they make projections for several future greenhouse gases scenarios and aerosol forcing (Flato et al. 2013). GCMs are one of the main models used in this thesis, so a more detailed description is given in Chapter 3.1.1.

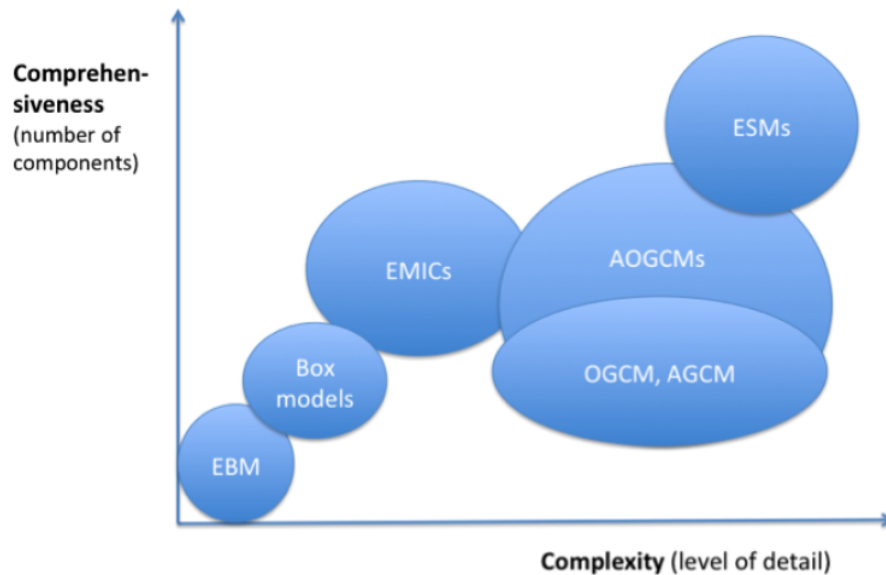


Fig. 3.1 Different kinds of climate models. The climate model hierarchy based on the computational complexity and the comprehensiveness of the individual model type (energy balance model (EBM), box models, Earth model of intermediate complexity (EMIC), ocean general circulation model (OGCM), atmosphere general circulation model (AGCM). A combination of the latter two is an atmosphere ocean general circulation model (AOGCM) and Earth system models (ESM)). From Eckers (2015).

#### 3.1.1 General Circulation Models

GCM stands for General Circulation Model but is also used for Global Climate Model. However, the last one is precisely an Atmosphere Ocean General Circulation Model (AOGCM) but currently it is common to use the term GCM for both. As already mentioned above, GCMs are the most precise and complex models for describing the climate system and projecting future climate conditions and the influence of increasing radiative forcing (Cubasch et al. 2013). They include the atmosphere, land surface, ocean circulations, simplified versions of sea ice dynamics, the carbon cycle and more. In the first place, GCMs are used to understand the internal dynamics of the different climate system components. Therefore, they can make projections with regard to aerosol



forcing and future greenhouse gases (GHG).

Due to limitations in available computational power, models are introduced with finite temporal and spatial resolution. GCMs raster the Earth into a 3-D grid with a typical resolution of the order of 150 km to 400 km, see Fig. 3.2 (Flato et al. 2013).

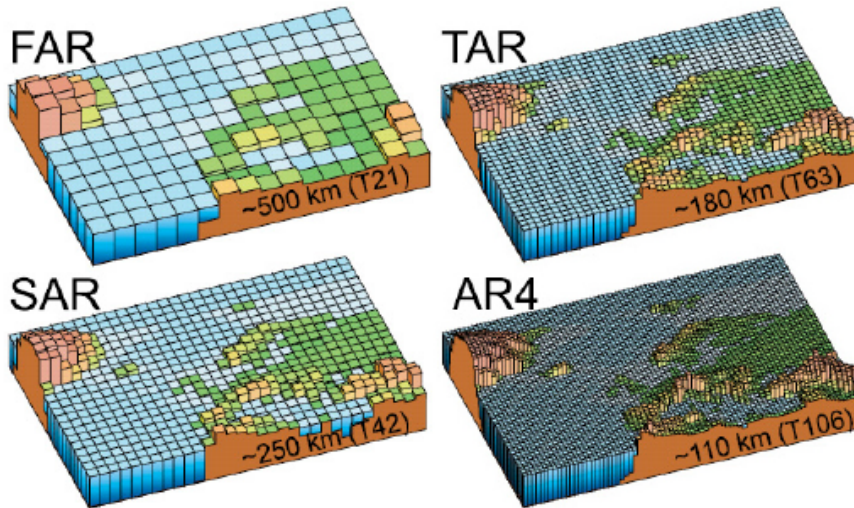


Fig. 3.2 Development of the GCMs. The improvements that have been taking place since the beginning of the first GCMs concern both the horizontal grid as well as a higher orographic resolution (Somerville et al. 2007).

In case of temporal resolution, the usual range is between 6-hourly data to monthly means. Calculations are performed with finite non-linear partial differential equation within every 3-D grid cell. Because the required equations for describing the conservation of energy, momentum, and mass cannot be solved analytically. Each cell has to calculate therefore all equations at each time step in a discrete form. For the conservation of energy, the thermal energy equation is needed. The total energy in a closed system is constant, although the energy of moving objects which are associated with heat, gravitational potential, etc. are able to transform into other forms of energy (IPCC 2007). Changes within a system can only occur over sinks and sources or inflows and outflows. Whereas the continuity equation is used for the conservation of mass. Furthermore, in an isolated system, the momentum is conserved for any interaction between two objects. So Newton's law of motion represents the conservation of momentum to a certain extent. To obtain a more accurate solution, the Navier-Stokes equations are needed. They describe hydrodynamic flows within the atmo- and hydrosphere and take account for acting forces like pressure gradient, gravity, the force of inertia, Coriolis force and friction. Besides that each grid cell not only has to calculate those equations in each

time step, they also have to take into account fluxes from their neighboring cells. Viner and Hulme (1997) are mentioning the existence of horizontal and vertical exchange between the atmospheric columns and layers of momentum, moisture, and heat. GCMs also consider the in- and outflows of SWR and LWR which is shown in Fig. 3.3. Thus, the surface characteristics including orography, vegetation, ice sheets, water, and soil as well as the internal dynamics must also be taken into account for every grid cell. In addition, one has also to consider that the exchange processes are happening on different time scales (Cubasch et al. 2013).

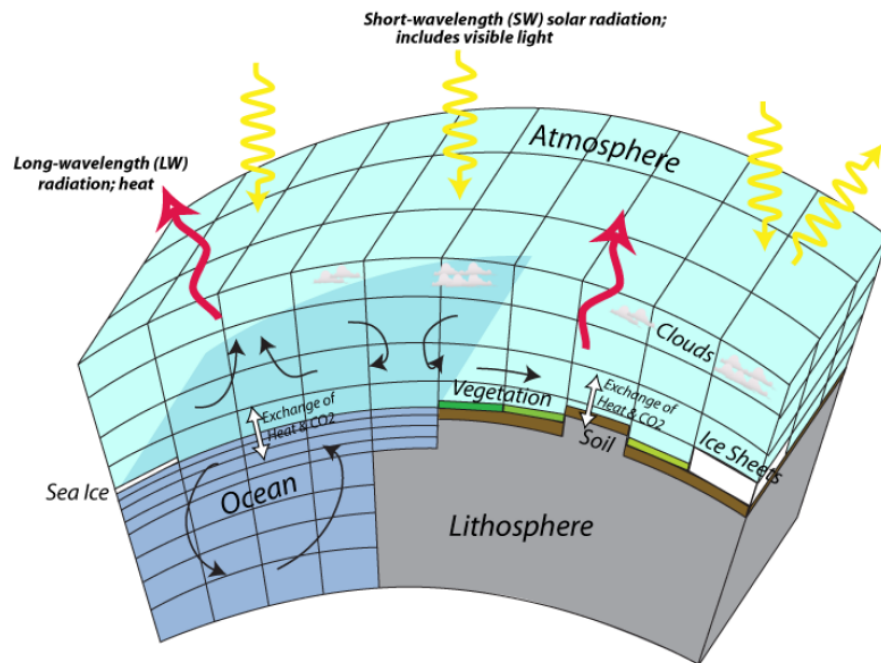


Fig. 3.3 Each sphere is represented by at least one box layer, whereas the atmo- and hydrosphere are the most represented ones. In addition, it also show the SWR and LWR as well as the exchanges within one sphere itself. From Bralower and Bice (2009)(based on Goosse, H., 2008).

Physical processes that are below the resolutions of the GCM aren't resolved sufficiently and therefore getting parameterized. Which means that the effects of these unresolved physical processes still have to be considered in the calculations. Therefore, the impacts of these processes are taken into account with the help of approximations, statistics or mathematical functions (Bony et al. 2007). One of the biggest problems in climate modeling is the reproduction of feedback loops due to their non-linear be-

havior. Bellenger et al. (2014) showed that hardly any model can reproduce the El Niño-Southern Oscillation (ENSO) phenomena in the Pacific although this phenomenon impacts the climate worldwide. As a result, one can say that if there are more cells, the model can approximate the real earth closer but this will also require much more computational power. In addition, GCMs usually run for at least one hundred model years (Bralower and Bice 2009).

Climate models exhibit systematic biases due to their internal physics, parametrization and inter-model differences. Statistical downscaling and bias correction methods can reduce some of those biases, nevertheless, climate models need evaluations (Rajib et al. 2014a). In fact, model evaluations aren't just only for raising the credibility of climate models. They also contribute to new insights in process understanding and boost confidence in model projections when a model performing well in terms of present atmospheric processes. In general, models can be evaluated by focusing on their performance itself or their reliability when it comes to how well they represent past and present climate condition by including the check of errors. This procedure is also known as model plausibility. Models get evaluated by comparing their performances regarding observational data including natural internal variability which will be explained further in Chapter 3.1.3. Confidence in a future model projection only exists, when the model simulates the historical climate condition well, including variability and changes (Flato et al. 2013). However, there are many works like van Ulden and van Oldenborgh (2006) which show that the comprehension and evaluation of model performances are hard due to the fact that the climate system as such is highly complex. For instance, Rajib et al. (2014b) found that in some Mediterranean areas the observed local temperature trends aren't compatible with the model mean trends. Thus, it is a difficult task to identify key factors to determine good model simulations (Räisänen 2007). An ensemble of many models and the sampling of model uncertainty like in phase 5 of the Coupled Model Intercomparison Project (CMIP5) should outperform an individual model in terms of robustness and the quality of the results (Palmer et al. 2004).

#### 3.1.2 Regional Climate Models

A Regional Climate Model (RCM) is a climate model which provides a more detailed simulation for a particular area than a GCM. Topographic factors like mountains, mesoscale turbulence in the atmosphere and other small-scale conditions are influencing the local climate significantly. Those factors are not resolved in GCMs because the resolution is too low, thus, they get parameterized. In comparison, RCMs have a finer spatial resolution. For example, within the COordinated Regional climate Downscaling EXperiment - EUROpean domain (EURO-CORDEX), typical resolutions of the models are either 50 km or 12.5 km with a temporal resolution up to 30 min values for some variables according to CLIPC (2018). Due to this fact, RCMs are computationally more costly and due to that they normally just run over a limited area. But the finer spatial and tem-

poral resolution leads to a better evaluation using regional observations. Additionally, more regional components can be taken into account (flooded areas, glaciers, lakes). RCMs also improve small-scale atmospheric turbulence, a higher forcing resolution regarding wind, coastal climate features, sea surface temperature, extreme precipitations and many more (Flato et al. 2013).

To achieve local model improvements, RCMs must be implemented into a driving GCM. The typical approach to accomplish these physical high-resolution climate information from a RCM is the so-called one-way nesting. For the one-way nesting method, a driving global model serves as the basis for describing large-scale forcing and general atmospheric circulation. Also included are information about GHG, solar activities and ENSO circulations. This global model is in most cases a GCM but also observational or reanalysis models can be used. For the RCM nesting, a limited-area domain with a lateral buffer zone gets implemented in a particular domain inside the driving GCM as seen in Fig. 3.4. Thus, the global model simulates the processes with a coarse spatial and temporal resolution. Whereas the nested domain has a finer resolution. After the nesting, the RCM receives initial conditions (IC), atmospheric time-dependent lateral boundary conditions (LBC) and surface boundary conditions from the driving GCM. Note, that a possible large systematic error like an incorrect ENSO simulation will also be transmitted from the driving GCM to the RCM which will most likely lead to an erroneous regional climate signal. This phenomenon is also known as garbage in, garbage out. After the nesting process the RCM try to take account for sub-GCM grid scale climate information. Therefore, effects which are normally parameterized within a GCM now get calculated in a physical-based way. Further, the RCM enhance the simulation of the atmospheric circulation at a finer spatial and temporal resolution to improve local impacts. Thus, this isn't the only possible approach but the most common one for nesting. Other methods are, for instance, high-resolution atmospheric GCMs or empirical statistical downscaling (Giorgi and Gutowski Jr. 2015).

Several studies like Seth and Giorgi (1998) showed that nesting a RCM domain over land areas or mountain regions influence the model sensitivity significantly. Which means that boundary domains over complex terrain lead to mismatches within the calculation processes. Therefore, a crucial part to consider is that the region of interest should be centered in the domain area and the nesting boundaries should always be as far away as possible as figure Fig. 3.4 shows. This prevents potential influences from spurious boundary effects within the region of interest. For the RCM equations itself, they require time-dependent LBC from the driving GCMs for their prognostic variables like wind or temperature and IC over the whole model domain to progress forward in time. Note, that the RCM just needs the LBC in the outermost regions, the boundary zone, at every time step so that the RCM equations itself can be freely integrated within the domain

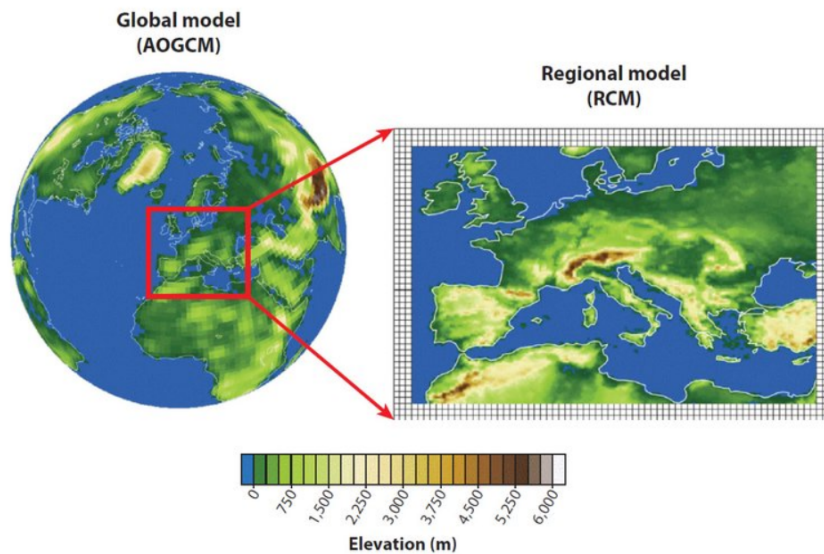


Fig. 3.4 Nesting of an RCM. A RCM gets embedded in a GCM, thus, additionally they pass on information at the edge per time step to the RCMs. This drives the RCMs and allow them to calculate the processes within the spheres at a higher resolution. Note, that the region of interest is centered while the boundary is as far away as possible from mountains and the area itself (Giorgi and Gutowski Jr. 2015).

region (Giorgi and Gutowski Jr. 2015). As for the evaluation of RCMs, it's basically the same as for GCMs. But to assess regional climate changes, one should use an ensemble of different global and/or regional model simulations due to the fact that different RCMs and GCMs lead to different projections. Based on that, it is also a possibility that e.g. different GCMs force the same RCM. Usually, the whole ensemble information will accomplish the best approximation for the most likely climate change signal (Teichmann et al. 2013).

### 3.1.3 Uncertainties in climate modeling

No climate model is absolutely accurate. As Hawkins and Sutton (2009) showed, uncertainty in combination with climate projections arise from three sources: Scenario uncertainty, model uncertainty, and internal variability. The relative importance of each uncertainty for projections varies due to the running time and spatial scale. Thus, internal variability and model uncertainty are the two dominant factors for regional scales within a short time period like one or two decades, see Fig. 3.5 (right). However, the contribution due to scenario uncertainty increases with time. Overall the model and the scenario uncertainty are the main sources of uncertainty for long-term climate projections on the regional and global scale (left picture in Fig. 3.5). In addition, model uncertainties are the main reason why model ensembles are used in climate research.

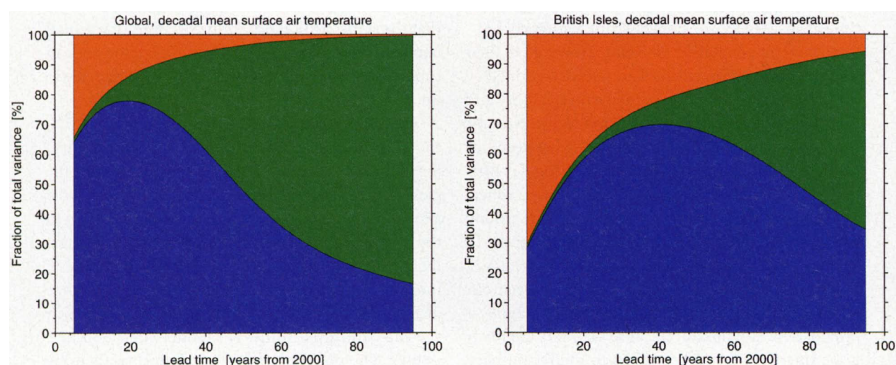


Fig. 3.5 Uncertainty overview. The three components of total uncertainty divided into fractions according to their influence over time on climate models (where orange describes the internal variability, green the scenario uncertainty and blue the model uncertainty). The figure references the respective share of uncertainty for the projected mean surface air temperature, once globally on the left side and over the British Isles on the right side (Hawkins and Sutton 2009).

#### Internal variability or initial condition uncertainty

Hawkins and Sutton (2009) describes internal variability as natural fluctuations occurring in climate. It is crucial to consider internal variability because it has the potential to reverse the longer-term climate trend for one or two decades (Cubasch et al. 2013; Deser et al. 2012). Furthermore, one has to take into account that different IC are leading to different results within a climate model. Two main components which are responsible for the varying results are the macroscopic and microscopic initial condition

uncertainty (ICU). While the macroscopic ICU refers to state variables within a large and slowly mixing scale, the microscopic ICU is linked to small rapidly mixing scales. Therefore, different IC produce different distributions of the climate model output within the timescale of interest (Stainforth et al. 2007).

#### Model uncertainty

Although the physical principles for every climate model are the same, each model computes a slightly different signal. This is caused by the fact that climate models are just approximations of the real climate system. The model uncertainty consists essentially of the parametric and the structural uncertainty.

- *structural uncertainty*: Climate models are just simplifications of reality and therefore, their structure is most likely inadequate. Only a few relevant parts of the real-world system can be represented correctly. This leads to several problems with extrapolation in case of climate projections. Even the most complex climate models with the highest resolution cannot describe all aspects and processes of the real-world system in a realistic way. Therefore it is hard to simulate unknown climate conditions (Cubasch et al. 2013).
- *parametric uncertainty*: It describes the fact that processes within a climate model can be represented in more than one way. As Smith (2001) pointed out, climate models can vary individually in their parametrization schemes, parameter values and can use different resolutions compared to each other. All these mentioned factors are representing the influence on large scale processes. Additionally, they react themselves to the large-scale behavior within a climate model. Therefore many models have difficulties to reproduce feedbacks correctly on a smaller scale (Stainforth et al. 2007).

#### Scenario uncertainty

It describes the uncertainty of different future radiative forcing depending on human actions. This includes, for instance, the emission of GHG as well as the changes in land-use. Based on the fact that the scenario uncertainty is connected with human actions and behavior, it is not possible to predict future changes. Therefore it makes no sense to quantify the so-called *human reflexive uncertainty* in a reasonable way (Patt and Dessai 2005). Nevertheless, to consider the impact of this form of uncertainty, different scenarios (socio-economic pathways) have been introduced. The aim is to cover the whole range of possible future developments of GHG concentrations and their influence on radiative forcing and hence climate itself (Hawkins and Sutton 2009). Climate statements about the future are called *projections* because the probability of each individual emission scenario cannot be taken into account. Instead, information about climate changes will be



provided by scenario simulations for defined GHG framework conditions (Collins et al. 2012). For the Intergovernmental Panel on Climate Change (IPCC)'s Fifth Assessment Report (AR5) several GCMs projected changes with four possible radiative forcing till the end of the century were introduced. In particular they are called representative concentration pathway (RCP)s and in special the four are RCP2.6, RCP4.5, RCP6.0 and RCP8.5 which are shown in Fig. 3.6. Note, that due to the unpredictability of human actions, each climate model projection is determined by just one of those climate scenarios (Cubasch et al. 2013). With regard to Chapter 5 only RCP8.5 is used in the thesis which contains a possible radiative forcing of  $8.5 \text{ W} \cdot \text{m}^{-2}$  till the end of the the 21<sup>th</sup> century.

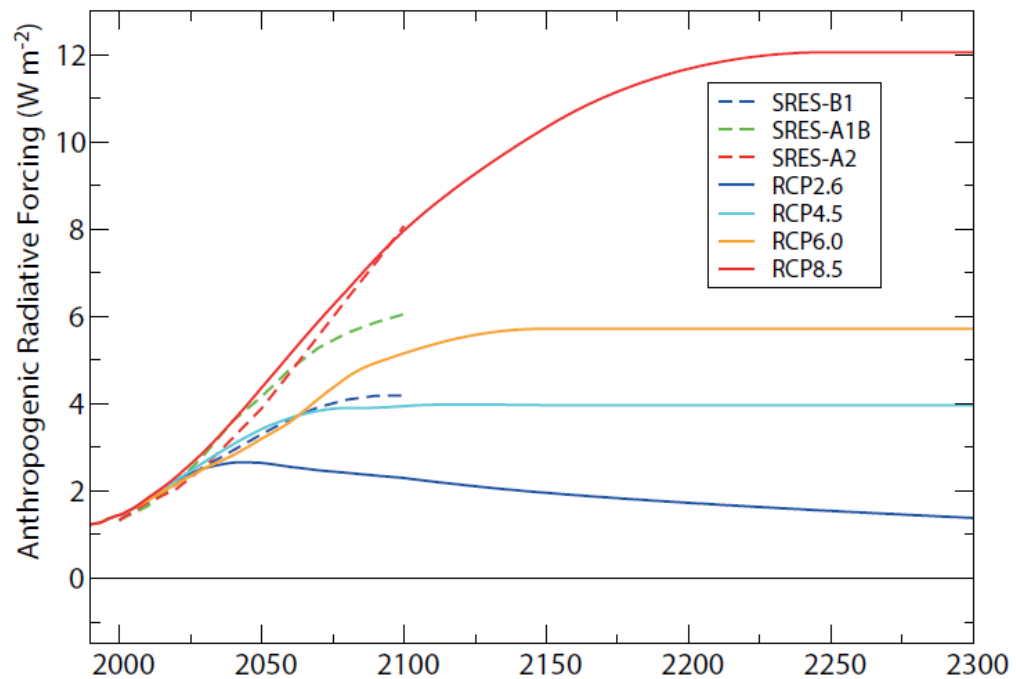


Fig. 3.6 Projections of the different scenarios. The RCPs represent the respective increase of the anthropogenetic radiative forcing of the newer scenarios in the AR5, while the SRES represent some scenarios from the Fourth Assessment Report (AR4). An increase between  $2.6 \text{ W} \cdot \text{m}^{-2}$  and  $8.5 \text{ W} \cdot \text{m}^{-2}$  is assumed. From Knutti and Sedláček (2012) (slightly modified).



## 3.2 Observations and reanalysis

Meteorological observational data just become available in the middle of the 19th century. All data before and even the present observations as well suffer from uncertainties including different measuring techniques and construction devices, although observational data are necessary to evaluate climate models. It is known that climate model performances can vary highly across regions Rajib et al. (2014b). In order to increase the confidence in climate projections, evaluations of past model performances are important. The trust in climate model projections can be boosted if the same models are able to manage and reproduce past observational values and changes in terms of mean state and other statistical quantities correctly (Bony et al. 2007). In order to evaluate the models, the observational grid data sets of E-OBS and ERA-Interim can be used.

### **European high-resolution observational gridded data set (E-OBS)**

Meteorological observations are spatially irregular and always station-based. But climate models usually represent area-averaged values, and the interpolation of the observed values to a gridded dataset is essential. To accomplish this, every grid cell represents the average value of all observation values within this cell. Over 2500 stations and their observed data are taken into account. E-OBS is a European land-only high-resolution data set on a rotated grid with  $0.22^\circ$  resolution. The data set include daily maximum, minimum and mean surface temperature as well as precipitation and sea level pressure. Note, that the observational data also hold uncertainties. They occur during the measurement of the meteorological parameter itself and throughout the interpolation process for a gridded dataset (Haylock et al. 2008). For the thesis, the E-OBS version 14 is used.

### **European Centre for Medium-Range Weather Forecasts Re-Analysis Interim (ERA-Interim)**

ERA-Interim is the product of the European Centre for Medium-Range Weather Forecasts (ECMWF). The ECMWF is an independent intergovernmental organization based in Reading, England. Their main tasks include producing global medium-term, monthly and seasonal based forecasts, development of numerical weather forecasting models as well as storing the forecasts and observational data. An essential part of a numerical weather model is the assimilation of observed data. The analysis of this data leads to a three dimensional and consistent representation of the atmospheric condition. Operational weather models and assimilation systems get enhanced and further developed over years. But in comparison to a normal analysis of station data, the calculations of ERA-Interim are carried out by an improved version of the original model- and assimilation system. This is called a reanalysis which is also an analysis of meteorological station data but besides the observation values which are years to decades ago, it also takes recent observational data into account. A reanalysis is generated with a single

version of an assimilation system, thus, changes in the method do not affect the output. The result is a multivariate, spatially complete and coherent description of the global atmospheric circulation. A forecast model with the associated reanalysis data as IC can, on one hand, extrapolate unknown parameters from nearby observed parameters and on the other hand propagate this information in time. ERA-Interim is one of those assimilating forecast models which uses observational data from 1979 to the present with a resolution of  $0.75^\circ \times 0.75^\circ$  (Dee et al. 2011).

## 3.3 Datasets and Variables

In this chapter, we give an overview of important variables and data sets which are used throughout the whole thesis.

### 3.3.1 Variables

The following variables are calculated values using physical laws, with comprehensible assumptions or are measured under standardized conditions. They are all available at ECMWF, E-OBS and on the Earth System Grid Federation (ESGF).

#### Near-surface air temperature (Tmean)

Simply said, the temperature is the mean kinetic energy of the molecules of an ideal gas. It is based on the four thermodynamic laws and if the amount  $\delta Q$  of heat is transferred from outside to a body with the mass  $M$ , the change in temperature  $\delta T$  follows

$$\delta Q = cM\delta T, \quad (3.1)$$

with the specific heat capacity  $c$ . Tmean describe the mean air temperature within a day or month, while maximum near-surface air temperature (Tmax) describe the maximum temperature within a day or month (Kraus 2007).

#### Total soil moisture content (Mrso)

Soil moisture influences air temperature, evaporation and to a certain amount also radiation due to changing albedo values. Therefore it is a key element in understanding the regional climate system.

The soil itself consists of solid organic and inorganic material. The free space in between, so-called pores, are containing air and/or water. The soil is saturated if all pores are filled with water although the average value of soil saturation is about 50%. During rain events, a certain amount of water drains away quickly through gravity and capillary actions. The infiltration rate is determined by the composition of the soil itself whereby

sandy soil show higher and clayey soil lower values. Thus, a runoff occurs when the precipitation rate exceeds the infiltration rate. However, not all of the drained water will end as groundwater. A part of it is stored within the soil itself known as total soil moisture content ( $Mr_{so}$ ) (Seneviratne et al. 2010). The amount of stored water is dependent on the field capacity. It describes the amount of water which can be held in the soil when the downward movement as well as the runoff and drainage rate of the water significantly decreases. Therefore the field capacity depends on the type of soil. The stored water can evaporate, be absorbed by plants or remain in the ground due to strong interactions in the soil. Which means that some of the water is bound so strongly to the ground, not even plants are able to use it. If the soil has dried out to this degree, that plants can no longer withdraw water from the ground than they will wither. This state is called wilting point (Veihmeyer and Hendrickson 1928). Soil moisture is also involved in a number of feedbacks as already mentioned in chapter 2 (Seneviratne et al. 2010). Non-linear responses influence the climate behavior due to the interaction of the  $Mr_{so}$  with the atmosphere. For instance, Jaeger (2011) found that moistening effects have a much higher influence within dry years than drying effects have within wet years. Additionally, a high accuracy in soil moisture values can lead to better forecasts e.g. in terms of air temperature (van den Hurk et al. 2012). Though, measuring soil moisture values is cost and time intensive and are the main reasons why not many observational data are available. Furthermore, the resolution of the data, as well as multi-year observations without gaps, are fundamental for every type of seasonal investigations but they are almost non-existing. There are no area-wide observational values in Europe, which is the reason why throughout this thesis ERA-Interim values are used as pseudo-observation values. In addition, available data for soil moisture is not homogenized between the different climate models in terms of included soil depth for calculations. Therefore, a comparison of absolute values doesn't make sense in this context. Due to this, only soil moisture trends and other statistical methods are used throughout the work.

### Surface net radiation (Rn)

This variable describes the product of the mean in- and outflowing radiant fluxes from SWR and LWR over a day or month. According to Kraus (2007) the Rn is defined like the following

$$Rn = SWR_{in} + LWR_{in} - (SWR_{out} + LWR_{out}). \quad (3.2)$$

### **Evapotranspiration (Evap)**

It shows the sum of transpiration and evaporation over land areas. Evap describes the transpiration from animals and plants as well as the evaporation from the ground and water areas in all phases. Transpiration represents a considerable proportion of the whole evapotranspiration, thus, a change in vegetation influences the evapotranspiration significantly. However, to evaporate water a certain amount of energy is needed which has a cooling effect on the atmosphere. The same amount of energy will be released again in case of condensation (Dee et al. 2011).

### **Potential evapotranspiration (PET)**

It describes the maximum value of possible Evap. More precisely, in case of the meteorological view, PET is defined as the maximum amount of liquid which can evaporate due to external environmental influences (e.g. wind, temperature, etc.) regardless of the available water volume. To calculate this amount, several methods have been developed. Two of them are the monthly based Blaney-Criddle (BC) and the daily based Priestley-Taylor (PT) method which are described in Section 5.3 (Brouwer and Heibloem 1997).

### **3.3.2 Model data**

Within chapter 3.1.1 and 3.1.2 the general operating procedure of GCMs as well as RCMs have already been mentioned. As an addition to this, table 3.2 contains all models that are used in the thesis with their specific resolution and the developing institute.

Tab. 3.1 Overview over the 9 GCM's as well as the 5 RCM's with their specific properties.

<b>GCM</b>				
Modelling Center	Institution	Model	spatial Resolution [lat × lon]	Reference
CSIRO	Commonwealth Scientific and Industrial Research Organisation and others	ACCESS1-3	1.25° × 1.875°	(Hirst and Uhe 2011)
CCCma	Canadian Centre for Climate Modelling and Analysis	CanESM2	2.812° × 2.812°	(Chylek et al. 2011)
NCAR	Royal Netherlands Meteorological Institute	CCSM4	0.942° × 1.25°	(Gent et al. 2011)
CNRM	Centre National de Recherches Meteorologiques	CNRM-CM5	1.401° × 1.406°	(Voltaire et al. 2013)
IPSL	Institute Pierre-Simon Laplace	IPSL-CM5A-MR	2.50° × 1.27°	(Hourdin et al. 2013)
MIROC	Atmosphere and Ocean Research Institute (The University of Tokyo) and others	MIROC-ESM	2.812° × 2.812°	(Watanabe et al. 2011)
		MIROC5	1.406° × 1.406°	(Watanabe et al. 2010)
MPI-M	Max-Planck-Inst. for Meteorology	MPI-ESM-LR	1.875° × 1.875°	(Raddatz et al. 2007)
NCC	Norwegian Climate Centre	NorESM1-M	1.875° × 2.5°	(Bentsen et al. 2013)
<b>RCM</b>				
CLMcom	Climate Limited-area Modelling Community	CCLM4-8-17	0.11° × 0.11°	(community.eu 2014) (Doms et al. 2011) (Bóhm et al. 2006)
SMHI	Swedish Meteorological and Hydrological Institute	RCA4	0.11° × 0.11°	(Strandberg et al. 2014)
KNMI	National Center for Atmospheric Research	RACMO22E	0.11° × 0.11°	(van Meijgaard et al. 2008)
DMI	Danish Climate Centre	HIRHAM5	0.11° × 0.11°	(Christensen et al. 2015)
GERICS	Helmholtz-Zentrum Geesthacht and others	REMO2009	0.11° × 0.11°	(Jacob and Podzun 1997)



# 4

## Statistics

Chapters 2 and 3 are the introductory chapters and are showing the basics regarding climate system and model types. In climatology the object of interest about longer-term mean conditions of the atmosphere and possible changes. In this Chapter is the focus on the methods which are used for this kind of investigation. A major part of this work is based on statistical calculations and findings between the individual variables from the climate models.

### 4.1 Arithmetic mean, variance and standard deviation

The arithmetic mean is used for central tendencies and is the sum of a numerical series of considered numbers divided by the number of those numbers. The arithmetic mean is defined as

$$\phi(x_1, \dots, x_n) = \bar{x} = \frac{1}{n} \sum_{i=1}^n x_i. \quad (4.1)$$

Another statistical quantity is the variance  $\sigma^2$ . It describes the squared deviation of a random variable  $x$  from its expected value,

$$\sigma^2 = \frac{1}{n} \sum_{i=1}^n (x_i - \bar{x})^2. \quad (4.2)$$

A disadvantage however is, that the variance contains a different unit than the used data. This can be fixed by taking the root of the variance to get the standard deviation  $\sigma = \sqrt{\sigma^2}$ .

## 4.2 Trend analysis

Trends can be used to point out statements or to estimate future developments and is a common tool in climatology. For this, a linear regression is performed with respect to the used variables in the form of

$$T(x, y, t) = C(x, y)t + \zeta(x, y, t), \quad (4.3)$$

with  $t$  as time relative and  $\zeta(x, y, t)$  as the residuals of the fit. To calculate the trend  $C(x, y)t$ , normally a least-square regression is used (van Oldenborgh et al. 2013).

## 4.3 Measure of coherence

Within statistics, absolute values provide information about quantitative features of data series and give an overview of their relationship to each other.

### Coefficient of correlation

*Bravais* and *Pearson* invented this coefficient to measure the relationship between two equally long, statistical series,  $(x_1, \dots, x_n)$  and  $(y_1, \dots, y_n)$  (Brückler 2017). The value is dimensionless and defined as follow:

$$r_{xy} = 1 - \frac{\sum_{i=1}^n (x_i - \bar{x})(y_i - \bar{y})}{\sqrt{\sum_{i=1}^n (y_i - \bar{y})^2} \sqrt{\sum_{i=1}^n (x_i - \bar{x})^2}}. \quad (4.4)$$

The coefficient of correlation ranges between  $-1 \leq r_{xy} \leq +1$ . If  $r_{xy}$  is exactly  $\pm 1$ , the relationship between the two data series is completely positiv (or negativ) .

### Coefficient of determination

It is a dimensionless value that measures the proportion of the variance in the dependent variables which can be predicted from the independent variables. Therefore one can make a statement about how well the line of regression approximate the real data points. The coefficient of determination is defined as follows:

$$R^2 = \frac{\sum_{i=1}^n (y_i - \hat{y}_i)^2}{\sum_{i=1}^n (y_i - \bar{y})^2}. \quad (4.5)$$

The coefficient of determination is ranged between  $0 \leq R^2 \leq +1$  with a complete explanation of the total variation by the explanatory variables  $x_1, x_2, \dots, x_n$  by  $R^2 = +1$ .



### p-Value (Probability value)

It is used in the context of testing the null hypothesis, thus, to estimate the extent of statistical significance based on evidence. The so-called probability value specifies whether the acceptance or rejection of the null hypothesis. So the null hypothesis will be retained if there is no evidence against it or gets rejected if the data are against it. This can be determined by the p-value. A guideline for confirming the null hypothesis is a p-value less than 0.05.

## 4.4 Remapping

In most cases, the placement of the model grid does not fit within the border of the area of interest. The decision which grid cell should be included in the analysis is hard because some grid cells are partly outside and/or partly inside the area of interest. Therefore a remap of the grid layout is needed. For this thesis, the approach from Mendlik et al. (2016) is used. All grid cells within the region of interest get summarized to a mean value within one big grid cell which has the same dimension as the region itself. Thus, the cells which are at the border and are only partly contributing get provided with a weighting which can be seen in figure Fig. 4.1. This means that the higher the participation within the area of interest is the higher the weighting will be.

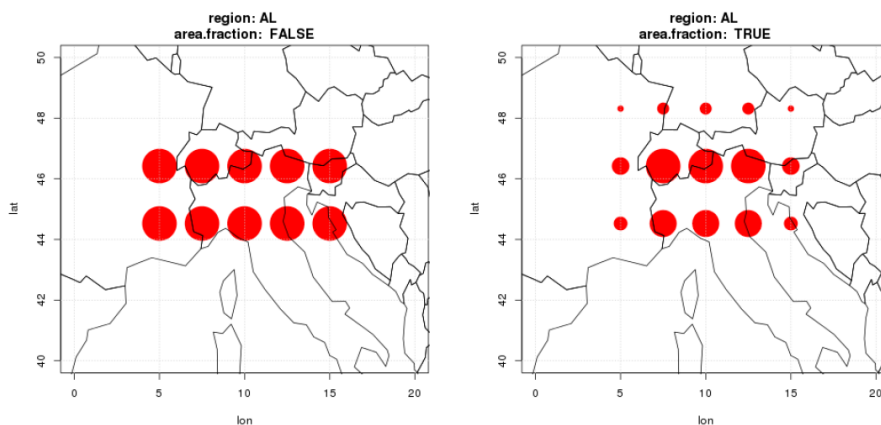


Fig. 4.1 With and without area fraction. It can be clearly seen that without weighting, there is a significant reduction in the amount of data. The areas which are not one hundred percent in the area of interest are still included and weighted in the calculations according to their respective share within the scope Mendlik et al. (2016).



# 5

## Results and Discussion

In the following Chapter, we discuss the results for soil moisture and temperature analysis within individual European regions. The aim is to show the different performances of Regional Climate Model (RCM)s and General Circulation Model (GCM)s and possible future changes. In Section 5.1 the basic approach for individual European regions and the verification between observation and model calculations is shown. The results of the statistical analysis related to maximum near-surface air temperature (Tmax) and total soil moisture content (Mrso) are presented in Section 5.2. Section 5.3 shows the results for present and future soil moisture-atmosphere coupling strengths.

### 5.1 Overview and verification of similarities between models and observations

Analyzing different climate models with each other requires a common data structure basis to ensure comparability between them. A particular challenge is in fact, that some climate models have different coordinate systems and different resolution. Hence, it is necessary to get all GCMs and all RCMs to the same initial state to make them comparable. Thus, within this thesis, the target areas are defined by the „Prediction of Regional scenarios and Uncertainties for Defining European Climate change risks and Effects (PRUDENCE)“ regions. The PRUDENCE project itself was part of the framework program for energy, sustainable development and the environment from the European Union (EU) (Christensen et al. 2007). Within this project, similar climate and orographic areas were summarized and combined with homogeneous surfaces close to

each other but with a heterogeneous surface compared to the other areas. The resulting eight European regions are shown in Fig. 5.1. For instance, mountainous areas like the Alps (Al) or Scandinavia (SC) are differentiated, same goes for coastal areas like the Mediterranean (MD) and the British Island (BI) (Christensen et al. 2001). These eight distinguished regions are used for the statistical analyses in the following chapters of the thesis. Therefore the first step is to adapt all climate model coordinates to the predetermined system as table 5.1 shows.

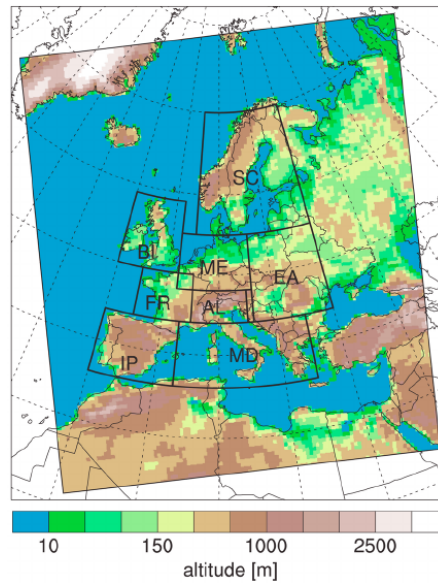


Fig. 5.1 European model domain with the PRUDENCE regions. The regions are similar within themselves in terms of climate and orographic aspects but different enough to each other (BI = British Isles, IP = Iberian Peninsula, Fr = France, ME = Mid- or Central Europe, SC = Scandinavia, AL = Alps, MD = Mediterranean, EA/EE = Eastern Europe). From Bellprat et al. (2012).

In case of the resolution, one can average over a specific PRUDENCE region and let the mean represent the whole area. Thus, each model is represented by a single grid box with a mean value which has exactly the same dimension as the selected area. The mean includes also those parts of the respective grid which are just partly within the targeting area. But this needs a weighting process that is described in the Remap-Section 4.4. However, a big part of the thesis is the interaction and coupling between Tmax and Mrso. So, before one should calculate the mean over a specific region it would be useful to get rid of the water areas within them, simply because they can distort the calculations. The temperatures over lakes and the ocean are usually more stable than

Tab. 5.1 PRUDENCE regions coordinates. Properties of the European domain are a rotated pole as well as areas with coordinates to stay consistent, thus, the table shows the coordinates of these individual regions (Bellprat et al. 2012)

<b>Area</b>	<b>West</b>	<b>East</b>	<b>South</b>	<b>North</b>
British Isles (BI)	-10	2	50	59
Iberian Peninsula (IP)	-10	3	36	44
France (FR)	-5	5	44	50
Mid- or Central-Europe (ME)	2	16	48	55
Scandinavia (SC)	5	30	55	70
Alps (AL)	5	15	44	48
Mediterranean (MD)	3	25	36	44
Eastern Europe (EE)	16	30	44	55

over land and Mrso values are also higher. With the help of a land-sea mask of the respective climate model, all grid cells which have a water share above 10% get cut out. This will help to keep the influence of rivers, lakes and the ocean as low as possible. After that process, the calculation of the mean values over a specific time period within each grid cell can be done. For the thesis, the data are evaluated for the summer season (JJA) which includes June, July, and August. Within each grid cell, the mean value over each summer month for each year gets calculated for a time period between 1979 to 2005. This leads to a data series of 27 values (summer mean) per grid cell for every used variable. Fig. 5.2 depicts the average Tmax of the year 2005 for a GCM and a RCM to clarify the resolution difference between those two. To complete the analysis pre-processing the averaging over the remaining land mass is carried out to obtain one representative value for each specific PRUDENCE domain for each year over the whole time period.

This kind of preliminary work is done for every climate model in the thesis. It is also accomplished for ERA-Interim and the European high-resolution observational gridded data set (E-OBS) which are used as observational data for the Mrso and Tmax throughout the thesis. Note, that due to the fact that there are no real observational data of Mrso for the whole European area, one can consider ERA-Interim as observations. So basically, ERA-Interim together with the E-OBS data define the verification basis for the reliability of the climate models and their projections of the climate system. However, it is useful to check the Mrso values first due to the inherit major role in the thesis.

ERA-Interim cannot project any future climate changes as other climate models because they take observational data into account. Additionally, it is very time-consuming to generate those data where no observations are available as already mentioned in Section 3.2. To trust those data, it is necessary that they are modeled correctly regarding

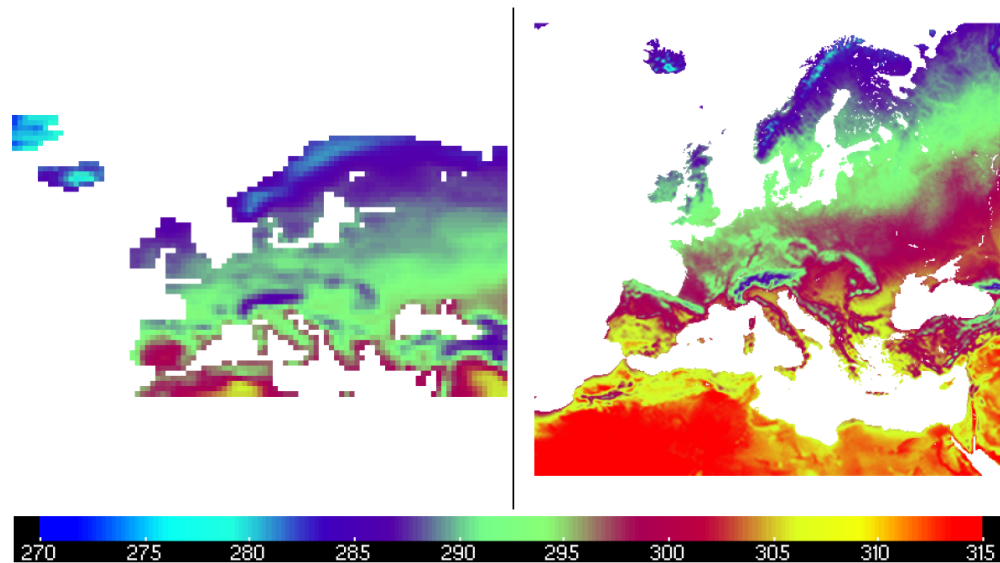


Fig. 5.2 Resolution difference between GCM and RCM. On the left side of the figure, the Tmax data are represented with the typical European Centre for Medium-Range Weather Forecasts Re-Analysis Interim (ERA-Interim) resolution of  $80 \text{ km} \times 80 \text{ km}$  for JJA. Compared to that, on the right side, there is the Tmax data from a *CCLM* driven by ERA-Interim with a resolution of  $12.5 \text{ km} \times 12.5 \text{ km}$ . Both figures represent the same time period. In addition, it also shows the results from the individual land-sea masked because the sea and bigger water amounts are cut out and replaced by no data (white space). The maps are displayed using the software *NC Viewer* (Pierce 2009).

physical laws and feedback influences. It makes sense that for instance evapotranspiration (Evap) increases when near-surface air temperature (Tmean) also rises. Higher Tmax leads to a higher evaporation rate which enhances the greenhouse effect because water vapor is a strong greenhouse gas (GHG) (Cubasch et al. 2013). Thus, a higher surface warming follows. But Evap can only increase to a certain extent. If there is no more water available, nothing can evaporate and the surplus energy which is normally needed for evaporation can now go into the sensible heat flux. This is common in southern European areas (Schönwiese 2003). Therefore, it is natural that surface net radiation (Rn), air temperature, and evaporative processes have a strong relationship with each other because the energy is linked directly to the amount of evaporation (Cubasch et al. 2013). A crucial part in the regional climate system is soil moisture. Within the thesis, ERA-Interim values for Mrso are calculated for the first meter of the surface with a water density of  $1000 \text{ kg}\cdot\text{m}^{-3}$  in cases of conversion measures. The relationship between Mrso

and Tmax as well as to net radiation should be similar. Although Schär et al. (1999b) suggested that there must be an enhancing of Rn by high values of Mrso due to albedo changes, Jaeger (2011) showed that there isn't a clear positive or negative relationship. For summer values, ERA-Interim shows a slight negative correlation between Mrso and net radiation as well as Tmax with shifted values for coastal areas like British Isles and the Mediterranean as Fig. 5.3 depicts. Hence, higher Tmax leads to lower Mrso values due to a rise in the evaporation rate. Hence, high temperatures lead to soil dehydration as shown for the Mediterranean, while low Mrso values for the British Isles in summer are resulting from blocking highs at this time of the year (Marsh et al. 2007).

No clear results regarding Mrso and Evap are possible although it shows a high evaporation rate as well as a high dehydration in the Mediterranean. In contrast, Scandinavia shows high Mrso and relatively low Evap values certainly has to do with the relatively low Tmax in this region. As for Tmean values from ERA-Interim and Tmax values from E-OBS, there is a clear positive relationship. This is not surprising since both reflect the observations. Further comparison between ERA-Interim values and the observational data from E-OBS (not shown) increases the reliability in addition because they are very similar to each other. Referring to Mrso and precipitation there is a positive connection which is influenced by discharges and infiltration. As far as Eastern Europe is concerned, there is a special interaction when it comes to Mrso because precipitation, as well as temperature, have a strong influence which results in a very variable soil dampness.

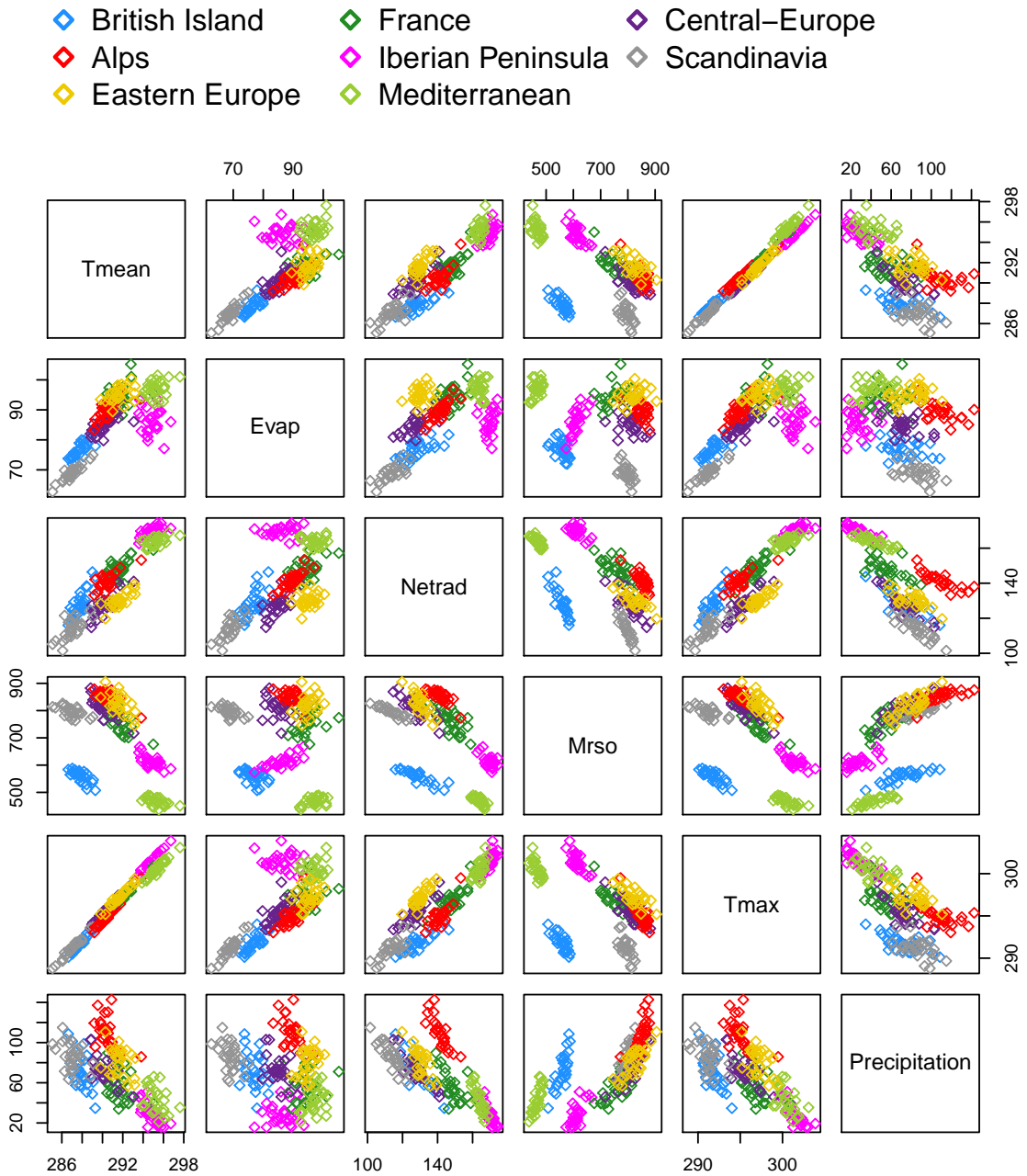


Fig. 5.3 Data overview of the PRUDENCE regions with ERA-Interim. The most important components of the soil moisture-air temperature feedback are plotted against each other to show their relationship within the individual regions. It is noticeable that both coastal areas, British Isles and Mediterranean, are separate from the rest in case of the soil moisture-air temperature relationship.



### 5.1.1 Model comparison

For the sake of readability, within figures in the following chapters, every climate model gets featured with a combination of a symbol and a color. Using colored marks ensures a quick separation between GCMs and RCMs, whereby colored crosses represent GCMs and other colored symbols like circles and squares represent RCMs. This combination maintains throughout the whole thesis and is shown in figure Fig. 5.4. With the list of GCMs on the left side as well as the list of RCMs on the right side with their specific recognition characteristics. Note, that this also functions as a legend for almost all figures within the thesis. On the right side, the driving GCM for the running RCM is also included, represented by the name before the point. For instance *CNRM-CM5.CLMcom-CCLM*, where *CNRM-CM5* represents the driving global model and *CLMcom-CCLM* the nested regional model. Furthermore, the color from a RCM is matched with the color of the driving GCM.

GCM ---	GCM/RCM combinations ---
✘ CNRM-CM5	△ CNRM-CM5.CLMcom-CCLM
✘ IPSL-CM5A-MR	▽ CNRM-CM5.SMHI-RCA4
✘ MPI-ESM-LR	▽ IPSL-CM5A.SMHI-RCA4
	○ MPI-ESM.CSC-REMO2009_v1
	○ MPI-ESM.CSC-REMO2009_v2
	△ MPI-ESM.CLMcom-CCLM
✘ NorESM	◇ NorESM.DMI-HIRHAM5
✘ ACCESS1.3	△ EC-EARTH.CLMcom-CCLM
✘ CanESM2	□ EC-EARTH.KNMI-RACMO22E
✘ CCSM4	◇ EC-EARTH.DMI-HIRHAM5
✘ MIROC5	△ HadGEM2.CLMcom-CCLM
✘ MIROC-ESM	□ HadGEM2.KNMI-RACMO22E
	▽ HadGEM2.SMHI-RCA4

Fig. 5.4 Model legend within the thesis. It contains a combination of shape and color for each individual model and is consistent throughout the whole thesis. Attention is also paid to the fact that the RCMs are color matched to the driving GCM.

Climate models are not only able to simulate past and present climate conditions it is also possible to project data from future climate scenarios. Although, some of the projected variables are not as robust as others according to Randall et al. (2007). For instance, precipitation is not as trustworthy in future scenarios as temperature values. However, the confidence in climate models arises from the fact that they are able to simulate the responding rise in global surface temperature values due to an increase in greenhouse gases (GHG) since the middle of the 19<sup>th</sup> century. Whereas the best results are gathered from multi-model means which are the closest to observational data (Bony et al. 2007; Cubasch et al. 2013). Overall, observational Tmax trends in the European region indicate an increase in surface temperature within the period 1979 to 2005. However, it can be interesting to study individual models and their output in certain local regions as well as the different projection results between them. Thus, one has to keep in mind that uncertainties of model runs have major impacts on the results, especially when it comes to natural variability.

A crucial part is the performance difference between GCMs and RCMs, especially in Europe. Overall both model types provide good results compared to present observational Tmax values in the European regions which is shown in Fig. 5.5. The possible spread for each model as well as for the observations is represented by the standard deviation that is also depicted. For instance, E-OBS data show a Tmax trend of  $0.04 K \cdot yr^{-1} \pm 0.02 K \cdot yr^{-1}$  for the period 1979 to 2005 over British Isles. Compared to that there is only one GCM, which is completely outside this range. A similar pattern occurs over the Iberian Peninsula, Central Europe and Scandinavia where the observational Tmax trends reach from  $0.05 K \cdot yr^{-1}$  to  $0.08 K \cdot yr^{-1}$  and only individual models are not within this range. Extrapolated for the entire 27-year period this is a maximum Tmax rise of  $1.35 K$  to  $2.16 K$  over these specific regions. However, in these three mentioned regions the outliers include both model types, GCMs, and RCMs.

For the other four regions France, the Alps, Mediterranean and Eastern Europe the situation is different because the amount of models which are outside or barely inside the observation range is higher. Over all four of these regions, it seems that a lot of climate models systematically underestimate the temperature trend compared to the observations. Especially the whole RCM ensemble have problems here. To emphasize this, the multi-model mean from the RCMs result in a Tmax trend value around  $0.03 K \cdot yr^{-1}$  over each of this four regions. This describes a deviation from the observations of at least  $0.02 K \cdot yr^{-1}$  or  $0.54 K$  in total. In contrast to that, at least half of the GCMs are within the observational range for every PRUDENCE region. Too low Tmax values have consequences in terms of Mrso, humidity and other climate variables. In particular, lower Tmax values imply higher Mrso values because the solar energy is used for evaporation and not for an increase of the surface flux as the observations show. So, van Oldenborgh et al. (2013) points out the possibility of a too high Mrso, because France heats up faster than the models project. However, there is no real evidence that there is indeed

an underestimation of the RCMs compared to the observational data. This is shown by the fact that not all RCMs underestimate the observational Tmax trend. And within this regions, not always the same models are underestimating the trend. Some models show this behavior only in one or two cases over the European regions. Most of the RCMs including the standard deviation is near the observational Tmax trend range. So the supposed underestimation can mostly be explained by uncertainties, in particular by natural variability within the individual model runs.

Taking into account Mrso values, the situation is different. Mrso has a strong impact on Tmax due to the cooling effect which occurs during evaporation. The hydration and the limitation of water within the soil embodied a crucial part in the soil moisture-atmosphere coupling. The amount of Mrso also affects cloud cover trends by the amplification of relative humidity in the atmosphere (Jaeger 2011). However, observational data of Mrso over the complete European area does not exist. This is also the reason why computationally generated data from ERA-Interim serve as observations. Since the availability of data regarding soil moisture is difficult, the use of absolute values is not justified. So throughout this thesis just relative values, trends and statistical metrics for Mrso related data are used. So the Mrso trend for all eight investigated European regions are between  $-2.904 \text{ kg}\cdot\text{m}^{-2}\cdot\text{yr}^{-1}$  and  $0.104 \text{ kg}\cdot\text{m}^{-2}\cdot\text{yr}^{-1}$  with the maximum in Scandinavia and the minimum in France for the period 1979 to 2005. It can be seen in Fig. 5.6. Based on the data, it seems that a general dehydration in Europe within the period of interest exists.

It is noteworthy that both northern regions, British Isles and Scandinavia are the only ones with a positive Mrso trend. Thus, according to the model data, are the only two European regions that increased in Mrso value during the study period. That suggests that there were either more rain events or lower Tmax values in the northern parts of Europe within the summer season. In addition, the trends from the climate models for these two regions agree very well with the trend from ERA-Interim. And the standard deviation is overall extremely low especially for Scandinavia, which indicates a relatively low change in Mrso values throughout the whole study period over each model. Similar situations appear over the Iberian Peninsula, Central Europe, and the Mediterranean. Although some outliers and relatively high standard deviations stand out, overall the climate model trends for Mrso matches well with the observational trend.

For France, the Alps and Eastern Europe the situation is different. Most climate models overestimate the Mrso trends compared to the observations. Although, one can argue that over the Alps, the Mrso values are still in the normal range if the standard deviation is included. The high deviation values, therefore, might be caused in this region due to a combination of heterogeneity of the orography, frequent precipitation events and many regional effects which are parameterized like thunderstorms. The situation for Eastern Europe looks similar because here, an overestimation of Mrso is possible.

However, there is no real evidence for this because some models are in the range of the observation. Therefore, the overestimation can be caused by uncertainties because some individual outlying values can happen due to natural variability and the related randomness of single model runs. According to that, a systematic overestimation cannot be confirmed for either Eastern Europe nor the Alps.

The last and most outstanding region in this context is France because the distribution of all model trend values for Mrso is an evidence for an overestimation compared to ERA-Interim. As Fig. 5.6 shows, no model matches the observational data range even with the consideration of standard deviation. So basically all climate models represent a higher trend value than ERA-Interim. This is also the region where the observations show the minimum of all Mrso trends in the European region. As a result, there is an increase in the moisture content over this region, which in turn affects all processes connected with the soil. According to the soil moisture-air temperature coupling the Tmax should be particularly affected. Due to the increased Mrso values, more solar radiation energy is needed for evaporation and therefore less energy can go into the sensible heat flux and the increase in air temperature. This would explain why, according to observations, this region warms up faster than the models project.

Especially the two *MIROC* models are interesting. Because the *MIROC5* model is underestimating the trend completely in Scandinavia as well as in Central Europe and Eastern Europe which are all located in the central parts of Europe. Whereas the *MIROC-ESM* model completely overestimates both southern regions, the Iberian Peninsula and the Mediterranean. This may either indicate a problem in the internal structure of the models or be simply due to natural variability within the model runs.

## 5.1 Overview and verification of similarities between models and observations

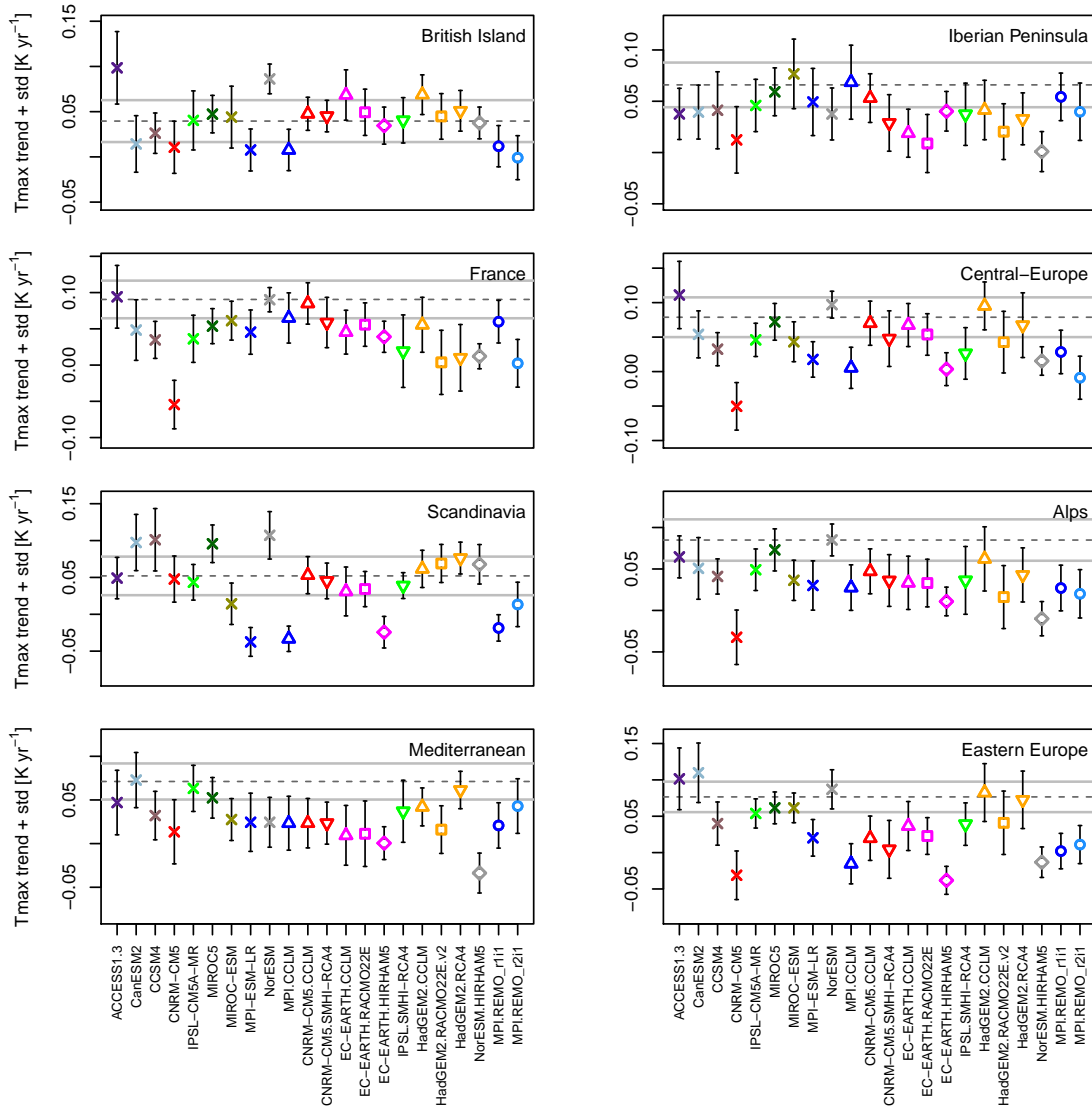


Fig. 5.5 Deviation of Tmax model data from observations. The Tmax observation trend of ERA-Interim are represented by the horizontal dashed line. In addition, the standard deviation is also added with gray lines. While the climate model Tmax trends are represented with the assigned color/shape combination plus the respective standard deviation.

## 5 Results and Discussion

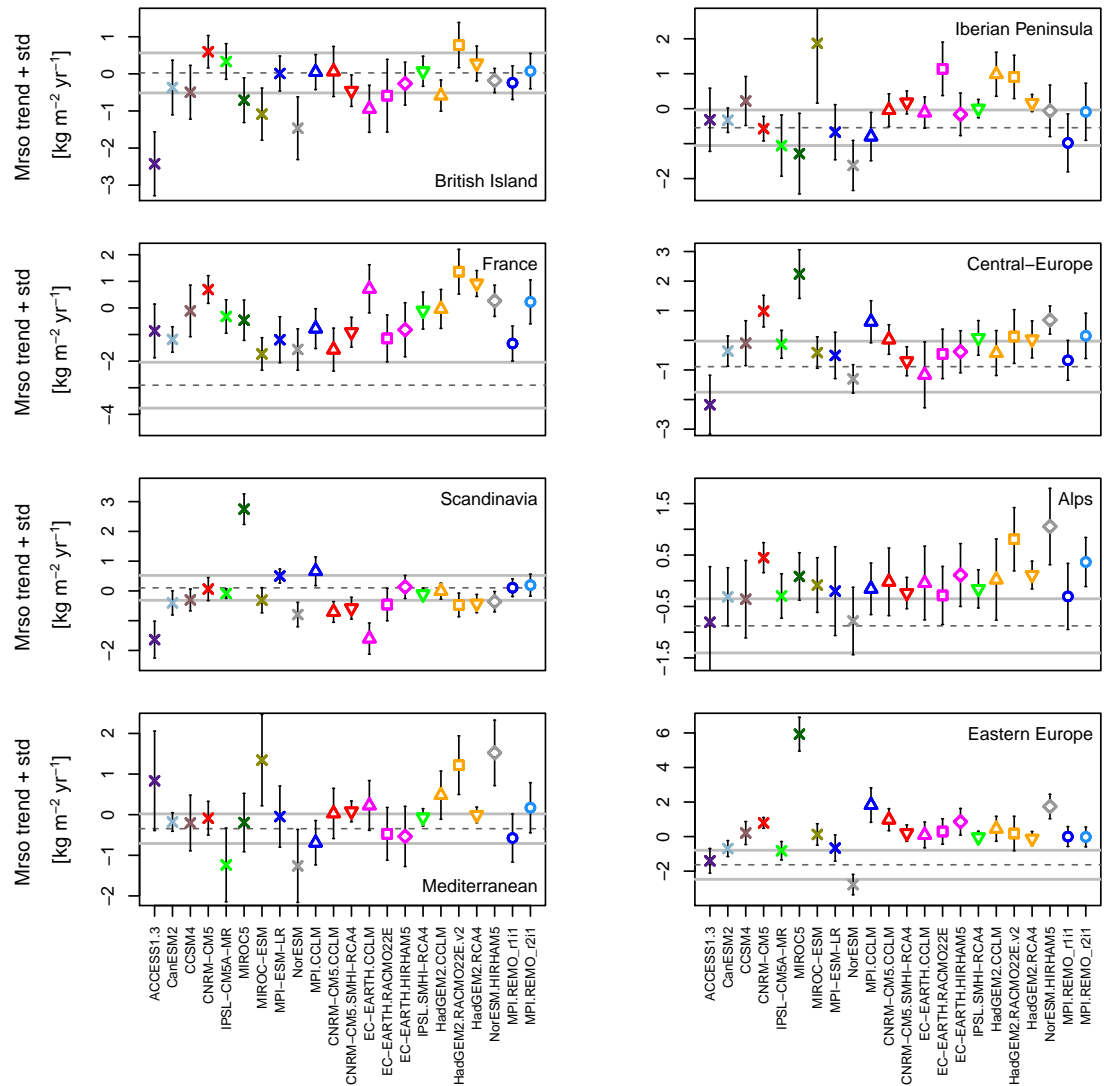


Fig. 5.6 Deviation from the Mrso model data compared to the observations. The climate model values of Mrso trends with the standard deviations are compared to the ERA-Interim trends (shown as a horizontal dashed line with gray lines representing the standard deviation).

### 5.1.2 Model differences

Nearly all GCMs and RCMs studied in this thesis show a similar behavior when their Tmax and Mrso trends are plotted against each other, shown in Fig. 5.7. Still, there are differences between the two model types. As one can see in Fig. 5.7, within six out of the eight PRUDENCE regions the data correlation of the RCMs and the GCM have the same negative direction in terms of a linear regression line. It follows that a higher Tmax trend is linked with a lower Mrso trend and therefore is in agreement with the soil moisture-air temperature coupling. The two exceptions are the Iberian Peninsula and Scandinavia where the GCM regression line represent a slight positive slope. However, the RCM slope is also negative in these two regions which imply that they show a completely negative correlation in all eight investigated European region between Tmax and Mrso. In general, the RCM regression slopes are between -0.036 and -0.012 with the highest over Mediterranean and the lowest over Scandinavia. In contrast, the GCMs have the lowest regression slope value over the Alps with -0.064 and the highest one over the Iberian Peninsula with 0.008. Since these are relatively small slope values, it is quite possible that natural variability is responsible for these two positive values of the GCMs. As a result, it can be assumed that both the RCMs as well as the GCMs have a negative linear relationship between Tmax and Mrso.

To emphasize the connection between Mrso and Tmax trend further, one have to look also at the coefficient of determination which indicates a significant correlation between the two variables. This is already explained in Section 4.3. It turns out that there are considerable differences between GCMs and RCMs over each PRUDENCE region. The two northern regions, British Isles and Scandinavia, show only a single significance between Mrso and Tmax trend. This is due to the low resolution of the GCMs combined with the partial occurrence of relatively high air temperatures in the British Isles during the JJA, which can also lead to droughts. In Scandinavia, the Tmax values are not quite as high due to the precipitation that also occurs in summer and does not lead to any major changes in Mrso (Marsh et al. 2007; Schönwiese 2003). Over the central European regions of France, Central Europe, the Alps, and Eastern Europe, the relationship between Mrso and Tmax is significant or almost significant as high temperatures and precipitation events that are moistening the soil again always alternate. Only in Eastern Europe are deviations between the two model groups, which is probably due to the different resolutions. The southern regions, the Iberian Peninsula and the Mediterranean are generally hot and dry in summer (Schönwiese 2003). Remarkable are the low  $R^2$  values in the Mediterranean. One explanation can be the change of the Hadley cell due to increased atmospheric temperatures which result in a northward expansion. As a result, a subsidence of dry air over the Mediterranean Sea gets induced which in turn leads to increased dehydration (Goosse 2015). And since the area is sometimes already dried out, it can not dry out further, but the Tmax can continue to

increase causing the constellation in Fig. 5.7.

Another notable point is the positioning of all climate models compared to the observational data. Within five regions, the majority of the models are bulking around the observational Tmax and Mrso trends from E-OBS and ERA-Interim. Within the three remaining regions where the comparison of the model trends with the observations does not match, France as well as the Alps and Eastern Europe, something special occurs. One can see in all three regions that they have a higher Mrso trend but at the same time a lower value for the Tmax trend than the observations. This, in turn, provides additional evidence for a strong soil moisture-air temperature coupling and its impact on the regional climate conditions.



## 5.1 Overview and verification of similarities between models and observations

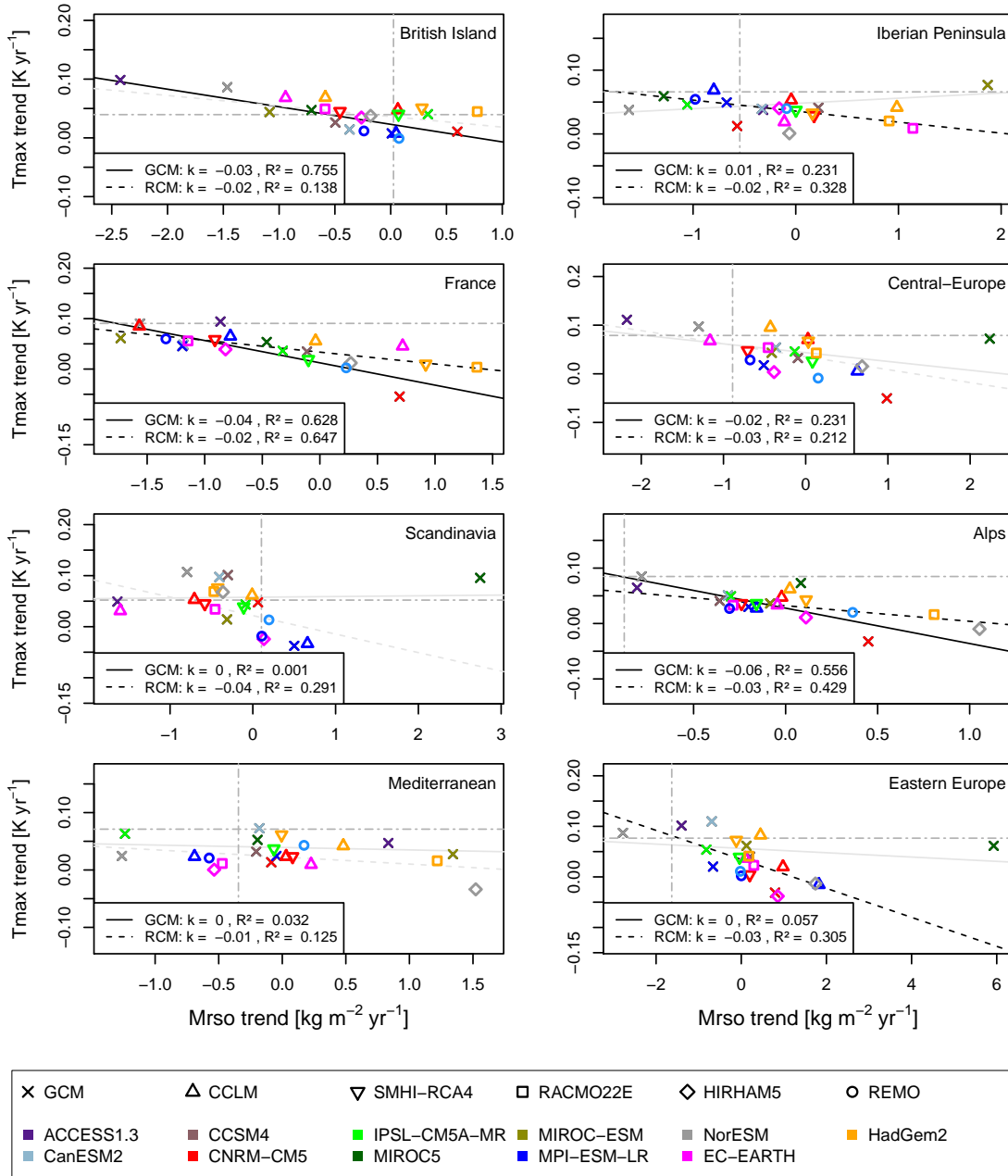


Fig. 5.7  $T_{max}$  trend against  $Mrso$  trend. All eight regions are in agreement with the soil moisture-air temperature coupling which implies a negative correlation between  $T_{max}$  and  $Mrso$ . For instance, this leads to an increase in  $Mrso$  while reducing  $T_{max}$ . The observational data are represented by the horizontal and vertical gray dashed lines while significant correlations of the climate model types are shown in black lines (GCM = solid lane, RCM = dashed line). Non-significant relationships are displayed in light gray.

By calculating the trend difference of Mrso and Tmax over the 27 years period of interest between a GCM and its corresponding RCMs, two interesting aspects appear. First, plotting the difference values against each other shows a negative correlation between Mrso and Tmax trends, which can be seen in Fig. 5.8. An increase in Mrso leads to a decrease in Tmax and vice versa. This leads to the assumption that the corresponding RCM amplifies the soil moisture-air temperature coupling mechanism due to an explicitly represented feedback process compared to the driving GCM. This behavior applies to all eight PRUDENCE regions. For instance, the *CNRM-CM5* driven RCMs show higher Tmax trends but weaker Mrso trends than the GCM itself in six regions. The strongest deviations are in the Alpine region, Central Europe and France with the highest value of  $0.139 K \cdot yr^{-1}$  which is nearly  $4 K$  over the whole period. Only in Scandinavia and in the Mediterranean region are the differences around zero between the corresponding RCMs and the driving GCMs. For the *NorESM* driven RCMs the picture is quite unique because they show in all eight PRUDENCE regions a higher Mrso trend than the GCM and therefore lower Tmax values. In fact, these are the highest Mrso differences throughout all GCM-RCM combinations in all regions. Related to that, they are also the ones with the lowest Tmax values. Due to the fact that the GCM is the base, the difference in the Tmax trend values are always negative and the Mrso values are always positive. In the case of the *MPI-ESM* driven RCMs, the difference values are around zero in all regions. Merely in France and Eastern Europe, one of the RCM shows a moister soil which in turn has the consequence to a lower Tmax value than the driving GCM.

Second, which is most likely the more important one, the dominant factor of these RCM-GCM combinations is probably the driving GCM itself. Over all European regions the different RCMs do not group around themselves regardless of the driving GCM, instead, the RCMs which are driven by the same GCM show a clustering. Therefore, the clustering depends on the GCM and not on the specific RCM. This can be shown for example by the arrangement of two non-specific RCMs. Assuming one of these two RCMs compute a stronger soil moisture-air temperature coupling and the other one simulates a systematic deviation from the driving GCM. Thus, all tries with the systematically deviant approaching RCM, driven with more than one GCM should be clustering around a certain area because it makes the same computations and deviations independent of the driving GCM. Whereas the values from the other RCM, that simulate the soil moisture-air temperature coupling in a certain way, should cluster in another specific area if it is driven by more than one GCM. As Fig. 5.8 show, this is not the case in terms of the *CLMcom-CCLM* or the *SMHI-RCA4*. The position of the *CLMcom-CCLM* differs from each other. It varies depending on the driving GCM, in this case, the *CNRM-CM5* or the *MPI-ESM*. Same applies for the *SMHI-RCA4* with the driving *CNRM-CM5* and the *IPSL-CM5A-MR*. Therefore the clustering cannot be the result of a systematic deviation or similar devices within the RCM themselves. Instead, it is more likely that the driving

GCM has a dominant influence on the corresponding RCM. This could be due to the driving data received by the RCMs. For example, one GCM generates a lot of heatwaves in summer while another one simulates a lot of cold rainy days. The corresponding RCM which receives this driving data is computing an amplification or a weakening of the soil dehydration based on these data. Resulting in a drier, moister or equal soil situation compared to the driving GCM. And due to the self-reinforcing effect of the soil moisture-air temperature feedback, different GCM driving data can lead to relatively large differences within the RCMs, that would explain the negative linear regression in Fig. 5.8. Therefore, the study of the major weather conditions of the individual driving GCMs would also be of interest, but it would go beyond the scope of this thesis.

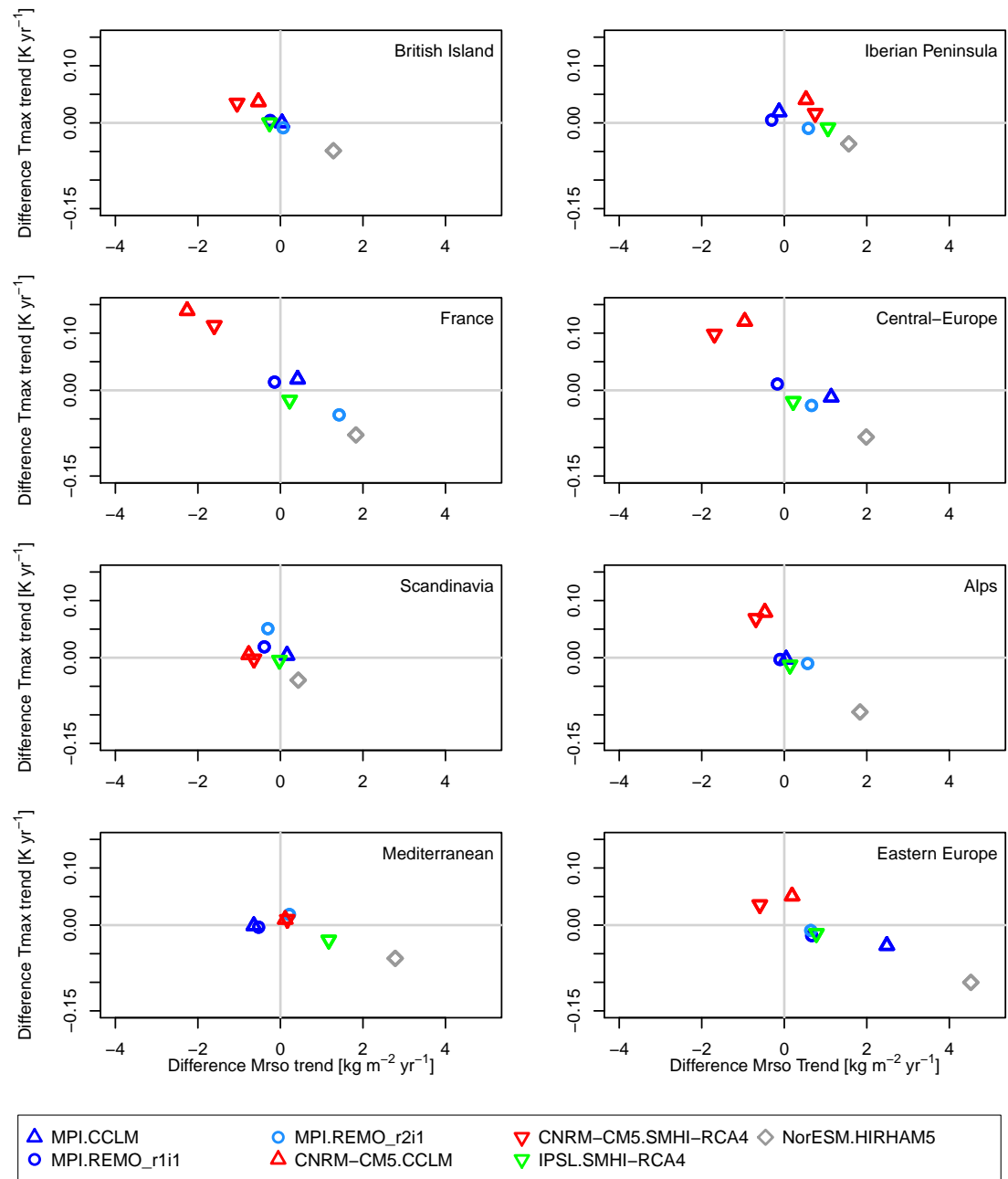


Fig. 5.8 Effects of the RCMs compared to the driving GCMs. Here, the GCM trend values of Mrso and Tmax are subtracted from the corresponding RCM trend values and then compared to each other. The dominating factor for the RCMs is the driving GCM.

To summarize the chapter, it is necessary to keep in mind that there are no observations available for some parameter, especially for Mrso. So observational data get generated to compensate for these lack of information within the time period of 1979 to 2005. Hence, this observational data are used as reference values to verify the different performances of RCMs and GCMs. In general all models show a good result for Tmax trend values compared to the E-OBS trends. Individual models are outside the observational range in different PRUDENCE regions, thus, this can be due to natural variability. In case of Mrso trends, the models are showing a possible overestimation in Eastern Europe and France. For Eastern Europe, the differences can be caused by uncertainties of individual model runs, however, a special case is France. There is evidence for an overestimation of the Mrso due to the fact that all models show this behavior compared to the observations. This is a possible explanation why France warms up faster than the models predict according to van Oldenborgh et al. (2013).

In addition, one can argue that there is a linear connection between Mrso and Tmax over the summer season. A change in one of the two variables immediately shows an opposite reaction of the other variable over a European region. For instance, an increase in Tmax immediately contributes to a reduction in Mrso, although there may be local deviations as for example in Scandinavia. Also, with regards to the performance comparison, there is evidence that the GCMs are the dominant influential factor on the performance of the corresponding RCM.

## 5.2 Uncertainty reduction through constraints

In this chapter, a brief overview of results concerning a relationship between current climate and long-term climate projections is given. Not only the results are discussed, but also the used method is centered within this chapter. Therefore, the first part of this chapter is focused on the explanation of so-called *Emergent constraints*. This is an approach where the current understanding of the climate system and projected future climate conditions are linked together. The second part of the chapter mainly shows the results from this approach with regard to the soil moisture-air temperature coupling.

### 5.2.1 Emergent constraints

It is hard to figure out which variables are trustworthy for the ability to project future climate conditions. Even if some realistically simulated variables exist for current climate conditions, there is no evidence that the exact same variables are more trustworthy in future climate projections (Klein and Hall 2015). Emergent Constraints can be a possible answer to this problem. According to Klein and Hall (2015) and Nijssen and Dijkstra (2017) emergent constraints are physical explainable empirical relationships over an ensemble of climate models. These relationships are connecting characteristic variables between present and long-term climate behavior, in which the long-term climate predictions are constraint by observations. Note, that the trust of emergent constraints is highest when the empirical relationship between predictor and predictand is based on simple physical laws (Collins et al. 2012). The combination of an observational estimate with a present model aspect leads to a constraint future climate prediction that can provide two things. First, the predictand is a single-valued function which depends on the predictor and second, it may be possible to make a statement if the observed uncertainty is able to explain the entire model spread (Klein and Hall 2015). Due to emergent constraints, future trends can be identified by past or current trends with restrictions due to observations. Thus, they can help to reduce uncertainties in climate model projections. This is possible because emergent constraints are able to narrow the uncertainty spread of climate projections of a single climate model or a model ensemble because the extent of the projected variable spread is limited by the physical connection on which the climate models are based on. It follows that a certain spread of the projection is physically unlikely and can therefore be restricted (Brient and Schneider 2016; Klein and Hall 2015). Additionally, model uncertainty and natural variability aren't non-negligible factors, so they should also be taken into account during the constraining of parameters for the observational data (Bracegirdle and Stephenson 2012).

There are a few examples where simple relationships between past or current observation and future projected variables exist. For instance, Bracegirdle and Stephenson (2012) used emergent constraints for regional polar warming estimates. For this, they

compare climate change signal (CCS) values from Tmean with present temperature model mean values and constrain them with observations, thus, a physical connection between both variables exists and the basic values are also measurable. Due to a significant connection between the mentioned variables, they show that a majority of the models which represent a colder average Tmean in the present are experiencing the stronger warming in the future. Another example is Klein and Hall (2015), where they show that emergent constraints can be used for investigations into cloud feedbacks where a climate change response exists on the strength of the optical depth of low-level clouds. According to Nijssen and Dijkstra (2017) emergent constraints are encountered if evidence for a linear correlation between the constrained present values and future projected values over the majority of the model ensemble occur. The estimated response to the present climate state and projected values can be calculated by a linear regression model (Bracegirdle and Stephenson 2012). The following trend model

$$y_i = \mu + \beta x_i \quad \text{for } i = 0, 1, \dots, n \quad (5.1)$$

is similar to the trend model in Section 4.2, where  $\mu$  and  $\beta$  can be calculated by using ordinary least squares (Draper and Smith 2014). Here,  $y_i$  describes the climate change response and  $x_i$  the present constrained aspect (Bracegirdle and Stephenson 2012). The strength of this method lies in its simplicity and the fact that both variables normally have a logical, physical connection to each other. Although not all variables are appropriate for such an approach (Collins et al. 2012).

### 5.2.2 Long-term climate projections with trend values

The main part of emergent constraints is the reduction of uncertainty and due to the statistical principles of this method, it can only happen if the characteristics have a physical relationship to each other which is mainly expressed by the coefficient of determination. Within this thesis, the emergent constraint response is represented by the CCS that is the result of a subtraction between two arithmetic Tmax means. According to Section 2.2 an increase in Tmean should strengthen the CCS, and therefore the Tmax, due to an amplification of the soil moisture-air temperature feedback. The first Tmax mean includes the data of an individual model over a specific PRUDENCE region within the reference period of 1979 to 2005. The second Tmax mean is calculated from the projected data of the same model and the same region within the future period 2070 to 2099. Projected Tmax values are under the assumption of the representative concentration pathway (RCP)8.5 that includes the maximum impact of GHG as well as the maximum effectiveness for them within a climate model ensemble. This will visualize a relationship between the present and projected data if one exists. This process is done for every model within the ensemble. The CCS itself shows a long-term variation in a cli-

mate state which is identifiable and statistically discernible (Carter et al. 2001). Fig. 5.9 depicts this connection for all eight PRUDENCE regions, whereas the most noticeable feature can be found in France. This is the only region where a specific model type, in this case, the RCMs, show a negative slope of the linear regression. Since this relationship is not significant, it can also be caused by model uncertainties. In comparison to that, the GCMs show more meaningful result in this region that is in accordance with the mentioned physical based theory.

As for the British Isles, Scandinavia, the Mediterranean, and the Alps, the ensemble behavior is quite similar over all these PRUDENCE regions. All four regions indicate a significant or almost significant relationship between CCS and Tmax trend for the RCMs. In contrast, the GCMs show no conspicuous relationship, except for the Mediterranean region. The different results between the two model types for the British Isles, Scandinavia, and the Alps, can be caused due to a more explicit computation of atmospheric processes associated with a higher resolution, as there are more frequent rainfall events in these areas. And these events are better represented by the RCMs. As for the Mediterranean region, it can be that it is only due to the model uncertainty since the GCM constellation is close to a significant connection. However, there is a big difference between the Mediterranean and the Iberian Peninsula. The signal from the RCMs is not meaningful, while the GCMs show a pretty strong connection with an  $R^2$  value of 0.605 in this region. Thus, the GCMs show a distinct relationship between present Tmax values and an increase in future air temperatures. The divergences between the two southern European regions may be affected by the shift of the Hadley cell, but further research would be needed to confirm this claim. Therefore, a reduction of uncertainties is unlikely for all the regions mentioned above because of the non-uniform results of the two model types.

Over the remaining two regions, Central Europe and Eastern Europe, the patterns of the model ensemble behavior are nearly the same. With regards to the regression model for both model types, the slopes of the linear regressions, as well as the coefficient of determination, match each other. With strikingly significant relationships between CCS and Tmax trend for the GCMs in both regions. And also the results of the  $R^2$  values for the RCMs indicate a connection between the two variables. Only the fact that most of the values don't match the observation very well, is tarnishing the result a bit. The unity in the Central and Eastern parts of Europe is due to the already influential soil moisture-air temperature feedback in these regions. A future warming has a reinforcing effect that leads to further dehydration and to a further increase in temperature. Thus, purely from the data, a reduction of uncertainties would be possible, but the deviation from the observations is questionable over these two regions.

An increase in Mrso leads to a rise in potential dampness which has an influence on evapotranspiration processes. Such an increase can be used for evaporation cooling and therefore to decrease Tmax. Based on physical laws, a negative regression should exist



## 5.2 Uncertainty reduction through constraints

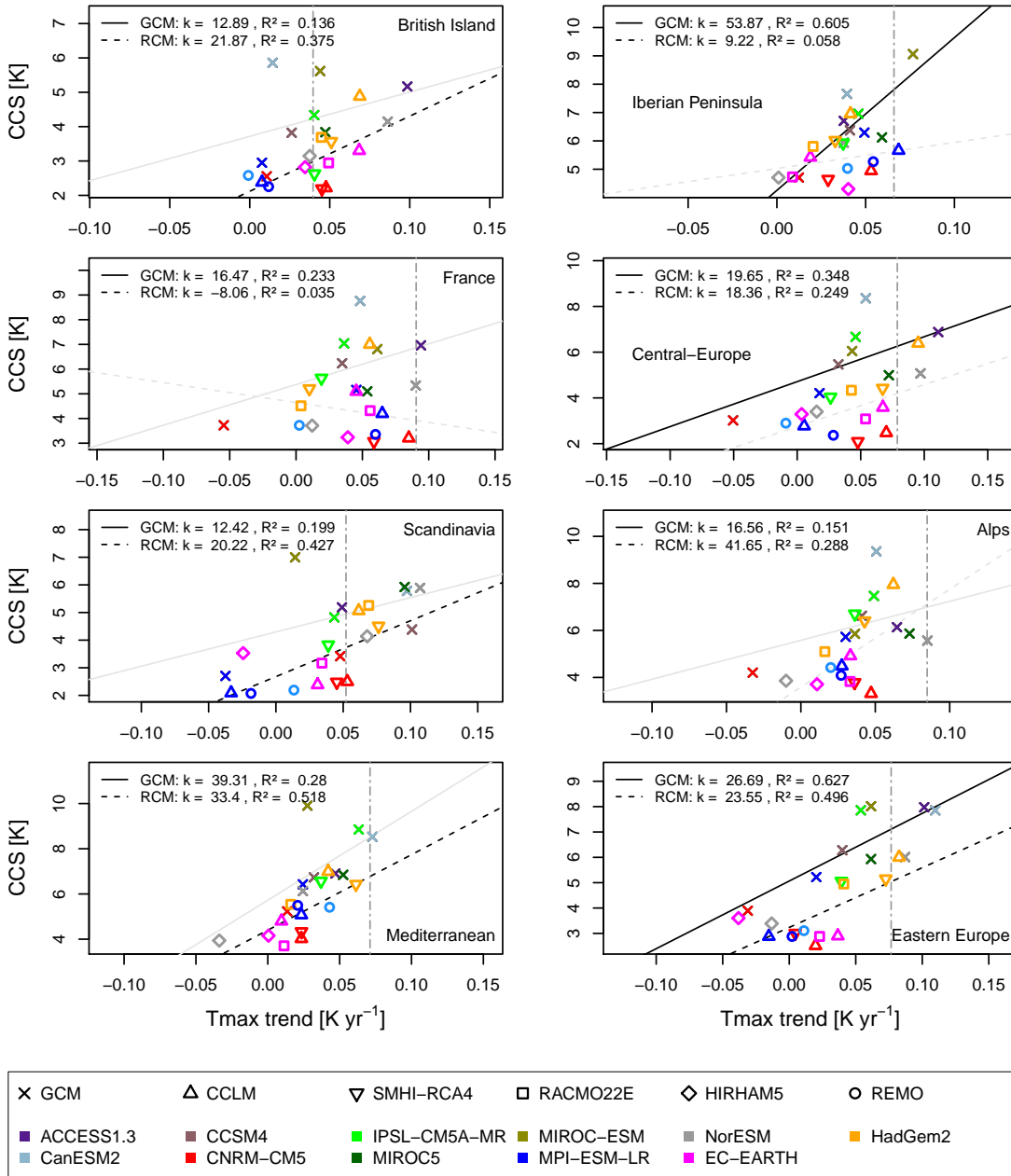


Fig. 5.9 CCS is plotted against the Tmax trend. This approach is for finding a relationship between current Tmax trends (period 1979 to 2005) which are constraint by observations, and projected CCS values to reduce uncertainty. The observational data are represented by the vertical gray dashed line while the correlations of the climate model types are shown in black lines if they are significant (GCM = solid lane, RCM = dashed line).

in terms of emergent constraints where an increase in Mrso trend implies a decrease in CCS and vice versa. However, within some PRUDENCE regions this relationship is not the case as Fig. 5.10 depicts. For instance, the regression for RCMs and GCMs over the Iberian Peninsula have a reverse relationship than expected. Even if the coefficient of determination for the RCMs is low in this case and therefore meaningless, the value for the GCMs together with the p-value (not shown in the figure) indicates a significant correlation. With regard to the Mrso trend-CCS pairing, it is the only statistical significant connection over all eight PRUDENCE regions. This can be caused by a change in the circulation pattern in the lower latitudes. The GCMs compute a warmer atmospheric condition, causing more humidity in the atmosphere which probably leads to increased rainfall events over the Iberian Peninsula. However, this does not have to be true as there are still ongoing studies on this topic but such an interaction is a possible outcome of the expansion of the Hadley cell northwards due to changing air temperatures (Wentz et al. 2007; Goosse 2015). The RCMs do not show this influence which indicates that a reduction with emergent constraints based only on the outcome of the GCMs is not feasible.

For France, British Isles, Central Europe, and the Alps the ensemble behavior is fairly similar over those four PRUDENCE regions. The GCMs, over all of them, indicate an increase in CCS with a reduction in Mrso trend while the RCMs are totally unrelated except France. A significant relationship cannot be confirmed between CCS and Mrso over these four regions although it is close over the British Isles with a  $R^2$  value of 0.295 for the GCMs.

Also, Scandinavia, the Mediterranean, and Eastern Europe are similar to each other. All three of them have in common that the two variables in Fig. 5.10 have absolutely no significant relationship to each other. Therefore, there is no statistical evidence for a significant value regarding the  $R^2$  values over the eight PRUDENCE regions with this set of variables. Further, not even the assumed physical relationship can be confirmed. To sum it up, there is no evidence that a reduction of uncertainties can be obtained with the Mrso trend values.

## 5.2 Uncertainty reduction through constraints

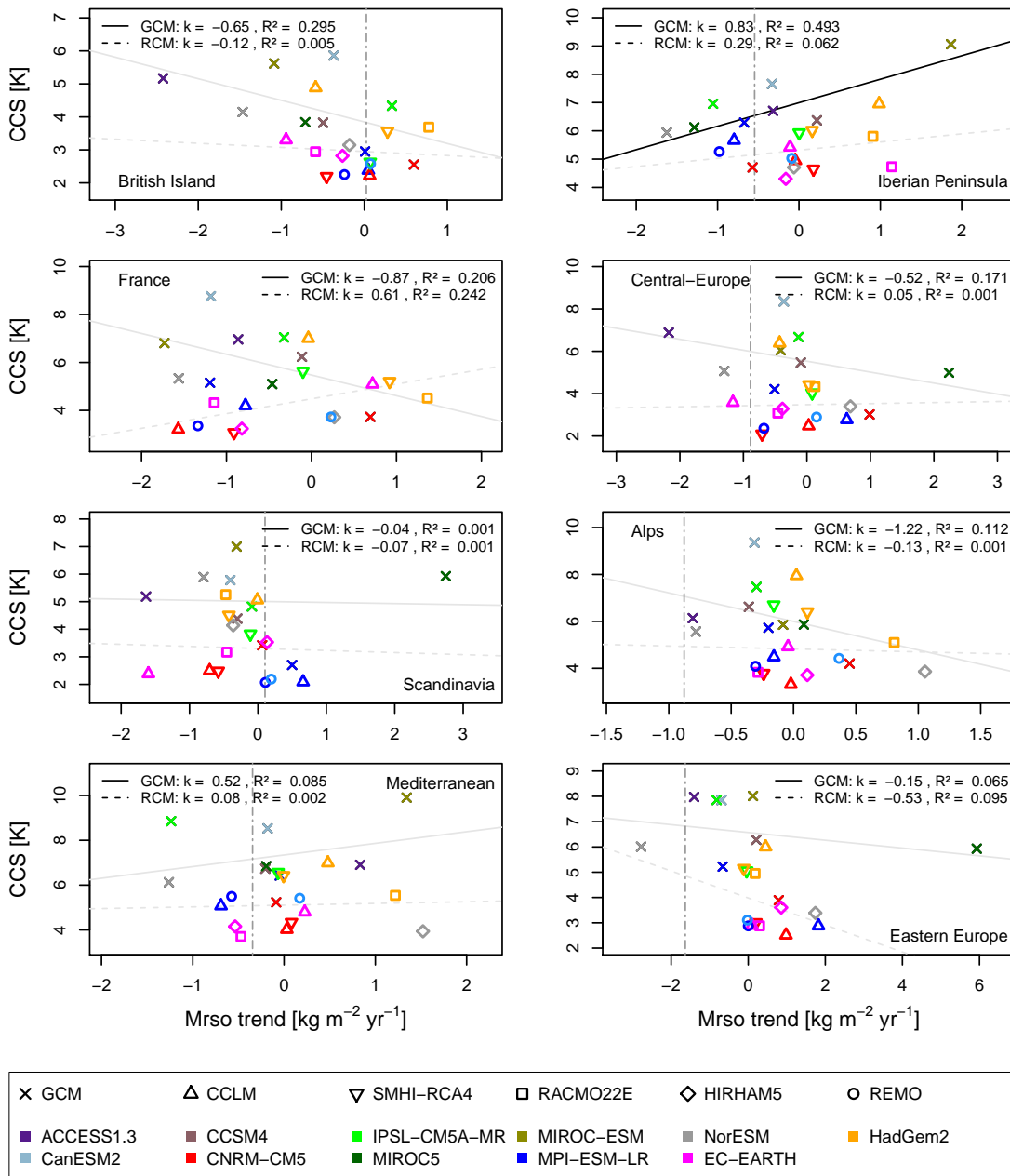


Fig. 5.10 CCS plotted against the Mrso trend. Besides the Tmax trends, the Mrso trends from 1979 to 2005 can also be used for reducing uncertainty. Again, the ERA-Interim values are represented by a vertical gray dashed line while significant correlations are illustrated in black lines. If the relationship is not significant, a light gray line is drawn.

### 5.2.3 Interannual variability by variances

Besides mean and trend statements, variances can also provide valuable statistical information about climate conditions. The variance is the mean square deviation of the results around their mean and therefore describes the spread of a variable. For the thesis, this can be an indicator of seasonal based Tmax or Mrso fluctuations which also provide information about the interannual variations (Kayano and Sansígolo 2009; Michaels et al. 1998). Same way as with other evaluations, first the variance is calculated on a monthly basis and after that, the average for JJA gets determined. Due to that, models with a higher variance can indicate a dryer soil that leads to higher Tmax values and perhaps a higher CCS. Usually, the JJA is dryer than other seasons and an additional drying of the soil should amplify the process further due to the lack of evaporative cooling.

Following this line of reasoning, a positive regression line between Mrso variance and CCS should exist. A dehydration of the soil results in a higher Tmax. In advance, Fig. 5.11 do not show any agreement with the theory above in any of the eight PRUDENCE regions except the two southern regions, the Iberian Peninsula and the Mediterranean. This indicates that there is a change in the southern circulation patterns that have local effects as otherwise more northern regions also are affected. A change in the Hadley cell due to higher air temperatures can cause this significant relationship between Mrso variance and CCS because this results in altered rainfall events and therefore a greater Mrso variance. However, only the GCMs indicate this correlation. None of the other six PRUDENCE regions indicate a connection between the two variables. As a result, under the consideration of the dehydration theory, a reduction of uncertainty with regard to the Mrso variance and the CCS is not feasible. The argument that there cannot be a relevant change in the basic data due to the coarse temporal resolution which results already in a dehydration at the beginning of summer is only partially correct. The variance was first calculated for each month and then the summer mean over each region. This would imply that during the entire investigation period there was no appreciable change of the Mrso by e.g. precipitation events which would have increased the Mrso. As a result of higher Mrso, the Tmax would have decreased and therefore also changes the CCS. But according to the data, one does not see anything of these.

Not only the Mrso variance can provide information for an emergent constraint setting, also Tmax variances can be useful for uncertainty related issues. But the results should be evaluated carefully because an increase in variance does not automatically mean a huge increase in temperature. Variances can reveal information about interannual variabilities but for instance, the temperature can drop in JJA due to heavy rainfalls or cold snaps which in return increase the Tmax variance although the maximum value of temperature itself does not change significantly. However, within the 27-year refer-

## 5.2 Uncertainty reduction through constraints

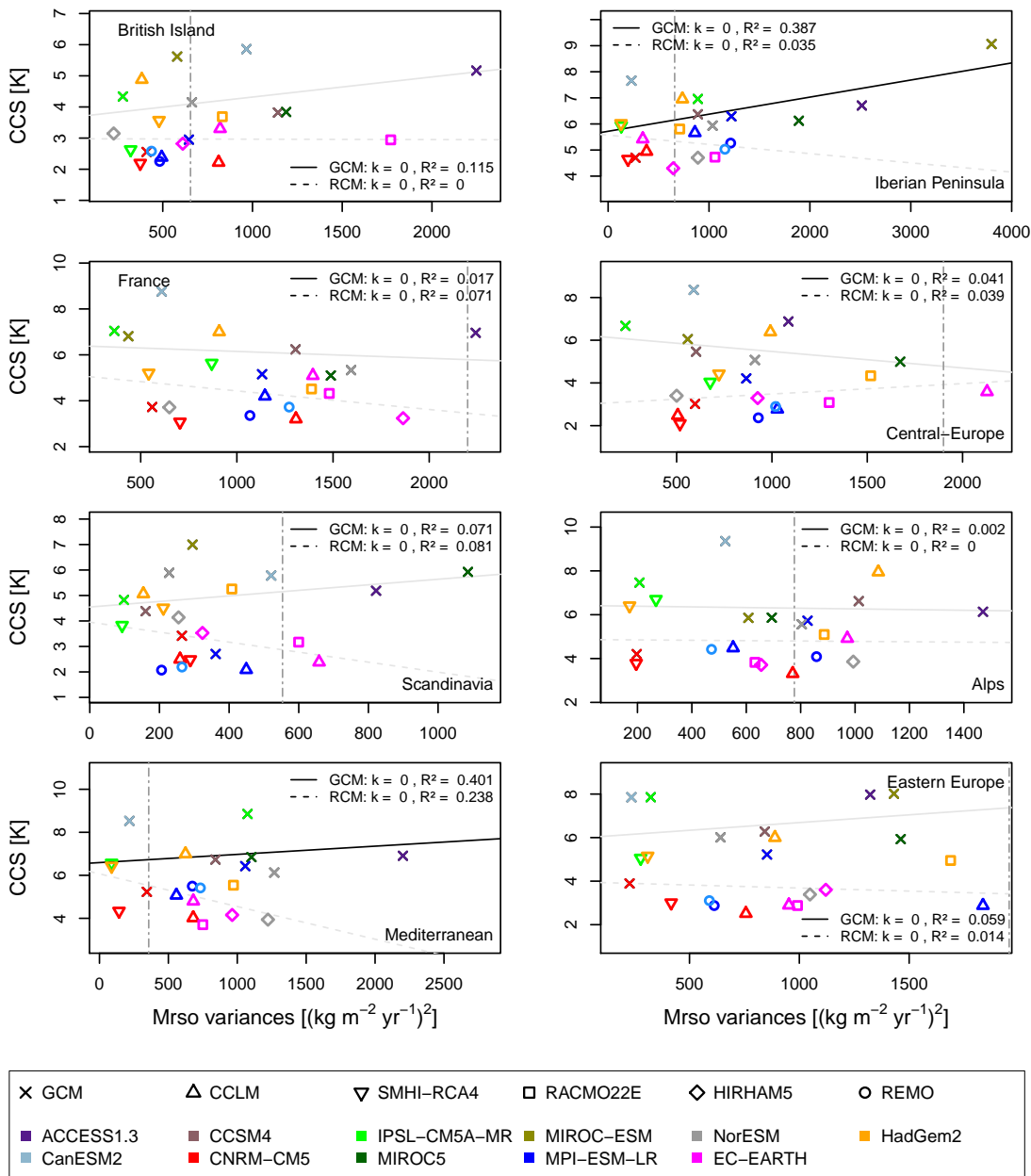


Fig. 5.11 Attempt to reduce uncertainty with variance values of Mrso. CCS is plotted against the interannual variability represented by the Mrso variance from the period 1979 to 2005 to get information about a possible uncertainty reduction (ERA-Interim trend is the vertical gray dashed line, the correlations are black with a solid line for the GCMs and a dashed line for the RCMs).

ence period of investigation between 1997 and 2005, the global mean temperature has increased (Hartmann et al. 2013). This may indicate that a general increase in variance results in an increase in Tmax. The relationship between Tmax variance and CCS for the PRUDENCE regions under this perspective can be seen in Fig. 5.12. In general, all regions show a positive correlation between these two variables with the exception of the GCMs in the Mediterranean.

It seems that all Central European regions that have a mountainous region show a significant relationship like France, the Alps, and Eastern Europe. Fig. 5.12 shows that especially the RCMs in these regions tend to have a more or less significant correlation with  $R^2$  above 0.150. This can be explained by the fact that the RCMs compute the complex orography more explicit, that leads to stronger fluctuations of the temperature. Both northern regions show a completely different behavior that indicates a significant relationship between CCS and Tmax trend by the RCMs over the British Isles while Scandinavia does not signal such a connection at all. This can be explained by the summer droughts over the British Isles, which occur alternately and increase the temperature, whereas Scandinavia is relatively consistent over the whole 27 year period. The two southern regions, the Mediterranean and the Iberian Peninsula, do not indicate a significant relationship, but there are differences between them. This may, as already mentioned above, be due to the extent of the Hadley cell which changes air flows and circulation patterns. Based on the results of this variable combination, a reduction of uncertainty is difficult to perform because just half of the regions show a significant relationship through at least one of the two model types. It is difficult to give a general statement although all results over the regions match the observation.

## 5.2 Uncertainty reduction through constraints

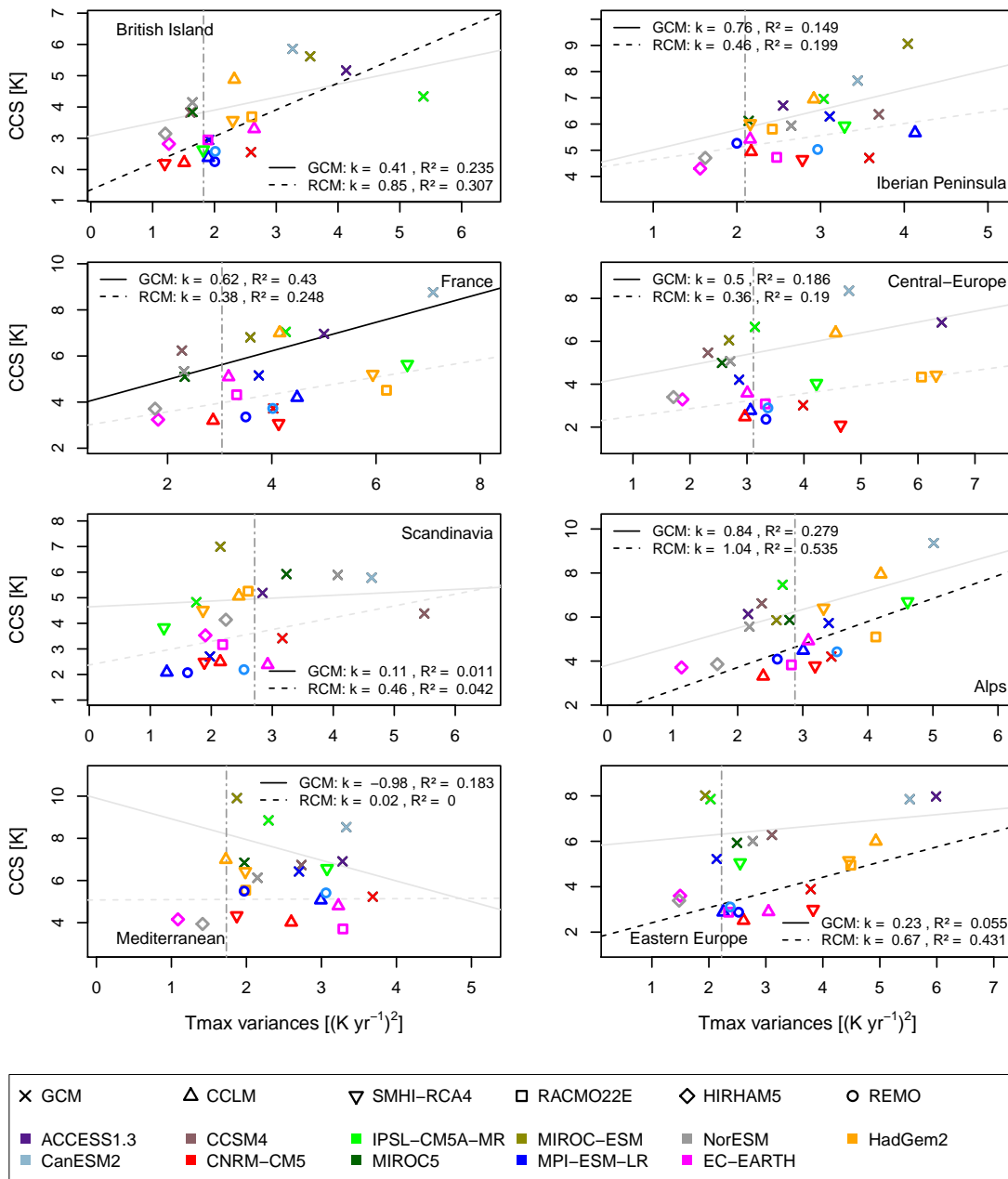


Fig. 5.12 CCS plotted against the Tmax variance from 1979 to 2005. The correlation between these two variables could possibly be used to reduce uncertainties, as there are some significant relationships (correlation between the two variables are shown in black lines). Although not all PRUDENCE regions have this correlation. Looking additionally at both model types together, the result differ within each region. Observations are represented with a vertical gray dashed line.

In summary, it can be said that projections from climate models have a rather large spread in terms of temperature, precipitation and other variables due to uncertainties. For this reason, emergent constraints are used for reducing these uncertainties with the help of a predictor-predictand relationship. The idea is based on the assumption that a physical connection exists between the present data, which are constraint by observations and long-term climate variables. The two aspects are connected with a linear regression approach. Thus, a possible relationship between them can help to reduce uncertainties for the projected values due to the fact that a certain spread of the projection is physically unlikely and can therefore be restricted. So, Tmax trends can probably be used for this purpose. In most regions, the regression line shows a significant result between the Tmax trend and the CCS with high coefficients of determination for both model types. However, one has to be careful because the ensemble values do not always match with the observations. Also, the Tmax variance represent in some regions a relationship with the CCS whereas in other regions they do not. Especially, RCMs in mountainous regions indicate a connection between the two variables. When it comes to Mrso trend and variance an additional benefit is hard to find. In case of the trend, the GCMs fit better with the theory than the RCMs, however, overall an approach for an uncertainty reduction is not possible. The same argument can be made for Mrso variance, thus, there is no strong evidence which could clearly assure a relationship with the CCS.



### 5.3 Soil moisture-air temperature feedback strength

A feedback is a mechanism between two or more variables where an initial process results in a change of a second process, that in turn influences the first one again. In general, this will lead to a non-linear response that can amplify or diminish the forcing that started the cause-and-effect chain reaction (Cubasch et al. 2013). As already mentioned the soil moisture-air temperature coupling is one of these feedback loops. Due to the fact that it is an important element within the climate system, not only the reaction itself but also the strength of it will be investigated in this Section. Therefore a standardized method is needed. Thus, the first part within this Section explains the approach which is used for detecting a feedback strength. The second part shows the interaction between the feedback strength and related quantities of the soil moisture-air temperature coupling mechanism.

Mrso and Tmax are linked together by evaporative processes. The interaction of these variables can be higher for certain events like heatwave or extreme rainfall. In the summer season, it is possible that the atmospheric demand for water is too big which can lead to a decrease in evaporation due to a lack of available moisture in the soil. Consequently, the result is an increase in Tmax that leads to a further demand for water (Miralles et al. 2012). Such processes have a significant impact within the climate system and can help to explain some changes in projections for summer events as Seneviratne et al. (2006b) showed. But not only the possible changes are relevant, also the strength of the feedback matters. In the case of soil moisture-air temperature coupling, however, the traditional diagnostic tools just indicate if there is a feedback or not, but they do not determine its strength. Because each climate model has its own degree of implementation when it comes to computing the land-atmosphere coupling. Which means that they calculate the same output but with different approaches. Therefore, a consistency does not exist over the whole ensemble (Miralles et al. 2012). Besides that, results of soil moisture changes cannot be validated due to the lack of field measurements and their uncertainty (Seneviratne et al. 2010).

A possible approach can be a workaround with the implementation of meteorological data as a replacement for missing or uncertain Mrso values. This allows an analysis of climatological conditions by explaining the interaction of soil moisture-air temperature coupling. Continuous data with a large spatial coverage and interaction with air temperature and soil moisture are needed. Some variables which satisfy these requirements are the surface net radiation and the evapotranspiration. Miralles et al. (2012) used those variables within equation 5.2 to calculate the strength of the land-atmosphere coupling for several days for the heatwave 2003 in Western Europe. The same approach is also applicable to long-term climatic analysis. In this thesis, the feedback metric  $\Pi$  is used to calculate the soil moisture-air temperature strength for the European subregions.

Mainly for the period 1979 to 2005. Thus, equation 5.2 describes the difference between two Pearson correlation coefficients ( $\rho$ ), which include the variables near-surface air temperature ( $T_{mean}$ ), evapotranspiration ( $Evap$ ), surface net radiation ( $Rn$ ) and potential evapotranspiration ( $PET$ ). With the definition of  $H' = Rn - \lambda * Evap$  and  $H'_p = Rn - \lambda * PET$  where  $\lambda$  describes the latent heat of vaporization, it comes to,

$$\Pi = \rho(H', T_{mean}) - \rho(H'_p, T_{mean}), \quad (5.2)$$

where  $T_{mean}$  is in  $K$ , and both  $H'$  and  $H'_p$  are in  $W/m^2$ . This approach originates from the PET estimation from Priestley and Taylor (1972). However, according to Miralles et al. (2012) the ground heat flux is not taken into account due to comparatively small values which is a modification of the Priestley-Taylor (PT) equation. Under the assumption that  $\sigma_H, \sigma_{H_p}$  and  $\sigma_{T_{mean}}$  are the standard deviations of  $H, H_p$  and  $T_{mean}$ , equation 5.2 can also be written as 5.3 but in terms of covariances ( $cov$ ). Therefore 5.3 can be expressed as follows:

$$\Pi = \frac{1}{\sigma_{T_{mean}} \cdot \left( \frac{cov(H', T_{mean})}{\sigma_H} - \frac{cov(H'_p, T_{mean})}{\sigma_{H_p}} \right)}. \quad (5.3)$$

A positive value of  $\Pi$  indicates that the lack of  $Mrso$  in combination with the surface energy distribution can explain a larger fraction of air temperature variability in an area. Although, many different methods for the calculation of PET exists (Miralles et al. 2012). For instance Ward and Robinson (2000) contains a small listing with:

- the Penman-Monteith formula.
- the Blainey-Criddle formula.
- the Turc equation.
- the Thornthwaite formula.
- the Priestley-Taylor equation.

Throughout the thesis, the feedback strength is calculated with the monthly based Blaney-Criddle formula. To show that the method reaches reasonable results with a minimum of required data, the results for four randomly selected climate models are listed in a comparative way in Fig. 5.14 with results from the daily based Priestley-Taylor equation. Before that, however, both methods are discussed below in more detail.

### Blaney-Criddle equation

Alongside precipitation and runoff, Evap is one of the most important variables in the hydrological cycle. It is relatively expensive and time-consuming to measure either the evapotranspiration itself or at least the demanded water for particular areas which represents some backup information for further researches. Especially, in regions where irrigation and water shortages are part of the day-to-day business. For this reason, certain formulas like the Blaney-Criddle (BC) equation are used to estimate and provide possible Evap data. These values serve as a basis for considerations about the hydrological cycle as well as water requirement information for cultivation crops and other plants. However, this equation can also be used for other question due to the fact that the PET can be calculated with very few variables. For instance, the BC method is based on two climate elements which are temperature and solar radiation. Even if measurements of daily sunshine hours over a large area are rare, the influence of solar radiation on PET is stronger than precipitation for example. Therefore the formula depends on air temperature and the mean solar radiation within a month in a specific geographical latitude as seen below:

$$PET = p \cdot (0.457 \cdot T_{mean} + 8.128). \quad (5.4)$$

Where  $p$  represents the mean daily percentage of annual daytime. This value is dependent on the geographical latitude and a specific month due to the position of the sun. The resulting values from that approach are depicted in Fig. 5.13, whereas the values above  $30^\circ$  latitude are interesting for the PRUDENCE regions according to table 5.1. The two numerical parameters 0.457 and 8.128 are empirical values which are applicable for all relevant latitudes. Originally, the BC equation was used for crop cultivations in the United States of America. But due to the simplicity and quite good results that the formula provides, it is used worldwide within governmental matters (Blaney and Criddle 1964).

### Priestley-Taylor equation (Pt)

Most daily based Evap equations require detailed meteorological and plant-specific data. For example, the Penman and the developed Penman-Monteith equation needs next to this data also detailed water flow knowledge or the mean stomata resistance of the plant stock within the area of interest. This would make the use of the method over all PRUDENCE regions virtually impossible. For this reason, Priestley and Taylor (1972) suggest a less time and data consuming method. The PT method is based on the Penman equation and is important where no detailed meteorological data are available. This equation is able to calculate the Evap even under circumstances where a lack

Latitude	North	Jan	Feb	Mar	Apr	May	June	July	Aug	Sept	Oct	Nov	Dec
	South	July	Aug	Sept	Oct	Nov	Dec	Jan	Feb	Mar	Apr	May	June
60°		.15	.20	.26	.32	.38	.41	.40	.34	.28	.22	.17	.13
55		.17	.21	.26	.32	.36	.39	.38	.33	.28	.23	.18	.16
50		.19	.23	.27	.31	.34	.36	.35	.32	.28	.24	.20	.18
45		.20	.23	.27	.30	.34	.35	.34	.32	.28	.24	.21	.20
40		.22	.24	.27	.30	.32	.34	.33	.31	.28	.25	.22	.21
35		.23	.25	.27	.29	.31	.32	.32	.30	.28	.25	.23	.22
30		.24	.25	.27	.29	.31	.32	.31	.30	.28	.26	.24	.23
25		.24	.26	.27	.29	.30	.31	.31	.29	.28	.26	.25	.24
20		.25	.26	.27	.28	.29	.30	.30	.29	.28	.26	.25	.25
15		.26	.26	.27	.28	.29	.29	.29	.28	.28	.27	.26	.25
10		.26	.27	.27	.28	.28	.29	.29	.28	.28	.27	.26	.26
5		.27	.27	.27	.28	.28	.28	.28	.28	.28	.27	.27	.27
0		.27	.27	.27	.27	.27	.27	.27	.27	.27	.27	.27	.27

Fig. 5.13 Global seasonal insolation of the sun. Depending on the orbital constellation Earth - Sun, the solar radiation changes according to season and latitude. The values above 30° latitude are meaningful for the PRUDENCE regions. From Blaney and Criddle (1964) and Brouwer and Heibloem (1997).

of soil water supply is a limiting factor. This is possible because the method for the calculation is based on the PET. This implies that the required meteorological elements can be provided by measurements or climate models. Including, for instance, the net solar radiation, air temperature, and surface pressure data (Flint and Childs 1991). According to Priestley and Taylor (1972) the dominant factor have to be the radiant energy terms for a specific surface area. To calculate the PET with the PT equation, Mcnaughton and Spriggs (1989) suggests the following version of the equation:

$$PET = \frac{1}{\lambda} \frac{s(R_n - G)}{s + \gamma} a. \quad (5.5)$$

Equation 5.5 includes the slope of the saturated vapor pressure  $s$ . Further, the surface net radiation  $R_n$ , the latent heat of vaporization  $\lambda$  and the soil heat flux  $G$  is needed. As already mentioned, according to Miralles et al. (2012) the soil heat flux  $G$  can be omitted. However, the PT method contains also the psychrometric constant  $\gamma$  and the Priestley-Taylor coefficient  $a$  (Flint and Childs 1991). The coefficient  $a$  itself is an empirical value with the best fitting value of 1.26 which has been found throughout several different sources (Mcnaughton and Spriggs 1989).

### 5.3.1 Different strength approaches

Values based on the BC equation generally overestimate the feedback strength a little compared to the PT approach. The results between the two methods in which the BC values are subtracted from the PT values for each European region is shown in Fig. 5.14. All four shown models, two GCMs and two RCMs, are selected randomly from the model ensemble. The results for both methods are calculated with the feedback equation 5.2 over the entire 27-year period (1979 to 2005) for each month separately. Afterward, the average is determined over three months (June, July, and August) to get the JJA mean. The difference between the two methods is the amount of data which are included in this procedure. The calculations after BC need one value from each required variable for each year. In comparison, the PT equation is a daily based method which requires 30 to 31 values from every variable within each selected month in one year. The total amount, therefore, is 2484 values from every variable for the whole 27-year period for each European region. For Fig. 5.14, the subtraction of the feedback strength between the two methods take place before the summer season mean gets calculated.

The first thing to be noticed is that the four selected models show almost the same behavior over all eight PRUDENCE regions. The only exceptions are the British Isles and the Iberian Peninsula. Here, the feedback strength between the two methods is almost the same for the *CNRM-CM5* as shown by Fig. 5.14 which is surprising because this model shows a high deviation in the remaining six regions. Together with the *HadGEM2.CCLM*, both models show a big difference between the two approaches with a deviation of  $\Pi$  -1.0. In comparison, the *MPI.CCLM* which shows overall the best result between the two approaches with a deviation range of -0.09 to -0.52 shows a big spread in the Iberian Peninsula. In the other regions, the model does not show such a big spread between the two feedback strength approaches. The last model is the *MPI-ESM-LR* which has a remarkable result in the Alps and Eastern Europe. These are the only two values with a positive  $\Pi$  value. That implies, that the feedback strength results with the daily based PT approach are higher than the BC results. For the other six regions, the metric differences of this model are negative. In fact, the BC approach shows a consistently different behavior than the PT approach where pretty much every model has the same deviation in the same direction. Therefore, if applied over the whole ensemble, the approach should still be viable because every model is equally affected.

The feedback strength describes the atmospheric demand for water over e.g. the European regions. Therefore it is not surprising, that the behavior of each climate model in terms of feedback strength differ from each other. In Fig. 5.15 the metric covariance as described in Equation 5.3 is shown for each model in comparison with the feedback strength from ERA-Interim. The feedback strength of the models are very close to the ERA-Interim data over the British Isles. Both model types are partially over- or

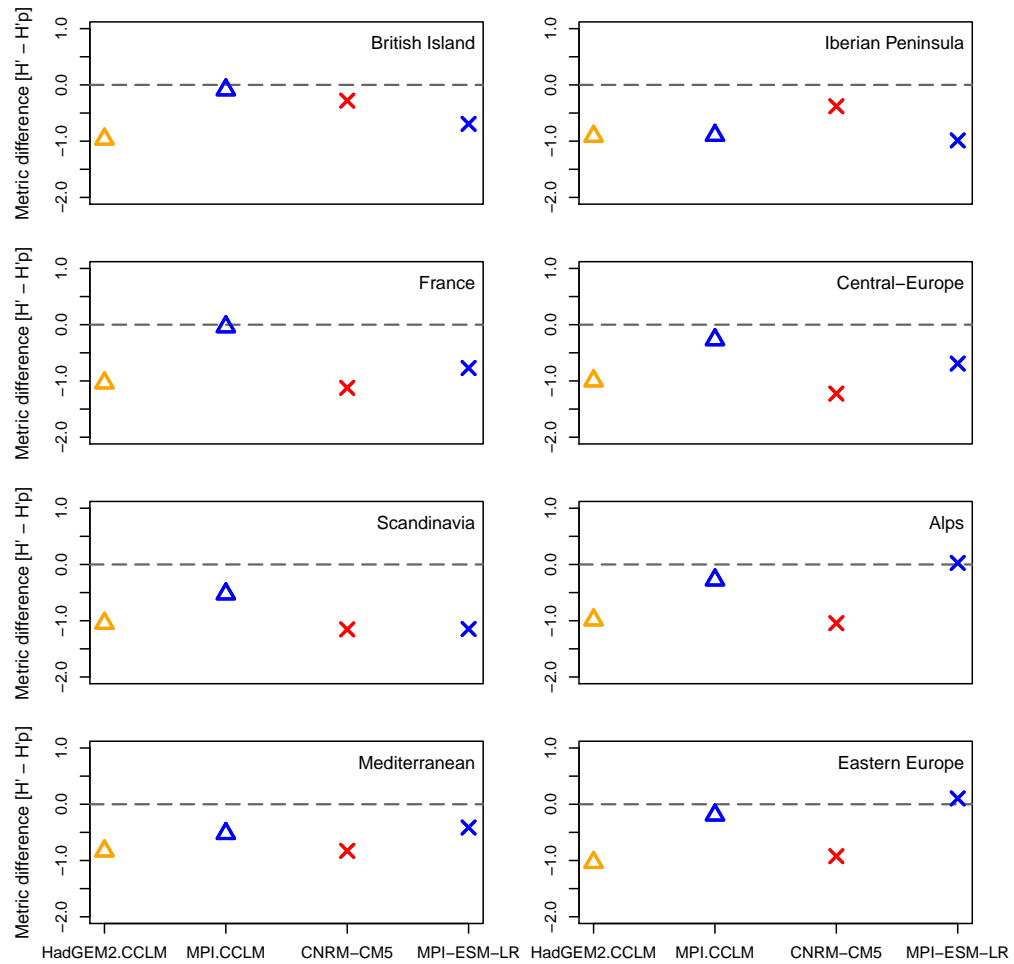


Fig. 5.14 Comparison of two different evapotranspiration methods with the same coupling method. A few randomly drawn climate models calculate the feedback strength by using two different methods for the Evap to determine a possible distinction between them. Shown is the subtraction of the metric results in which the simpler Blaney-Criddle method was subtracted from the more complicated Priestley-Taylor method. The data for this comparison are from the period 1979 to 2005.

underestimating the observational data but the entirety of all models are matching the ERA-Interim feedback value quite well. Over Scandinavia, the situation is quite similar because the majority of the models are very close to the feedback strength value of ERA-Interim. Only two models are further away with a maximum difference of 1.66. Thus, the entire model ensemble shows a relatively good match whereby individual outliers can be caused by uncertainties.

In France and Central Europe, the situation is fairly similar to each other. In both regions are one-third of the GCMs under- or overestimating ERA-Interim. As for the RCMs two-thirds of all models are overestimating and one-third is underestimating the ERA-Interim value. In both regions, each individual model behavior is the same, only the feedback values are stronger. That implies that each model is either over- or underestimating the strength in both cases in the same direction. However, it should be mentioned that the ensemble mean (not shown) in both regions, despite some outliers, are near the ERA-Interim value.

For the Iberian Peninsula and the Alps, an overestimation of the feedback strength from the RCMs is recognizable. Some models are near the ERA-Interim value, however, most of them are clearly overestimating it in these two regions. It is striking, though, that not a single RCM is underestimating the feedback strength compared to ERA-Interim. In addition, it is noteworthy that the feedback strength in the Iberian Peninsula is about three times as high as in all other regions except the Mediterranean. The consequences of such a strong coupling can be, that a small change in  $T_{max}$  or  $M_{rso}$  have a huge impact due to the self-reinforcing effect of the feedback. Depending on the direction in which the feedback is working, some of the RCMs may experience excessive dehydration or too little air temperature warming due to changes in the surface heat flux. This implies, that the impacts can be massive in terms of climate projections because the soil moisture-air temperature coupling re-affects itself even further and a strong coupling can lead to particularly strong changes since the region reacts very sensitively to the respective influencing variable. The GCMs, on the other hand, gather relatively well with minor deviations around the ERA-Interim value, which can be an effect of the model resolution.

Besides the last two mentioned regions also the Mediterranean and Eastern Europe show a similar behavior. The only difference is, that not only the majority of the RCMs, also at least half of the GCMs are also overestimating the feedback strength. Therefore, the total model ensemble describes an overestimation. As already mentioned above, the feedback value in the Mediterranean is relatively high compared to other European regions. It follows that a small change of one variable is sufficient enough to change the environment in this area due to the sensitivity of the coupling. So both southern regions have a high feedback value. This contributes to the fact that the Mediterranean, as well as the Iberian Peninsula, tend to dehydration and the occurrence of drought events in JJA. In general, an overestimation of the feedback strength over certain PRUDENCE regions cannot be dismissed even if there are few models which are near to ERA-Interim.

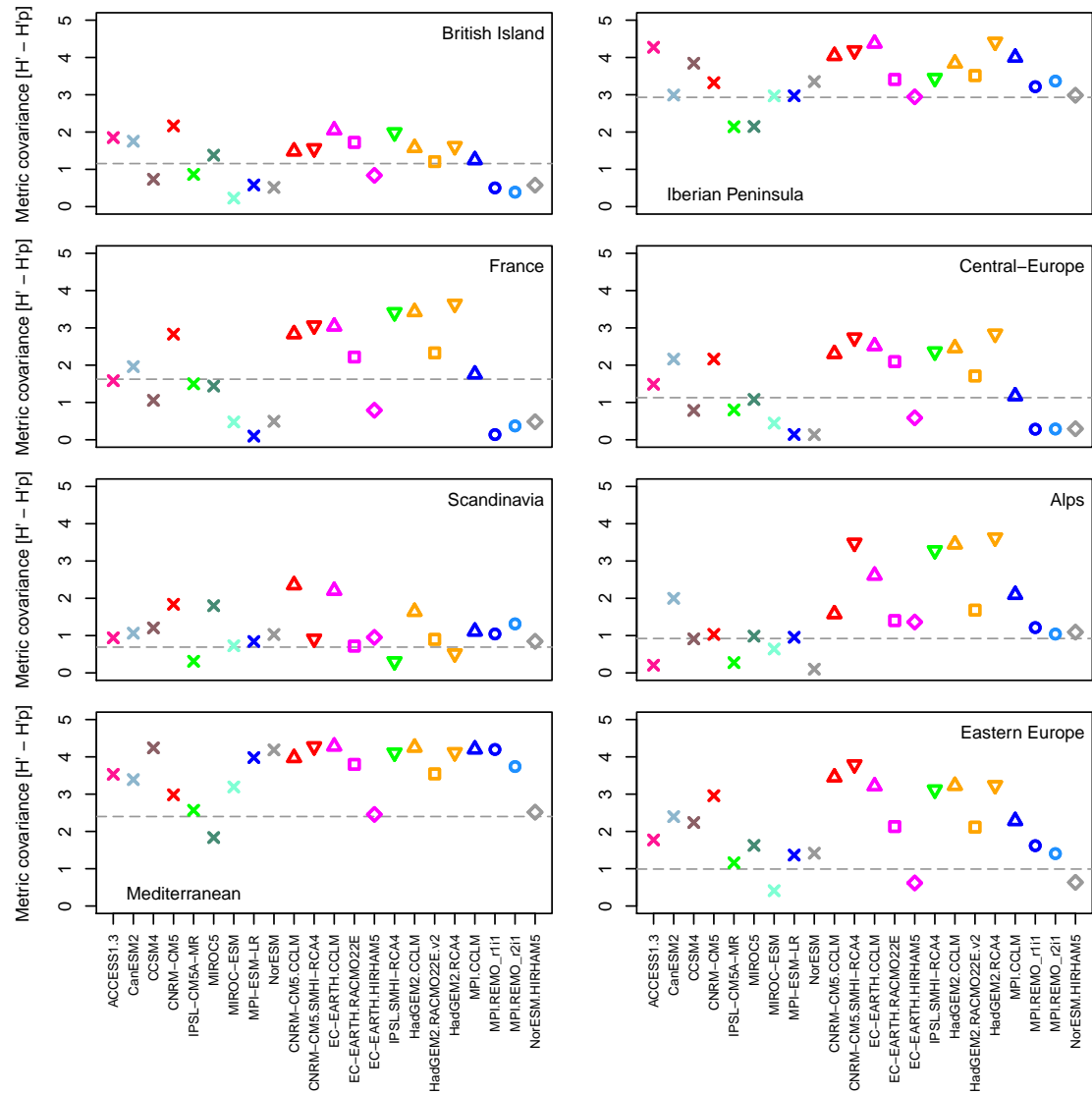


Fig. 5.15 Feedback strength in GCM and RCM compared to ERA-Interim data in JJA from 1979 to 2005. It is noteworthy, that the RCM values are relatively far away from ERA-Interim over the Alps and the Mediterranean region.



Considering  $Mr_{so}$  as a function of coupling strength, information about dehydration should be recognizable. Because a low feedback value implies that the soil is able to meet the water demand of the atmosphere. On the other hand, if  $Mr_{so}$  is not able to fulfill the demand of the atmosphere than high strength values indicate a dry climate condition. Therefore a high feedback strength in combination with high  $T_{max}$  or low  $Mr_{so}$  values are indicators that the local energy balance has a strong influence on local air temperature (Miralles et al. 2012).

Fig. 5.16 depicts the relationship between the  $Mr_{so}$  trend and the feedback strength for each region. It is noticeable that there is just one significant relationship over all eight regions. It seems like that the GCMs over Scandinavia represent a coupling process in which the  $Mr_{so}$  amount leads to a lower  $T_{max}$  and in turn again to a moister soil, whereas RCMs indicate no or the opposite effect. Thus, the  $Mr_{so}$  trends from the GCMs are higher than the atmospheric demand. This implies, due to the self-reinforcement of the feedback, lower  $T_{max}$  and at the same time as a consequence, higher  $Mr_{so}$  values. For all other PRUDENCE regions, there is no clear indication for a relationship between the two plotted variables in Fig. 5.16. Neither is a statement possible to classify which one of the two model types is closer to the truth because no coefficient value represents a level with a clear indication. The highest  $R^2$  are close to 0.1 which is too low for an evidence of a relationship. Also, the consideration over the whole model ensemble gives no further information.

## 5 Results and Discussion

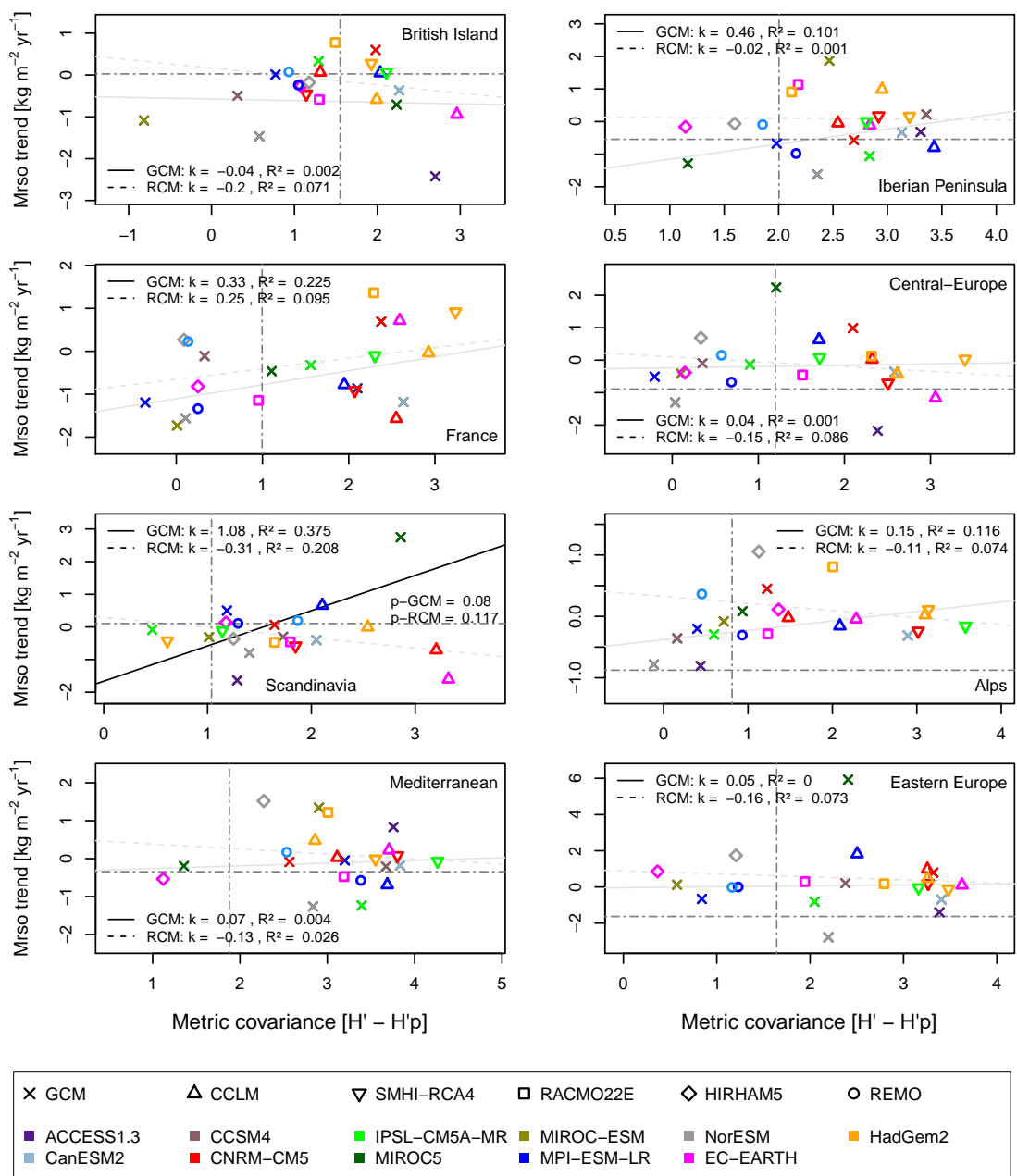


Fig. 5.16 Relationship between feedback strength and Mrso trend. There is no significant relationship within the PRUDENCE regions between these two variables. The ERA-Interim data from 1979 to 2005 are represented as gray dashed lines for comparison while the correlations are shown as black lines.

Based on the idea of Miralles et al. (2012), a strong soil moisture-air temperature coupling is detectable by a positive linear connection between the feedback strength and high Tmax values. The relationship between these two variables is shown in Fig. 5.17. As for the British Isles, the GCMs show no significant connection between the feedback strength and the Tmax trend, whereas the RCMs depict a result that is closer to the theory above. This implies that there is evidence that the coupling strength and Tmax are positively connected with each other. As a result of these, high Tmax values are reinforcing themselves through the soil moisture-air temperature coupling or cooling itself down within the RCMs. This would not be so far off because the British Isles experienced a few summer droughts within the last century according to Marsh et al. (2007). In comparison to that, the regions Scandinavia and the Mediterranean are further away from a meaningful feedback strength-air temperature connection. Because the significance of the relationship cannot confirm the feedback hypothesis. Basically, none of the indicators from both model types in these two regions are significant. Same results can be obtained by considering the total ensemble because there is no evidence for a relationship in these regions between Tmax and the feedback metric. As for Scandinavia, the non-significant result is not really astonishing since there are other influences which probably contribute more to the climate condition like precipitation than just the feedback alone in JJA (Schönwiese 2003). For the Mediterranean region, it is a surprise, considering the dry, hot summers with a lot of sunshine in the Mediterranean climate (Schönwiese 2003). One can, therefore, assume that there should be a connection between the mentioned variables but it does not exist. Similar cases arise in the Iberian Peninsula and France. There is no evidence for a significant relationship between the feedback strength and the Tmax trend within these two regions.

The interesting regions in this particular context are Central Europe, the Alps, and Eastern Europe and these although the GCMs do not show any significant relations. Despite that, the RCMs show a different behavior. In all three regions, the value of  $R^2$  is rather high and all of them have a significant relationship between Tmax and the feedback metric II. The highest coefficient value even achieves a value above 0.600. Overall, there are some regions where the local energy balance has an influence on the Tmax value. But it does not affect those areas with the highest feedback strength value. It turns out that especially those areas are affected that are located in the central parts of Europe. An interesting point is added, that these connections can only be seen in conjunction with the RCMs.

## 5 Results and Discussion

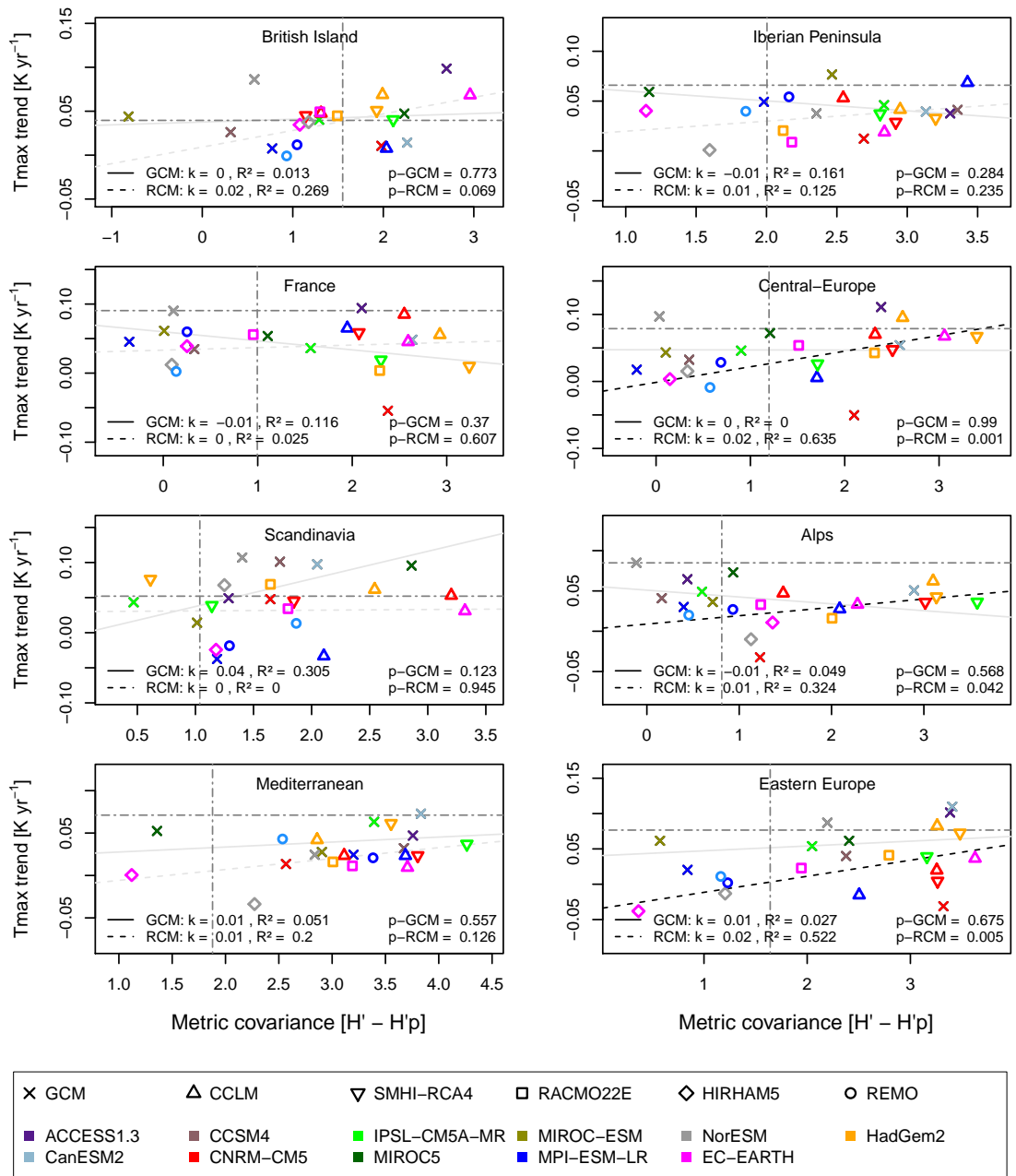


Fig. 5.17 Tmax trend plotted against the feedback strength. Within some PRUDENCE regions the RCM show a significant correlation (black dashed line) between those two variables while there is no indication for the GCMs (light gray solid line). The two observational data are represented with gray dashed lines.

The influence of a feedback does not determine the direction of a system, it only amplifies or balances the original orientation. Due to this reason, a system can tip over and escalate as well as returning to a resting state. But the stronger the feedback, the stronger the influence on a system can be and therefore, bigger fluctuations within a system can happen (Cubasch et al. 2013). The following pages are focusing mainly on the relationship between the variance of Tmax and Mrso to the feedback strength because the variance detects such fluctuation and therefore the interannual variations as Kayano and Sansígolo (2009) pointed out. For example, the variance increases greatly when a region is normally moist, and a sudden dry period occurs. Or the reverse case occurs where a region is dry and a rainy summer takes place. Both cases can be the result of the feedback effect because often only small changes are sufficient enough to trigger a whole chain reaction or self-amplification. Therefore, considering the variance, one can assume that the range of values is most likely higher where a higher metric value exists. Because the change in Tmax and Mrso within a season can vary greatly, especially during summer because a succession of heavy thunderstorms as well as a dehydration event is possible. One of the first considerations is to check if mutual influence towards one of the variables exists. Thus, whether there is a connection respectively a dependency between the variance of Tmax and the strength of the feedback is depicted in Fig. 5.18.

The first noticeable point is, that both, the RCMs as well as the GCMs show a positive regression slope in all eight PRUDENCE regions. However, there are still differences between them in terms of significance. For instance, Scandinavia and the Iberian Peninsula are the only regions in this context where neither the RCMs nor the GCMs show a significant correlation.

Besides that, another group of regions which are more similar to each other than to all other regions are the British Isles, the Alps, and the Mediterranean. Over those three regions, at least one model type describes a significant relationship between Tmax and  $\Pi$ . Here, typically the RCMs are the ones which are indicating this representative connection, whereas the GCMs just have a striking correlation in the Alps. One possible explanation for the difference between the two southern regions, the Iberian Peninsula and the Mediterranean, could be their location. The Mediterranean is more maritime while the Iberian Peninsula is rather continental. Due to this fact, more precipitation events in the Mediterranean in summer occurs, which decreases the Tmax values while it remains relatively dry and stable in the continental areas, resulting in steady high temperatures. This could mean that the Iberian Peninsula is already so dry in JJA that it does not matter if a rain event occurs because the dehydration is so strong that not even the soil moisture-air temperature coupling can counteract against it.

Over the remaining three regions France, Central Europe and Eastern Europe the coefficient of determination is for both model types high and therefore, they are representing significant relationships. Especially Eastern Europe seems to be particularly dependent on the feedback mechanism in terms of atmospheric conditions.

So, overall it seems that there is a significant connection between the feedback strength and the Tmax variance, especially for RCMs. However, these results should be treated with caution. The metric for the feedback strength itself contains a temperature covariance according to Miralles et al. (2012). Therefore, there might be the chance that this influences the results to a certain extent. However, there is evidence that an increase in  $\Pi$  within the European regions leads to a rise in Tmax.

As for the connection between Mrso variance and the feedback strength, only two regions indicate a significant relationship (see Appendix: Fig. 6.1). The GCMs depict a strong positive relationship with a significant connection in Scandinavia, whereas the RCMs indicate the same signal in the Mediterranean region. For Scandinavia, this implies that the soil in this region tends to dry out and become humid again during rainfalls in summer. It makes sense due to the climate conditions and the orography since this region has relatively low Tmax compared to the rest of Europe and high precipitation values (Schönwiese 2003). But with additional information, that the RCMs do not show the same behavior in the least. Same goes for the Mediterranean, with the difference that the RCMs are representing a significant relationship instead of the GCMs. Since the Iberian Peninsula does not show any sign of a correlation between the two variables, it indicates again that this is possibly due to the fact that the Mediterranean is maritime and therefore frequent precipitation events occur that moisten the soil again and cooling down the air temperature in JJA.

### 5.3 Soil moisture-air temperature feedback strength

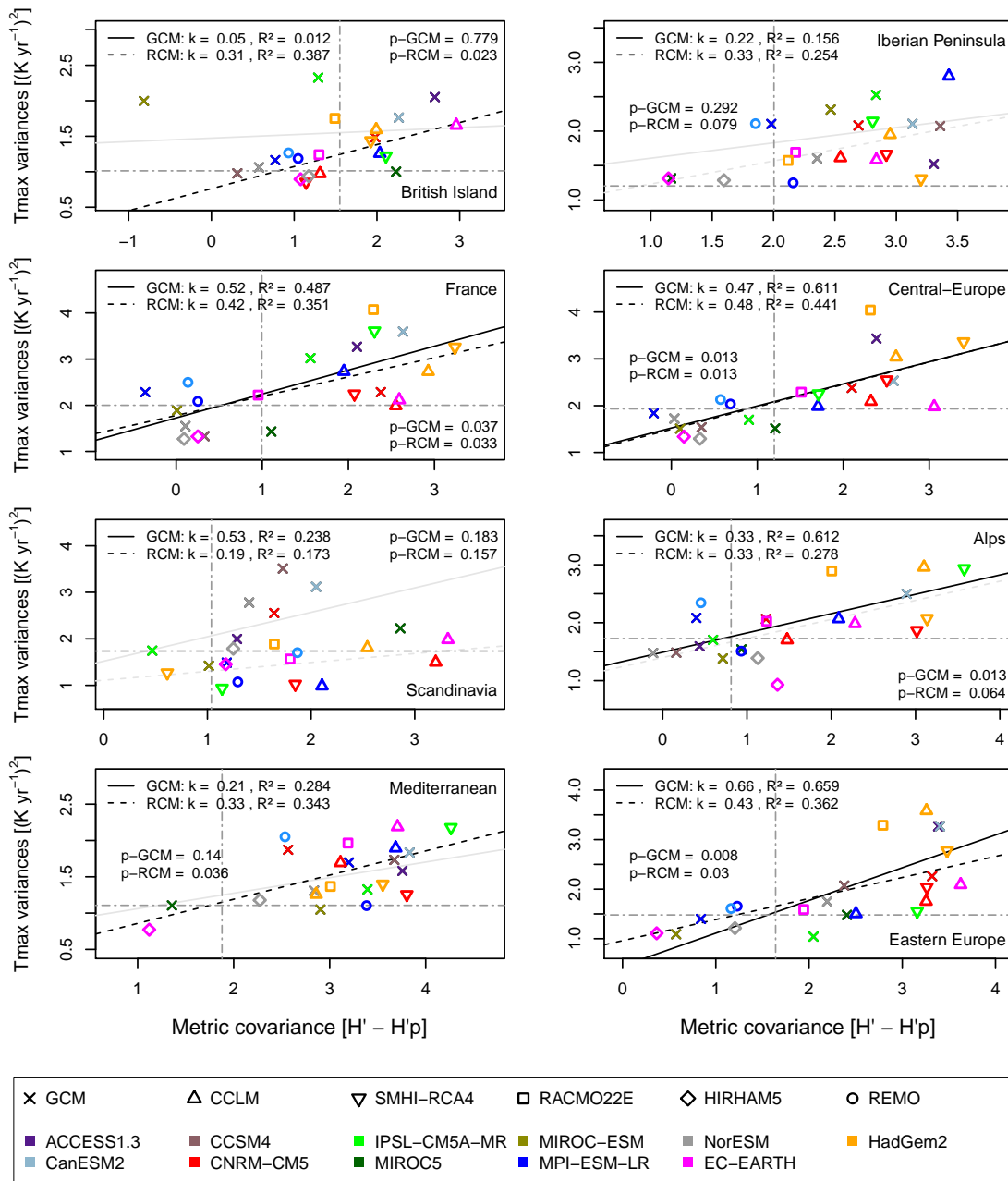


Fig. 5.18 Scatterplot between the Tmax variance and the feedback strength. A strong feedback should express a higher Tmax variance because the drying of the soil has an increase in air temperature as a consequence. In some regions the model data are a bit off the bench compared to the observations and ERA-Interim (gray dashed lines) over the period 1979 to 2005. However, the correlations (black lines) are often significant between these two variables.

### 5.3.2 Projected feedback strength

To get an idea of possible future feedback impacts on a particular system, a comparison between current and projected future variables can be a feasible approach. Therefore, to determine the change of the feedback strength is important. This, in turn, suggests shifts of the impact factors in a region for the future. For this purpose, the same metric approach from equation 5.3 for present values is used for the projected values of the ensemble models. This allows a comparison between consistent values which is depicted in Fig. 5.19. The projected values are those from the RCP8.5 runs of the period 2070 to 2099. It becomes clear that with the given projected values, the feedback strength is raised in all eight PRUDENCE regions. This applies to the whole model ensemble.

The only ambiguous case is Scandinavia where the models are close to the equilibrium line. As a consequence of the raising feedback strength, all current impacts from the coupling mechanism are additionally reinforced. Theoretically, there is a high chance that current processes which increase the air temperature or the cooling effect due to evapotranspiration in particular areas will increase further in the future. Whereas, areas, where the feedback influence has a much higher weighting than other factors in terms of changes, will receive the biggest impacts. So for instance, if the  $T_{max}$  increases much stronger than the evaporative cooling, then this will lead to a further increase in temperature due to the self-reinforcing effect of the feedback mechanism. So this basically means that within a domain two things can happen. First, in regions where the tipping point has been reached, the system leaves the equilibrium state and revolves till a new balance is found. This is the situation that would affect the environment the most. Or the second possible result, where only the predominant feedback impact within a region is reinforced, so the balance between the feedback variables will just shift a little bit because it is already at the final state. For example, the Iberian Peninsula is generally quite warm and an additional increase in  $T_{max}$  does not change the system completely. Same with Scandinavia where only the predominant system is reinforced or does not change at all as Fig. 5.19 shows.

But the situation is different for Central Europe and Eastern Europe. As Seneviratne et al. (2006a) mentioned, a possible northwards shift of the climate regimes in Europe will imply with great likelihood a stronger change in the soil moisture-air temperature coupling within these two regions. These two regions are also the ones that show the biggest change in Fig. 5.19. So an increase of  $T_{max}$  variability in JJA can be explained by a stronger soil moisture-air temperature coupling mechanism. Therefore, an increase in  $T_{max}$  can lead to a stronger drying of  $Mrso$  than within other regions. So there is a high chance that these two regions are experiencing the highest changes in Europe in the future. In addition, the current  $T_{max}$  and  $Mrso$  trends are plotted against the future feedback values as Fig. 6.2 and Fig. 6.3 in the Appendix depict. It shows that there is no significant relationship between the future feedback strength and the  $Mrso$  trend values in any PRUDENCE region. In comparison, the British Isles, Central Europe, the



### *5.3 Soil moisture-air temperature feedback strength*

---

Alps and Eastern Europe have a correlation between the future strength values and the Tmax trend but only with the RCMs. The GCMs do not indicate anything, thus, it shows that especially the whole Central European areas are particularly dependent on the location and the orography. Furthermore, the existence of a strong dependency with the soil moisture-air temperature feedback confirms the suspicion that these regions are very susceptible to future atmospheric changes.

## 5 Results and Discussion

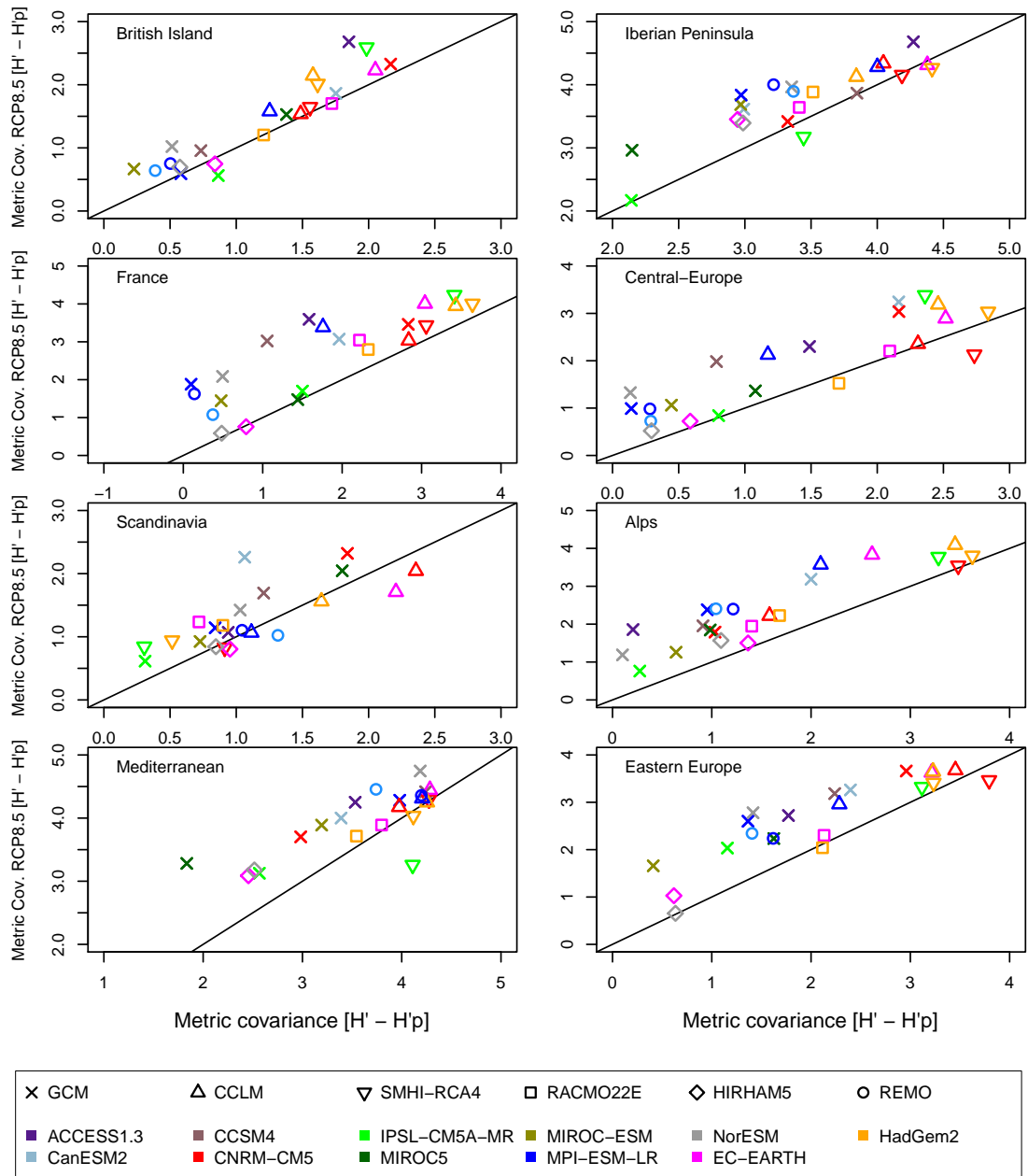


Fig. 5.19 An approach to estimate future feedback strengths. The feedback strength for the period 2070 to 2099 is calculated with the projected values and plotted against the current (period 1979 to 2005) strength. It shows that there is an increase in almost all PRUDENCE regions, whereas the equilibrium is being marked with a black line. Especially within Central Europe and Eastern Europe, both climate model types agree with a large number of models with this trend.

In Chapter 5.3 we showed interesting results in terms of feedback strengths and their effect on different European regions. First, the metric analysis equation from Miralles et al. (2012) states that methods that can describe the impact of the soil moisture-air coupling mechanism only requires the net radiation, evapotranspiration, and air temperature. This points out those areas where the local energy balance is controlling the Tmax (Miralles et al. 2012). The advantage, therefore, is based on the fact, that the method does not depend on Mrso values but is able to make statements about the influence of it on other climate components. Regarding the soil moisture-air temperature coupling it shows that the strength of the feedback is too strong in certain climate models compared to observational data especially over the Mediterranean and Eastern Europe.

However, the relationship between the feedback strength and the Mrso trend show no results in terms of dependencies. The Tmax values indicate a different outcome. Although GCMs do not provide any results in terms of the correlation between the metric values and the Tmax, the RCMs represent a significant relationship in some European regions like Central Europe, the Alps, and Eastern Europe. In addition, the variance of Tmax and Mrso is also taken into account because it reflects the interannual variability within the whole period. This shows that the Tmax variance correlates with the feedback strength in almost all regions. That applies to both, the RCMs and the GCMs, with the former ones showing a higher significance. Also, the Mrso variance indicates a significant connection with the feedback strength in some European regions like the Iberian Peninsula, Scandinavia, and the Mediterranean. With the focus on Eastern Europe, only the Tmax variance values are showing a meaningful relationship with high values of  $R^2$ .

The future development of the feedback strength is also important because it has a decisive influence on the environment. A change may, for example, lead to increased drought occurrence, heat waves or a change in precipitation events. The current data of the climate models show a future increase of the soil moisture-air temperature coupling in all regions which coincides with the statements of the Fifth Assessment Report (AR5) (IPCC 2013). Thus, the biggest impact of these developments will be seen in areas which are currently in an unstable balance between Mrso and Tmax. If the tipping point is reached then a self-reinforced process can occur which massively change the environment such as drying out landscapes where the soil is currently fertile. We found out that these areas are mainly Central Europe and Eastern Europe. Seneviratne et al. (2006a) already pointed out the possibility that these two areas will change in the future due to a stronger coupling mechanism. We can now deposit these evidence with numbers that include the relationship of Mrso and Tmax.



# 6

## Conclusion and Outlook

Among other things, model analysis and evaluation are important in order to demonstrate their feasibility and to strengthen confidence in climate models. Climate models are useful for discussing specific behavior and characteristics of climate components and to learn more about their impacts on the climate system. Two climate properties which are analyzed in this thesis are maximum near-surface air temperature (Tmax) and total soil moisture content (Mrso), the latter being especially crucial on the regional scale. To accomplish this, both model types General Circulation Model (GCM)s and Regional Climate Model (RCM)s are used and evaluated on distinctive European regions (PRUDENCE) for the summer season.

Even though RCMs have a higher resolution and an explicitly computation of certain climate processes the most dominant factor for them are the driving GCMs as shown in Section 5. It can be seen by the clustering of the individual RCMs to their corresponding driving GCM based on the RCM-GCM difference values of Tmax and Mrso trends against each other. The individual RCMs are not distributed randomly and they are clustering in such a way that specific RCMs do not show any signs of independence regarding their driving GCM. Instead, the different RCMs cluster around the corresponding GCM, indicating that the receiving data of the driving GCM is the most dominant influence. In their entirety, however, there are differences between RCMs and GCMs. And the differences between the two model types are consistent in all analytical approaches throughout the thesis. Here, it is important to note, that one model alone does not provide robust information due to uncertainties like natural variability. Therefore, in this thesis, an entire model ensemble is necessary for robust statements. The whole ensemble of RCMs and GCMs on a first glance show a good agreement with the

observations and are consistent with them in both, Mrso as well as Tmax trends, with exception of France. Over this region, climate models overestimate Mrso compared to reanalysis data (ERA-Interim). This implies that the soil is too moist in the climate models, which in turn reduces Tmax due to evapotranspiration processes in the summer season. And as van Oldenborgh et al. (2008) already guessed, a faster warming in observations compared to climate model projections may be based on soil moisture differences. Because this would result in a stronger conversion of solar radiation into air temperature, which can be confirmed based on the results in chapter 5.

Future uncertainties in projections are more diverse and influential than the present ones and moreover, depend on several factors like CO<sub>2</sub> concentrations. A possible approach to reduce these uncertainties are emergent constraints which are shown in Section 5.2. Here, the attempt is to find a relationship between present model data, which are constraint by observations and long-term climate variables. Current and projected values are plotted against each other and are connected with a linear regression line. A possible relationship between these two aspects can help to reduce uncertainties for statements about future climate changes. This attempt, however, fails in terms of Mrso trends and variance with respect to the periods 1979 to 2005 and 2070 to 2099. Only GCMs show a relationship over the Iberian Peninsula and the Mediterranean, while RCMs are not indicating a connection over any European region. A reduction based on the results of one model type alone is therefore hard and usually not justifiable. For the emergent constraint approach with Tmax values the situation is different since there is a connection between the current and the projected values in almost all regions. Looking at both model types as a whole, six out of the eight regions show a significant relationship between the projected climate change signal (CCS) values of either the Tmax trend or variance. Only France and Central Europe are not affected by this.

Furthermore, in order to pay attention to the decisive soil moisture-air temperature coupling, the metric from Miralles et al. (2012) has been adapted for longer time periods and not just for daily analysis. The advantage is, that this approach not only indicates areas with a distinct soil moisture-air temperature coupling mechanisms like the diagnostic tool from Seneviratne et al. (2006b), it also provides a value for the strength of the coupling interaction. Thus, the feedback metric shows that two Prediction of Regional scenarios and Uncertainties for Defining European Climate change risks and Effects (PRUDENCE) regions are strongly connected. These two regions are the Iberian Peninsula and the Mediterranean area and are the same ones that have already been classified as so-called *transitional zones* from Seneviratne et al. (2006b) and van den Hurk et al. (2012) which shows that the feedback metric provides meaningful values. According to the models, Eastern Europe may also be such a transitional zone while the reanalysis data does not indicate this and leads therefore to an overestimation of the feedback strength in the climate models in this area. One possible explanation could

---

be the strong dependence of evapotranspiration, precipitation and air temperature on each other which is indicated by reanalysis data. Another possible explanation is the fact, that the resolution of the ERA-Interim data is with  $80\text{ km} \times 80\text{ km}$  grid spacing too coarse and leads to distortions. This is of particular importance because there is evidence that Eastern Europe experiences a dehydration in future climate projections (IPCC 2007). Seneviratne et al. (2006a) also consider that due to a northward shift of the climate regime in Europe, the coupling mechanism in central Europe will get stronger. This idea is supported by currently available model projections which are indicating an increase of future feedback strengths in all regions, except Scandinavia (see Section 5.3). Furthermore, the two regions mentioned earlier, Central Europe and Eastern Europe, are exactly the two regions in which a particularly strong increase in the soil moisture-air temperature coupling strength can happen according to the analysis in chapter 5.3. By assuming that temperature will rise in the future, see Cubasch et al. (2013), this suspicion is further underpinned by the nature of the feedback.

It turns out that both model types are relatively uniform in projecting future feedback strengths, only the RCMs show a stronger influence of T<sub>max</sub>. Therefore, they indicate that the environment can change significantly due to the self-reinforcing effect of the coupling mechanism. Thus, a change in T<sub>max</sub> can have an extreme impact in those two regions and it could also explain the dehydration results in the Fifth Assessment Report (AR5). Further analysis shows a strong relationship between the T<sub>max</sub> and the feedback metric whereas the Mrso show no significant correlation within any European region. In general, the T<sub>max</sub> trend or variance shows significant correlations with either the anthropogenetic climate warming expressed in terms of the climate change signal, the feedback metric or both in many regions. However, this is not too surprising because both variables, CCS and the feedback metric, are based on temperature values. Whereas the Mrso seems to have no correlation except the temperature, although the feedback strength should reflect both the temperature and the soil moisture at the same time.

A look across all regions shows that the British Isles, Central Europe, and the Alps behave similarly in general. One reason could be that these regions are very affected by precipitation events. Another possible reason could be, that this is a consequence of a wrong storm track representation in the climate models, which Zappa et al. (2013) shows. A special region is Scandinavia because here the T<sub>max</sub> values are not necessarily depending on just Mrso alone due to the fact that the results from RCMs and GCMs contradict each other. More likely is the fact, that precipitation and the coarse resolution of the steep orography play a crucial role in this area. It is possible that the region is experiencing a warming and also an increase in precipitation in the future (Jaeger 2011). Although there is no evidence that the soil moisture-air temperature coupling will get stronger.

Finally, our results indicate a strong feedback mechanism in the Iberian Peninsula and the Mediterranean region that are largely in agreement with Seneviratne et al. (2010) and Jaeger (2011). This implies that the soil dehydration in these two regions is the re-

sult of high air temperature and evapotranspiration effects caused by strong interactions of the soil moisture-air temperature coupling. However, there are some major differences between these two regions. In this context, it is possible that the experimental setup contributes also to the differences. Due to the applied water mask and the subsequent averaging of the values, it is likely that this causes a distortion of possible similarities between these regions because the number of averaged grid values differ from each other. And in combination with the location, because the Mediterranean region is more maritime influenced while the Iberian Peninsula is more continental influenced, some climatic distinctions can occur. Nonetheless, the northwards shift of the Hadley cell due to the increasing air temperatures can particularly affect these two regions, especially in the future.

### **Prospects and proposal**

Although soil moisture is a key variable in the climate system, there are still lots of problems associated with it. One key issue is the lack of observations, while there are new direct and indirect measurement methods in use (Seneviratne et al. 2010). For example, Mrso values in climate models are not fully homogenized in terms of depths and calculation methods. The layer depth is also decisive because, at some point, both the wilting point and the area where the plants can no longer use the capillarity is reached. It would be meaningful to define a standard model output so that the ground output is available in at least two, maybe even three layers (e.g. 0.30 m, 1 m and rest). A different way for future investigations could be to dispense the soil moisture itself completely and instead use the water content in the soil as an analysis variable. It may also be necessary to make further improvements to the feedback metric as there is no relationship between the metric and the soil moisture. Therefore, the potential of RCMs is immediately evident, even if they make just small corrections and improvements. Because soil moisture is regionally very heterogeneous due to the varying soil depth and different types of soil. Also, investigations of Mrso representation in models and their biases are needed to avoid mistakes at the initial state because of its importance for projections as van den Hurk et al. (2012) show. Nevertheless, climate models are currently the best tools for future estimates of the climate system, if their simplifications and deviations are kept in mind. It might also be a good idea to use a finer resolution for ERA-Interim for future analysis because soil properties vary very much in space. At the time of this thesis, long data periods on such a fine resolution are not available. Another approach for future investigations could be the considerations of precipitation as well as the analysis of model values under the assumption of the RCP4.5 and RCP6.0 scenario. One point that should be maintained for future analysis is the use of a land-sea mask.



# Appendix

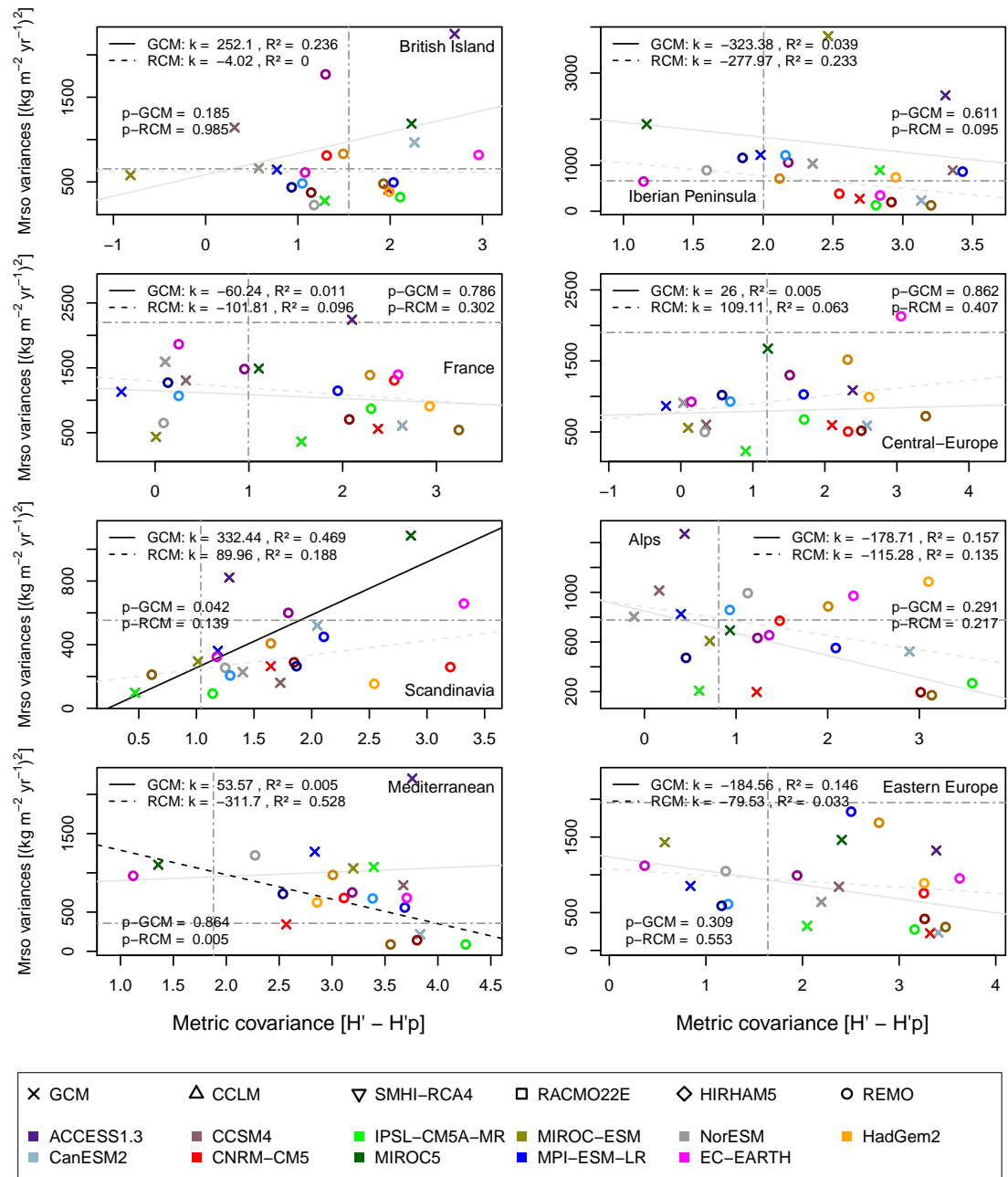


Fig. 6.1 Scatterplot between Mrso variance and the feedback strength. The interannual variability of Mrso is higher when rainfall and subsequent dehydration occurs during the summer months. However, droughts and other factors can affect this relationship. Observation are again in gray lines while significant correlations of the climate models are represented by a black line (non-significant relationships are marked with a light gray line).

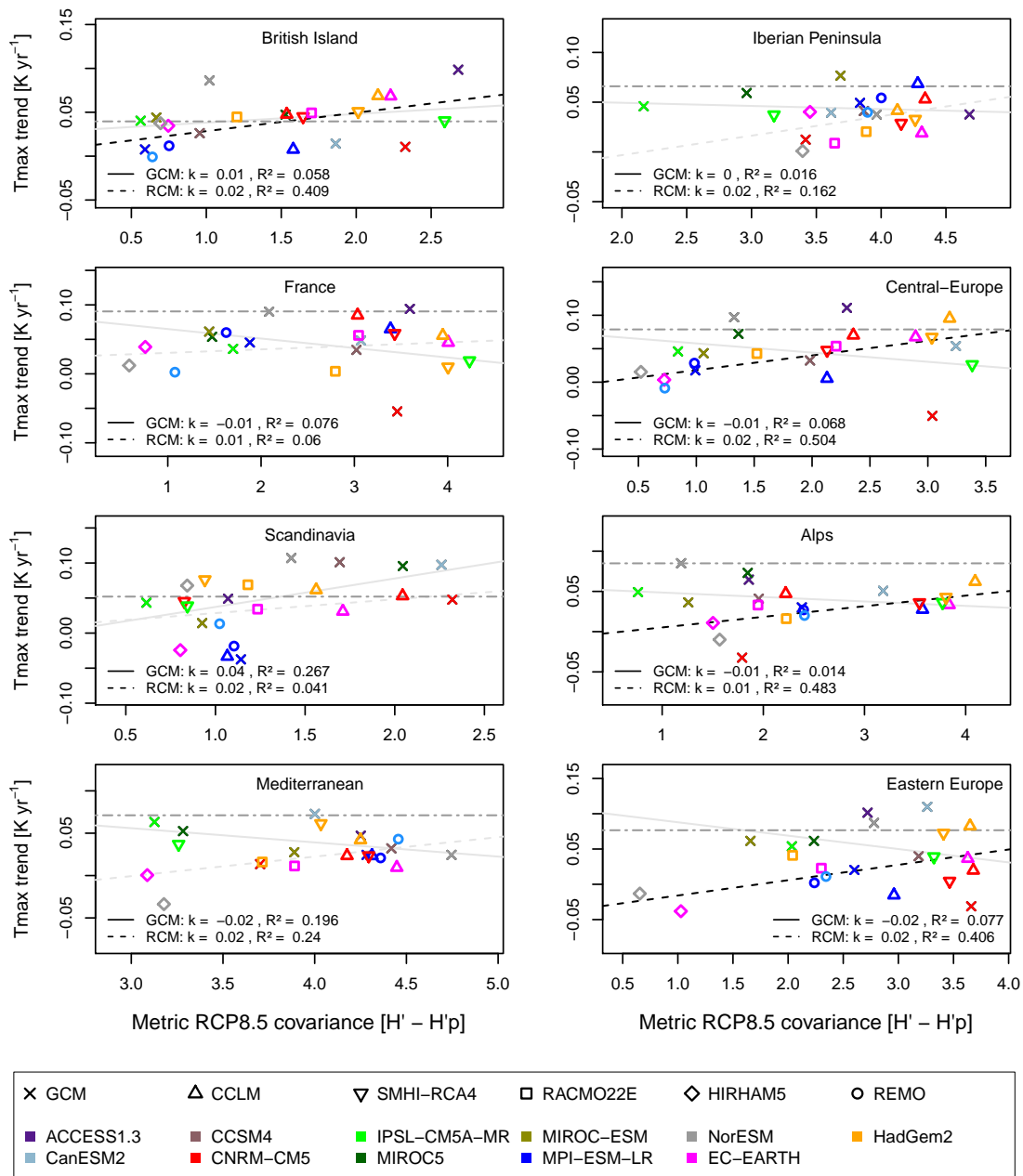


Fig. 6.2 Scatterplot between the Tmax trend and the future feedback strength. The feedback strength for the period 2070 to 2099 is calculated with the projected RCP8.5 values and plotted against the current (1979 to 2005) Tmax values. It shows significant relationships between the two variables for the RCMs in some region, especially in the central areas of Europe (represented by a dashed black line). The GCMs do not show any significant correlation (light gray line) while the observational data are marked with a dashed gray line.

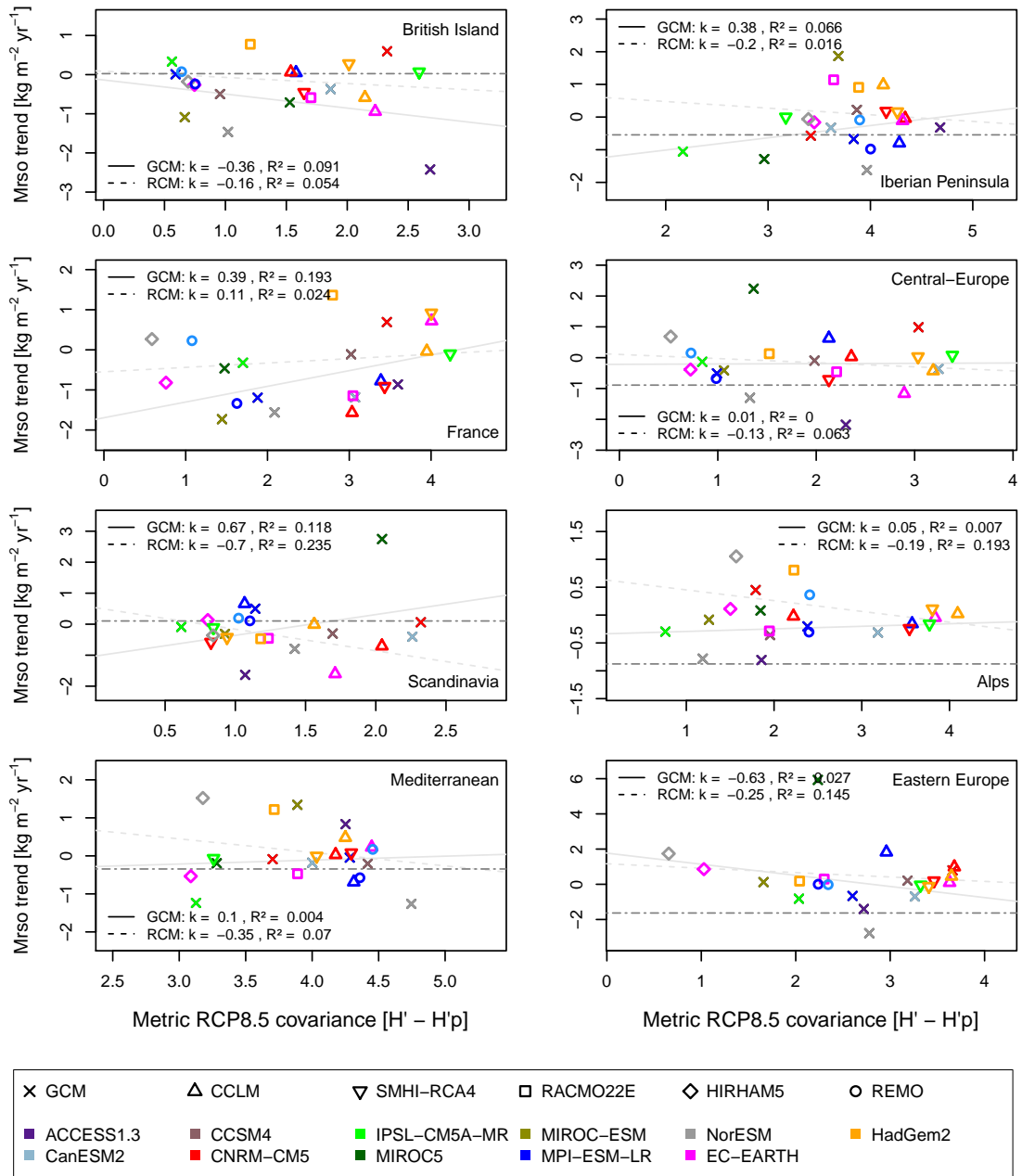


Fig. 6.3 Mrso trend is plotted against the future feedback strength. The feedback values are from the RCP8.5 projections and are plotted against the current Mrso trend values. It can be seen that there are no significant relationships between these two variables, neither for the RCMs nor for the GCMs. Therefore, the correlations are represented with light gray lines instead of black lines and the observational data are shown with a dashed gray line.

# List of Figures

1.2	Soil moisture-temperature coupling estimation based on a diagnose formula	2
2.1	Interaction between solar radiation and Earth's atmosphere	7
2.3	Contributing processes for the soil moisture-land atmosphere coupling	9
3.1	Different kinds of climate models	12
3.2	Development of the GCMs	13
3.3	Typical structure of a GCM	14
3.4	Nesting of an RCM	17
3.5	Overview of the uncertainties	18
3.6	Projections of the different scenarios	20
4.1	With and without area fraction	29
5.1	European model domain with the PRUDENCE regions	32
5.2	Resolution difference between GCM and RCM	34
5.3	Data overview of the PRUDENCE regions with ERA-Interim	36
5.4	Model legend within the thesis	37
5.5	Deviation of Tmax model data from observations	41
5.6	Deviation from the Mrso model data compared to the observations	42
5.7	Tmax trend against Mrso trend	45
5.8	Effects of the RCMs compared to the driving GCMs	48
5.9	CCS is plotted against the Tmax trend	53
5.10	CCS plotted against the Mrso trend	55
5.11	Attempt to reduce uncertainty with variance values of Mrso	57
5.12	CCS plotted against Tmax variance	59
5.13	Global seasonal insolation of the sun	64
5.14	Comparison of two different evapotranspiration methods with the same coupling method	66
5.15	Feedback strength in GCM and RCM compared to ERA-Interim data in the summer season from 1979 to 2005	68
5.16	Relationship between feedback strength and Mrso trend	70
5.17	Tmax trend plotted against the feedback strength	72

*List of Figures*

---

5.18	Scatterplot between the Tmax variance and the feedback strength . . . . .	75
5.19	Approach to estimate future feedback strengths . . . . .	78
6.1	Scatterplot between Mrso variance and the feedback strength . . . . .	86
6.2	Scatterplot between the Tmax trend and the future feedback strength with RCP8.5 . . . . .	87
6.3	Mrso trend is plotted against the future feedback strength . . . . .	88

## List of Tables

3.1	Overview of all used climate models . . . . .	25
5.1	PRUDENCE region coordinates . . . . .	33





# Acronyms

**AL** Alps. 32

**AOGCM** Atmosphere Ocean General Circulation Model. 12

**AR4** Fourth Assessment Report. 6, 20

**AR5** Fifth Assessment Report. 5, 19, 20, 79, 82

**BC** Blaney-Criddle. 24, 62–65

**BI** British Isles. 32

**CCS** climate change signal. 50–52, 54, 56, 59, 60, 82

**CMIP5** phase 5 of the Coupled Model Intercomparison Project. 15

**E-OBS** European high-resolution observational gridded data set. 21, 22, 33, 38, 44, 49

**EBM** Energy balance model. 11

**ECMWF** European Centre for Medium-Range Weather Forecasts. 21, 22

**EE** Eastern Europe. 32

**EMIC** Earth System Models of Intermediate Complexity. 11

**ENSO** El Niño-Southern Oscillation. 14, 16

**ERA-Interim** European Centre for Medium-Range Weather Forecasts Re-Analysis Interim. 21, 22, 33, 35, 39, 41, 42, 44, 54, 56, 65, 67, 69, 74

**ESGF** Earth System Grid Federation. 22

**EU** European Union. 31

**EURO-CORDEX** COordinated Regional climate Downscaling EXperiment - EUROpean domain. 15

**Evap** evapotranspiration. i, 8, 23, 24, 33, 61–63, 65

**FR** France. 32

**GCM** General Circulation Model. 11–16, 19, 24, 31–33, 37, 38, 43, 44, 46, 47, 49, 51, 52, 56, 60, 64, 65, 67, 69, 71, 73, 76, 79, 81, 82, 87, 88

**GHG** greenhouse gases. 1, 5, 6, 12, 16, 19, 38, 51

**IC** initial conditions. 16, 18, 21

**ICU** initial condition uncertainty. 18

**IP** Iberian Peninsula. 32

**IPCC** Intergovernmental Panel on Climate Change. 5, 19

**JJA** summer season. 32, 33, 43, 56, 64, 65, 67, 71, 73, 76

**LBC** lateral boundary conditions. 16

**LWR** longwave radiation. 6, 11, 13, 14, 23

**MD** Mediterranean. 32

**ME** Mid- or Central-Europe. 32

**Mrso** total soil moisture content. i, 8, 22, 31–33, 38, 39, 42–44, 46, 47, 49, 52, 54, 56, 60–62, 65, 69, 73, 76, 79, 81, 82, 84, 85, 88

**PET** potential evapotranspiration. 24, 61–64

**PRUDENCE** Prediction of Regional scenarios and Uncertainties for Defining European Climate change risks and Effects. 31, 32, 35, 38, 43, 46, 49, 51, 52, 56, 59, 63, 65, 69, 71, 73, 76, 77, 82

**PT** Priestley-Taylor. 24, 62–65

**RCM** Regional Climate Model. 15, 16, 24, 31–33, 37, 38, 43, 44, 46, 47, 49, 51, 52, 56, 60, 64, 65, 67, 69, 71, 73, 76, 79, 81, 82, 84, 87, 88

**RCP** representative concentration pathway. 19, 20, 51, 76

**Rn** surface net radiation. i, 23, 33, 61, 64

**SC** Scandinavia. 32

**SWR** shortwave radiation. 6, 11, 13, 14, 23

**T<sub>max</sub>** maximum near-surface air temperature. i, 8, 22, 31–33, 38, 39, 41, 43, 44, 46, 47, 49, 51, 52, 54, 56, 59–61, 65, 69, 71, 73, 74, 76, 79, 81, 82, 87

**T<sub>mean</sub>** near-surface air temperature. 8, 22, 33, 50, 51, 61–63

**UNEP** United Nations Environment Programme. 5

**WMO** World Meteorological Organization. 5



## Bibliography

- Agrawala, S. (1998). “Context and Early Origins of the Intergovernmental Panel on Climate Change.” In: *Climatic Change* 39, pp. 605–620. ISSN: 1573-1480. DOI: 10.1023/A:1005315532386 (cit. on p. 5).
- Bellenger, H., E. Guilyardi, J. Leloup, M. Lengaigne, and J. Vialard (2014). “ENSO representation in climate models: from CMIP3 to CMIP5.” In: *Climate Dynamics* 42.7, pp. 1999–2018. ISSN: 1432-0894. DOI: 10.1007/s00382-013-1783-z (cit. on p. 15).
- Bellprat, O., S. Kotlarski, D. Lüthi, and C Schär (2012). “Objective calibration of regional climate models.” In: *Journal of Geophysical Research (Atmospheres)* 117 (cit. on pp. 32, 33).
- Bentsen, M., I. Bethke, J. B. Debernard, T. Iversen, A. Kirkevåg, Seland, H. Drange, C. Roelandt, I. A. Seierstad, C. Hoose, and J. E. Kristjansson (2013). “The Norwegian Earth System Model, NorESM1-M – Part 1: Description and basic evaluation of the physical climate.” In: *Geoscientific Model Development* 6, 687–720. DOI: 10.5194/gmd-6-687-2013 (cit. on p. 25).
- Blaney, H. F. and W. D. Criddle (1964). “Determining Water Requirements for Settling Water Disputes.” In: *National Resources Journal* 4.29, pp. 29–40 (cit. on pp. 63, 64).
- Bóhm, U., M. Kúcken, W. Ahrens, A. Block, D. Hauffe, K. Keuler, B. Rockel, and A. Will (2006). “CLM-the climate version of LM: Brief description and long-term applications.” In: *COSMO newsletter* 6, pp. 225–235 (cit. on p. 25).
- Bony, S., C. R., R. Fichet, J. Fyfe, V. Kattsov, A. Pitman, J. Shukla, J. Srinivasan, R. Stouffer, A. Sumi, and K. Taylor (2007). “Climate Models and Their Evaluation.” In: *Climate Change 2007: The Physical Science Basis. Contribution of Working Group I to the Fourth Assessment Report of the Intergovernmental Panel on Climate Change*. Ed. by S. Solomon, D. Qin, M. Manning, Z. Chen, M. Marquis, K. Averyt, M. Tignor, and H. Miller. Cambridge, United Kingdom and New York, NY, USA: Cambridge University Press. Chap. 8 (cit. on pp. 14, 21, 38).

- Bracegirdle, T. J. and D. B. Stephenson (2012). “Higher precision estimates of regional polar warming by ensemble regression of climate model projections.” In: *Climate Dynamics* 39.12, pp. 2805–2821. ISSN: 1432-0894. DOI: 10.1007/s00382-012-1330-3 (cit. on pp. 50, 51).
- Bralower, T. and D. Bice (2009). *Module 4: Introduction to General Circulation Models*. <https://www.e-education.psu.edu/earth103/node/524> (cit. on pp. 14, 15).
- Brient, F. and T. Schneider (2016). “Constraints on Climate Sensitivity from Space-Based Measurements of Low-Cloud Reflection.” In: *Journal of Climate* 29.16, pp. 5821–5835. DOI: 10.1175/JCLI-D-15-0897.1 (cit. on p. 50).
- Brouwer, C. and M. Heibloem (1997). “Irrigation Water Management: Training Manual No. 3: Irrigation water needs.” In: ed. by B. Snellen (cit. on pp. 24, 64).
- Brückler, F. (2017). *Geschichte der Mathematik kompakt: Das Wichtigste aus Arithmetik, Geometrie, Algebra, Zahlentheorie und Logik*. Springer Berlin Heidelberg. ISBN: 9783662553527 (cit. on p. 28).
- CLIPC (2018). *CLIPC: Constructing Europe’s Climate Information Portal*. URL: <http://www.clipc.eu/home> (cit. on p. 15).
- Carter, T., R. Leemans, M. Lal, P. Whetton, L. Mearns, M. Hulme, L. Hay, R. Jones, R. Katz, R. Kittel, J. Smith, and R. Wilby (2001). *Climate Change 2001: The Scientific Basis: Contribution of Working Group I to the Third Assessment Report of the Intergovernmental Panel on Climate Change*. Ed. by J. Houghton, Y. Ding, D. Griggs, M. Noguer, P. van der Linden, X. Dai, K. Maskell, and C. Johnson. Cambridge University Press. ISBN: 0521807670 (cit. on pp. 8, 52).
- Charney, J., W. J. Quirk, S.-H. Chow, and J. Kornfield (1977). “A comparative study of the effects of albedo change on drought in semi-arid regions.” In: *Journal Atmospheric Science* 34, pp. 1366–1385. DOI: 10.1175/1520-0469(1977)034<1366:ACSOTE>2.0.CO;2 (cit. on p. 9).
- Christensen, J. H., T. Carter, and F. Giorgi (2001). “PRUDENCE kick-off meeting.” In: *Technical report* 1-8 (cit. on p. 32).
- Christensen, J. H., T. R. Carter, M. Rummukainen, and G. Amanatidis (2007). “Evaluating the performance and utility of regional climate models: the PRUDENCE project.” In: *Climatic Change* 81.1, pp. 1–6. ISSN: 1573-1480. DOI: 10.1007/s10584-006-9211-6 (cit. on p. 31).
- Christensen, O. B., M. Drews, J. H. Christensen, K. Dethloff, K. Ketelsen, I. Hebestadt, and A. Rinke (2015). *The HIRHAM Regional Climate Model Version 5*. URL: [www.dmi.dk/dmi/tr06-17](http://www.dmi.dk/dmi/tr06-17) (cit. on p. 25).

- Chylek, P., J. Li, M. K. Dubey, M. Wang, and G. Lesins (2011). “Observed and model simulated 20th century Arctic temperature variability: Canadian Earth System Model CanESM2.” In: *Atmospheric Chemistry and Physics Discussions* 11, pp. 22893–22907. DOI: 10.5194/acpd-11-22893-2011. URL: <https://www.atmos-chem-phys-discuss.net/11/22893/2011/> (cit. on p. 25).
- Claussen, M., L. Mysak, A. Weaver, M. Crucifix, T. Fichet, M.-F. Loutre, S. Weber, J. Alcamo, V. Alexeev, A. Berger, R. Calov, A. Ganopolski, H. Goosse, G. Lohmann, F. Lunkeit, I. Mokhov, V. Petoukhov, P. Stone, and Z. Wang (2002). “Earth system models of intermediate complexity: closing the gap in the spectrum of climate system models.” In: *Climate Dynamics* 18.7, pp. 579–586. ISSN: 1432-0894. DOI: 10.1007/s00382-001-0200-1 (cit. on p. 11).
- Collins, M., R. E. Chandler, P. M. Cox, J. M. Huthnance, J. Rougier, and D. B. Stephenson (2012). “Quantifying future climate change.” In: *Nature Climate Change* 2, pp. 403–409. DOI: doi:10.1038/nclimate1414 (cit. on pp. 20, 50, 51).
- Cubasch, U., D. Wuebbles, D. Chen, M. Facchini, D. Frame, N. Mahowald, and J.-G. Winther (2013). “Introduction.” In: *Climate Change 2013: The Physical Science Basis. Contribution of Working Group I to the Fifth Assessment Report of the Intergovernmental Panel on Climate Change*. Ed. by T. Stocker, D. Qin, G.-K. Plattner, M. Tignor, S. Allen, J. Boschung, A. Nauels, Y. Xia, V. Bex, and P. Midgley. Cambridge, United Kingdom and New York, NY, USA: Cambridge University Press. Chap. 1, 119–158. ISBN: ISBN 978-1-107-66182-0. DOI: 10.1017/CB09781107415324.007 (cit. on pp. 3, 5, 6, 12, 14, 18–20, 34, 38, 61, 73, 83).
- Dee, D. P. et al. (2011). “The ERA-Interim reanalysis: configuration and performance of the data assimilation system.” In: *Quarterly Journal of the Royal Meteorological Society* 137.656, pp. 553–597. DOI: 10.1002/qj.828 (cit. on pp. 22, 24).
- Deser, C., A. Phillips, V. Bourdette, and H. Teng (2012). “Uncertainty in climate change projections: the role of internal variability.” In: *Climate Dynamics* 38.3, pp. 527–546. ISSN: 1432-0894. DOI: 10.1007/s00382-010-0977-x (cit. on p. 18).
- Doms, G., E. Förstner, E. Heise, H.-J. Herzog, D. Mironov, M. Raschendorfer, T. Reinhardt, B. Ritter, R. Schrodin, J.-P. Schulz, and G. Vogel (2011). “A description of the nonhydrosotatic regional COSMO Model, Part II: Physical parameterization.” In: *Deutscher Wetterdienst* (cit. on p. 25).
- Draper, N. R. and H. Smith (2014). “Fitting a Straight Line by Least Squares.” In: *Applied Regression Analysis*. Wiley-Blackwell. Chap. 1, pp. 15–46. ISBN: 9781118625590. DOI: 10.1002/9781118625590.ch1 (cit. on p. 51).

- Durre, I., J. M. Wallace, and D. P. Lettenmaier (2000). “Dependence of Extreme Daily Maximum Temperatures on Antecedent Soil Moisture in the Contiguous United States during Summer.” In: *Journal of Climate* 13.14, pp. 2641–2651. DOI: 10.1175/1520-0442(2000)013<2641:DOEDMT>2.0.CO;2 (cit. on p. 9).
- Eckers, A. (2015). *In the climate model jungle*. <https://www.scisnack.com/2015/04/13/in-the-climate-model-jungle/> (cit. on p. 12).
- Flato, G., J. Marotzke, B. Abiodun, P. Braconnot, S. S. Chou, W. Collins, P. Cox, F. Driouech, S. Emori, V. Eyring, C. Forest, P. Gleckler, E. Guylyardi, C. Jakob, V. Kattsov, C. Reason, and M. Rummukainen (2013). “Evaluation of Climate Models.” In: *Climate Change 2013: The Physical Science Basis. Contribution of Working Group I to the Fifth Assessment Report of the Intergovernmental Panel on Climate Change*. Ed. by T. Stocker, D. Qin, G.-K. Plattner, M. Tignor, S. Allen, J. Boschung, A. Nauels, Y. Xia, V. Bex, and P. Midgley. Cambridge, United Kingdom and New York, NY, USA: Cambridge University Press. Chap. 9 (cit. on pp. 11–13, 15, 16).
- Flint, A. L. and S. W. Childs (1991). “Use of the Priestley-Taylor evaporation equation for soil water limited conditions in a small forest clearcut.” In: *Agricultural and Forest Meteorology* 56.3, pp. 247–260. ISSN: 0168-1923. DOI: [https://doi.org/10.1016/0168-1923\(91\)90094-7](https://doi.org/10.1016/0168-1923(91)90094-7) (cit. on p. 64).
- Forster, P., V. Ramaswamy, P. Artaxo, T. Berntsen, R. Betts, D. Fahey, J. Haywood, J. Lean, D. Lowe, G. Myhre, J. Nganga, R. Prinn, G. Raga, M. Schulz, and R. van Dorland (2007). “Changes in Atmospheric Constituents and in Radiative Forcing.” In: ed. by S. Solomon, D. Qin, M. Manning, Z. Chen, M. Marquis, K. Averyt, M. Tignor, and H. Miller (cit. on p. 7).
- Gent, P. R., G. Danabasoglu, L. J. Donner, M. M. Holland, E. C. Hunke, S. R. Jayne, D. M. Lawrence, R. B. Neale, P. J. Rasch, M. Vertenstein, P. H. Worley, Z. Yang, and M. Zhang (2011). “The Community Climate System Model Version 4.” In: *Journal of climate* 24. DOI: 10.1175/2011JCLI4083.1 (cit. on p. 25).
- Giorgi, F. and W. J. Gutowski Jr. (2015). “Regional Dynamical Downscaling and the CORDEX Initiative.” In: *Annual Review of Environment and Resources* 40.1, pp. 467–490. DOI: 10.1146/annurev-environ-102014-021217 (cit. on pp. 16, 17).
- Goosse, H. (2015). *Climate System Dynamics and Modeling*. Cambridge University Press. ISBN: 9781107083899 (cit. on pp. 8, 9, 43, 54).



- Hartmann, D., A. Klein Tank, M. Rusticucci, L. Alexander, S. Brönnimann, Y. Charabi, F. Dentener, E. Dlugokencky, D. Easterling, A. Kaplan, B. Soden, P. Thorne, M. Wild, and P. Zhai (2013). “Observations: Atmosphere and Surface.” In: *Climate Change 2013: The Physical Science Basis. Contribution of Working Group I to the Fifth Assessment Report of the Intergovernmental Panel on Climate Change*. Ed. by T. Stocker, D. Qin, G.-K. Plattner, M. Tignor, S. Allen, J. Boschung, A. Nauels, Y. Xia, V. Bex, and P. Midgley. Cambridge, United Kingdom and New York, NY, USA: Cambridge University Press. Chap. 2, 119–158. ISBN: ISBN 978-1-107-66182-0. DOI: 10.1017/CB09781107415324.007 (cit. on p. 58).
- Hawkins, E. and R. Sutton (2009). “The Potential to Narrow Uncertainty in Regional Climate Predictions.” In: *Bulletin of the American Meteorological Society* 90.8, pp. 1095–1108. DOI: 10.1175/2009BAMS2607.1 (cit. on pp. 18, 19).
- Haylock, M., N. Hofstra, A. Klein Tank, L. Klok, P. Jones, and M. New (2008). “A European daily high-resolution gridded dataset of surface temperature and precipitation for 1950–2006.” In: *Journal of Geophysical Research: Atmospheres* 113. DOI: <http://dx.doi.org/10.1029/2008JD010201> (cit. on p. 21).
- Hirst, T. and P. Uhe (2011). *ACCESS1-3 model output prepared for CMIP5*. URL: <http://wiki.csiro.au/confluence/display/ACCESS/Home> (cit. on p. 25).
- Houghton, J. (2009). *Global Warming: The Complete Briefing*. Cambridge University Press. ISBN: 9781107049291 (cit. on p. 1).
- Hourdin, F., M.-A. Foujols, F. Codron, V. Guemas, J.-L. Dufresne, S. Bony, S. Denvil, L. Guez, F. Lott, J. Ghattas, P. Braconnot, O. Marti, Y. Meurdesoif, and L. Bopp (2013). “Impact of the LMDZ atmospheric grid configuration on the climate and sensitivity of the IPSL-CM5A coupled model.” In: *Climate Dynamics* 40.9, pp. 2167–2192. ISSN: 1432-0894. DOI: 10.1007/s00382-012-1411-3 (cit. on p. 25).
- IPCC (2007). “Climate Change 2007: The Physical Science Basis. Contribution of Working Group I to the Fourth Assessment Report of the Intergovernmental Panel on Climate Change.” In: ed. by S. Solomon, D. Qin, M. Manning, Z. Chen, M. Marquis, K. Averyt, M. Tignor, and H. Miller. Cambridge, United Kingdom and New York, NY, USA: Cambridge University Press (cit. on pp. 2, 3, 5, 6, 13, 83).
- (2013). “Summary for Policymakers.” In: *Climate Change 2013: The Physical Science Basis. Contribution of Working Group I to the Fifth Assessment Report of the Intergovernmental Panel on Climate Change*. Ed. by T. Stocker, D. Qin, G.-K. Plattner, M. Tignor, S. Allen, J. Boschung, A. Nauels, Y. Xia, V. Bex, and P. Midgley. Cambridge, United Kingdom and New York, NY, USA: Cambridge University Press. Chap. SPM, 1–30. ISBN: ISBN 978-1-107-66182-0. DOI: 10.1017/CB09781107415324.004 (cit. on pp. 8, 79).

- Jacob, D. and R. Podzun (1997). "Sensitivity studies with the regional climate model REMO." In: *Meteorology and Atmospheric Physics* 63.1, pp. 119–129. ISSN: 1436-5065. DOI: 10.1007/BF01025368 (cit. on p. 25).
- Jacob, D. et al. (2014). "EURO-CORDEX: new high-resolution climate change projections for European impact research." In: *Regional Environmental Change* 14.2, pp. 563–578. DOI: 10.1007/s10113-013-0499-2 (cit. on p. 2).
- Jaeger E. B. and Seneviratne, S. I. (2011). "Impact of soil moisture-atmosphere coupling on European climate extremes and trends in a regional climate model." In: *Climate Dynamics* 36.9, pp. 1919–1939. ISSN: 1432-0894. DOI: 10.1007/s00382-010-0780-8 (cit. on pp. 1, 9, 23, 35, 39, 83).
- Kayano, M. T. and C. Sansígolo (2009). "Interannual to decadal variations of precipitation and daily maximum and daily minimum temperatures in southern Brazil." In: *Theoretical and Applied Climatology* 97.1, pp. 81–90. ISSN: 1434-4483. DOI: 10.1007/s00704-008-0050-4 (cit. on pp. 56, 73).
- Keeling, C., A. Carter, and W. Mook (1984). "Seasonal, latitudinal, and secular variations in the abundance and isotopic ratios of atmospheric CO<sub>2</sub>: 2. Results from oceanographic cruises in the tropical Pacific Ocean." In: *Journal of Geophysical Research: Atmospheres* 89, pp. 4615–4628. ISSN: 2156-2202. DOI: 10.1029/JD089iD03p04615 (cit. on p. 5).
- Klein, S. A. and A. Hall (2015). "Emergent Constraints for Cloud Feedbacks." In: *Current Climate Change Reports* 1.4, pp. 276–287. ISSN: 2198-6061. DOI: 10.1007/s40641-015-0027-1 (cit. on pp. 50, 51).
- Knutti, R. and J. Sedláček (2012). "Robustness and uncertainties in the new CMIP5 climate model projections." In: *Nature Climate Change* 3. DOI: <http://dx.doi.org/10.1038/nclimate1716> (cit. on p. 20).
- Koster, R. D. et al. (2004). "Regions of Strong Coupling Between Soil Moisture and Precipitation." In: *Science* 305.5687, pp. 1138–1140. DOI: 10.1126/science.1100217 (cit. on pp. 3, 9).
- Kraus, H. (2007). *Die Atmosphäre der Erde: Eine Einführung in die Meteorologie*. Springer Berlin Heidelberg, pp. 45–60, 95–132. ISBN: 9783540350170 (cit. on pp. 22, 23).
- Landsberg, H. (1945). "Climatology." In: *Handbook of Meteorology*. Ed. by F. Berry, E. Bollay, and N. Beers. McGraw-Hill Inc. ISBN: ISBN 978-0070050303 (cit. on p. 1).
- Le Treut, H., R. Somerville, Y. Cubasch U. and Ding, C. Mauritzen, A. Mokssit, T. Peterson, and M. Prather (2007). "Historical Overview of Climate Change Science." In: ed. by S. Solomon, D. Qin, M. Manning, Z. Chen, M. Marquis, K. Averyt, M. Tignor, and H. Miller (cit. on p. 8).

- Marsh, T., G. Cole, and R. Wilby (2007). “Major droughts in England and Wales, 1800–2006.” In: *Weather* 62.4, pp. 87–93 (cit. on pp. 35, 43, 71).
- Menaughton, K. and T. Spriggs (1989). “An evaluation of the Priestley and Taylor equation and the complementary relationship using results from a mixed-layer model of the convective boundary layer.” In: *IAHS Publication* 177 (cit. on p. 64).
- Mendlik, T., G. Heinrich, A. Gobiet, and A. Leuprecht (2016). “From climate simulations to statistics - Introducing the wux package.” In: *Austrian Journal of Statistics* 45.1, pp. 81–96. DOI: <https://doi.org/10.17713/ajs.v45i1.98> (cit. on p. 29).
- Michaels, P., R. Balling, R. Vose, and P. Knappenberger (1998). “Analysis of trends in the variability of daily and monthly historical temperature measurements.” In: *Climate Research*. 1st ed. Vol. 10, pp. 27–33 (cit. on p. 56).
- Miralles, D. G., M. J. van den Berg, A. J. Teuling, and R. A. M. de Jeu (2012). “Soil moisture-temperature coupling: A multiscale observational analysis.” In: *Geophysical Research Letters* 39.21. ISSN: 1944-8007. DOI: 10.1029/2012GL053703 (cit. on pp. 1, 3, 61, 62, 64, 69, 71, 74, 79, 82).
- Nijse, F. J. and H. A. Dijkstra (2017). *A mathematical approach to understanding emergent constraints*. Tech. rep. (cit. on pp. 50, 51).
- Palmer, T. et al. (2004). “DEVELOPMENT OF A EUROPEAN MULTIMODEL ENSEMBLE SYSTEM FOR SEASONAL-TO-INTERANNUAL PREDICTION (DEMETER).” In: *Bulletin of the American Meteorological Society* 85.6, pp. 853–872. DOI: 10.1175/BAMS-85-6-853 (cit. on p. 15).
- Patt, A. and S. Dessai (2005). “Communicating uncertainty: lessons learned and suggestions for climate change assessment.” In: *Comptes Rendus Geoscience* 337.4, pp. 425–441. ISSN: 1631-0713. DOI: <https://doi.org/10.1016/j.crte.2004.10.004> (cit. on p. 19).
- Pierce, D. W. (2009). *Ncview 1.93g*. URL: [http://meteora.ucsd.edu:80/~pierce/ncview\\_home\\_page.html](http://meteora.ucsd.edu:80/~pierce/ncview_home_page.html) (cit. on p. 34).
- Priestley, C. H. B. and R. J. Taylor (1972). “On the Assessment of Surface Heat Flux and Evaporation Using Large-Scale Parameters.” In: *Monthly Weather Review* 100.2, pp. 81–92. DOI: 10.1175/1520-0493(1972)100<0081:0TAOSH>2.3.CO;2 (cit. on pp. 62–64).
- Raddatz, T. J., C. H. Reick, W. Knorr, J. Kattge, E. Roeckner, R. Schnur, K.-G. Schnitzler, P. Wetzler, and J. Jungclaus (2007). “Will the tropical land biosphere dominate the climate-carbon cycle feedback during the twenty-first century?” In: *Climate Dynamics* 29, pp. 565–574. DOI: 10.1007/s00382-007-0247-8 (cit. on p. 25).

- Räisänen, J. (2007). “How reliable are climate models?” In: *Tellus* 59, pp. 2–29. DOI: 10.1111/j.1600-0870.2006.00211.x (cit. on p. 15).
- Rajib, M., S. Sultana, M. Saha, and M. Rahman (2014a). “A Multi- Model Ensembling Approach for Developing Plausible Country-scale Climate Change Scenarios for Future.” In: *Journal of Earth Science Climate Change* 5.2. DOI: 10.4172/2157-7617.1000179 (cit. on p. 15).
- (2014b). “A Multi- Model Ensembling Approach for Developing Plausible Country-scale Climate Change Scenarios for Future.” In: *Journal of Earth Science Climate Change* 5.2. DOI: 10.4172/2157-7617.1000179 (cit. on pp. 15, 21).
- Randall, D., R. Wood, S. Bony, R. Colman, T. Fichefet, J. Fyfe, V. Kattsov, A. Pitman, J. Shukla, J. Srinivasan, R. Stouffer, A. Sumi, and K. Taylor (2007). “Climate Models and Their Evaluation.” In: *Climate Change 2007: The Physical Science Basis. Contribution of Working Group I to the Fourth Assessment Report of the Intergovernmental Panel on Climate Change*. Ed. by S. Solomon, D. Qin, M. Manning, Z. Chen, M. Marquis, K. Averyt, M. Tignor, and H. Miller. Cambridge, United Kingdom and New York, NY, USA: Cambridge University Press. Chap. 8 (cit. on p. 38).
- Robock, A. (1978). “Internally and Externally Caused Climate Change.” In: 35 (cit. on p. 8).
- Schär, C., D. Lüthi, U. Beyerle, and E. Heise (1999a). “The Soil–Precipitation Feedback: A Process Study with a Regional Climate Model.” In: 12, pp. 722–741 (cit. on p. 9).
- Schär, C., D. Lüthi, U. Beyerle, and E. Heise (1999b). “The Soil–Precipitation Feedback: A Process Study with a Regional Climate Model.” In: *Journal of Climate* 12.3, pp. 722–741. DOI: 10.1175/1520-0442(1999)012<0722:TSPFAP>2.0.CO;2 (cit. on p. 35).
- Schönwiese, C. (2003). *Klimatologie*. UTB für Wiessenschaft : Uni-Taschenbücher. Ulmer. ISBN: 9783825217938 (cit. on pp. 34, 43, 71, 74).
- Seneviratne, S. I. and R. Stöckli (2008). “The Role of Land-Atmosphere Interactions for Climate Variability in Europe.” In: *Climate Variability and Extremes during the Past 100 Years*. Ed. by S. Brönnimann, J. Luterbacher, T. Ewen, H. F. Diaz, R. S. Stolarski, and U. Neu. Springer Netherlands, pp. 179–193. ISBN: 978-1-4020-6766-2 (cit. on p. 1).
- Seneviratne, S. I., D. Lüthi, M. Litschi, and C. Schär (2006a). “Land–atmosphere coupling and climate change in Europe.” In: *Nature* 443. DOI: <http://dx.doi.org/10.1038/nature05095> (cit. on pp. 1, 3, 76, 79, 83).

- Seneviratne, S. I., R. Koster, Z. Guo, P. A. Dirmeyer, E. Kowalczyk, D. Lawrence, P. Liu, D. Mocko, C.-H. Lu, K. W. Oleson, and D. Verseghy (2006b). “Soil Moisture Memory in AGCM Simulations: Analysis of Global Land–Atmosphere Coupling Experiment (GLACE) Data.” In: *Journal of Hydrometeorology* 7.5, pp. 1090–1112. DOI: 10.1175/JHM533.1 (cit. on pp. 1, 2, 8, 61, 82).
- Seneviratne, S. I., T. Corti, E. L. Davin, M. Hirschi, E. B. Jaeger, I. Lehner, B. Orlowsky, and A. J. Teuling (2010). “Investigating soil moisture–climate interactions in a changing climate: A review.” In: *Earth-Science Reviews* 99.3, pp. 125–161. ISSN: 0012-8252. DOI: <https://doi.org/10.1016/j.earscirev.2010.02.004> (cit. on pp. 2, 3, 9, 10, 23, 61, 83, 84).
- Seth, A. and F. Giorgi (1998). “The Effects of Domain Choice on Summer Precipitation Simulation and Sensitivity in a Regional Climate Model.” In: *Journal of Climate* 11.10, pp. 2698–2712. DOI: 10.1175/1520-0442(1998)011<2698:TEODC0>2.0.CO;2 (cit. on p. 16).
- Smith, L. A. (2001). “Disentangling Uncertainty and Error: On the Predictability of Nonlinear Systems.” In: *Nonlinear Dynamics and Statistics*. Ed. by A. I. Mees. Birkhäuser Boston, pp. 31–64. ISBN: 978-1-4612-0177-9 (cit. on p. 19).
- Somerville, R., H. Le Treut, Y. Cubasch U.and Ding, C. Mauritzen, A. Mokssit, T. Peterson, and M. Prather (2007). “Historical Overview of Climate Change Science.” In: ed. by S. Solomon, D. Qin, M. Manning, Z. Chen, M. Marquis, K. Averyt, M. Tignor, and H. Miller, pp. 93–128 (cit. on p. 13).
- Stainforth, D., M. Allen, E. Tredger, and L. Smith (2007). “Confidence, uncertainty and decision-support relevance in climate predictions.” In: *Philosophical Transactions of the Royal Society of London A: Mathematical, Physical and Engineering Sciences* 365.1857, pp. 2145–2161. ISSN: 1364-503X. DOI: 10.1098/rsta.2007.2074 (cit. on p. 19).
- Strandberg, G., L. Bärring, U. Hansson, C. Jansson, C. Jones, E. Kjellström, M. Kupiainen, G. Nikulin, P. Samuelsson, and A. Ullerstig (2014). “CORDEX scenarios for Europe from the Rossby Centre regional climate model RCA4.” In: *Report meteorology and climatology* 116 (cit. on p. 25).
- Teichmann, C., B. Eggert, A. Elizalde, A. Haensler, D. Jacob, P. Kumar, C. Moseley, S. Pfeifer, D. Rechid, A. R. Remedio, H. Ries, J. Petersen, S. Preuschmann, T. Raub, F. Saeed, K. Sieck, and T. Weber (2013). “How Does a Regional Climate Model Modify the Projected Climate Change Signal of the Driving GCM: A Study over Different CORDEX Regions Using REMO.” In: *Atmosphere* 4.2, pp. 214–236. ISSN: 2073-4433. DOI: 10.3390/atmos4020214 (cit. on p. 17).

- Veihmeyer, F. J. and A. H. Hendrickson (1928). "SOIL MOISTURE AT PERMANENT WILTING OF PLANTS." In: *Plant Physiology* 3.3, pp. 355–357. ISSN: 0032-0889. DOI: 10.1104/pp.3.3.355 (cit. on p. 23).
- Viner, D. and M. Hulme (1997). "The Climate Impacts LINK Project: applying results from the Hadley Centre's climate change experiments for climate change impacts assessments Climatic Research Unit." In: *School of Environmental Sciences* (cit. on p. 14).
- Voldoire, A. et al. (2013). "The CNRM-CM5.1 global climate model: description and basic evaluation." In: *Climate Dynamics* 40.9, pp. 2091–2121. ISSN: 1432-0894. DOI: 10.1007/s00382-011-1259-y (cit. on p. 25).
- WMO (1979). "Eighth World Meteorological Congress(Cg-VIII):abridged final report with resolutions." In: *WMO Bulletin* 533 (cit. on pp. 1, 5).
- Ward, R. C. and M. Robinson (2000). *Principles of Hydrology*. McGraw-Hill Publishing Co. ISBN: 978-0077095024 (cit. on p. 62).
- Watanabe, M., T. Suzuki, R. O'ishi, Y. Komuro, S. Watanabe, S. Emori, T. Takemura, M. Chikira, T. Ogura, M. Sekiguchi, K. Takata, D. Yamazaki, T. Yokohata, T. Nozawa, H. Hasumi, H. Tatebe, and M. Kimoto (2010). "Improved Climate Simulation by MIROC5: Mean States, Variability, and Climate Sensitivity." In: *Journal of Climate* 23 (cit. on p. 25).
- Watanabe, S., T. Hajima, K. Sudo, T. Nagashima, T. Takemura, H. Okajima, T. Nozawa, H. Kawase, M. Abe, T. Yokohata, T. Ise, H. Sato, E. Kato, K. Takata, S. Emori, and M. Kawamiya (2011). "MIROC-ESM: model description and basic results of CMIP5-20c3m experiments." In: 4 (cit. on p. 25).
- Wentz, F. J., L. Ricciardulli, K. Hilburn, and C. Mears (2007). "How Much More Rain Will Global Warming Bring?" In: *Science* 317.5835, pp. 233–235. ISSN: 0036-8075. DOI: 10.1126/science.1140746 (cit. on p. 54).
- White, R. (1979). "The World Climate Conference: Report by the Conference Chairman." In: *WMO Bulletin* 28, pp. 177–178 (cit. on p. 1).
- Zappa, G., L. C. Shaffrey, and K. Hodges (2013). "The Ability of CMIP5 Models to Simulate North Atlantic Extratropical Cyclones." In: *Journal of Climate* 26.15, pp. 5379–5396. DOI: 10.1175/JCLI-D-12-00501.1 (cit. on p. 83).
- community.eu, www.clm (2014). *CLMcom-CCLM4-8-17 model output prepared for CORDEX*. <http://www.clm-community.eu/> (cit. on p. 25).
- van Meijgaard, E., L. van Ulft, W. van de Berg, F. C. Bosveld, B. van den Hurk, G. Lenderink, and A. Siebesma (2008). "The KNMI regional atmospheric climate model RACMO version 2.1." In: *Technical report* 302 (cit. on p. 25).

- van Oldenborgh, G., F. Doblas Reyes, S. Drijfhout, and E. Hawkins (2013). “Reliability of regional climate model trends.” In: *Environmental Research Letters* 8.1, p. 014055 (cit. on pp. 1, 2, 28, 38, 49).
- van Oldenborgh, G. J., S. Drijfhout, A. van Ulden, R. Haarsma, A. Sterl, C. Severijns, W. Hazeleger, and H. Dijkstra (2008). “Western Europe is Warming Much Faster than Expected.” In: 5, pp. 1–12 (cit. on p. 82).
- van Ulden, A. P. and G. J. van Oldenborgh (2006). “Large-scale atmospheric circulation biases and changes in global climate model simulations and their importance for climate change in Central Europe.” In: *Atmospheric Chemistry and Physics* 6.4, pp. 863–881. DOI: 10.5194/acp-6-863-2006 (cit. on p. 15).
- van den Hurk, B., F. Doblas-Reyes, G. Balsamo, R. D. Koster, S. I. Seneviratne, and H. Camargo (2012). “Soil moisture effects on seasonal temperature and precipitation forecast scores in Europe.” In: *Climate Dynamics* 38, pp. 349–362. ISSN: 1432-0894. DOI: 10.1007/s00382-010-0956-2 (cit. on pp. 3, 23, 82, 84).







---

### *Abstract:*

Earth's climate system is influenced and controlled by solar radiation factors as well as crucial feedback mechanisms and their components. One of these components is the soil moisture, which plays an important role not only globally, but especially at the regional scale. In order to better understand impacts and changes of soil moisture, General Circulation Models (GCM) and Regional Climate Models (RCM) are used. In this thesis three aspects regarding soil moisture and its impact on maximum temperature as well as the soil moisture-air temperature coupling mechanism within Europe are discussed. In the first step, it is shown how well the climate models can reproduce observations in summer season. To be more specific, the soil moisture-air temperature coupling as well as the zoning for various European regions will be discussed. Furthermore, we consider the relationship between the different climate model types to each other. Next, we take the consideration of soil moisture and maximum air temperature as possible elements for the reduction of uncertainty in climate projections into account. The use of so-called Emergent Constraints is resorted to this approach. Additionally, an overview for a method to determine the strength of the soil moisture-air temperature coupling is given. This is done with the help of net radiation and evaporation to get accurate results. This shows how differentiated the impact of the soil moisture-air temperature within the European summer season is. The approach to reflect possible changes for these feedback strengths are also taken into account.

### *Zum Inhalt:*

Das Klimasystem der Erde wird von vielen Faktoren wie z.B. der Energie der Sonne sowie die damit verbundenen Rückkoppelungsschleifen beeinflusst und gesteuert. Einer dieser Faktoren stellt die Bodenfeuchte dar, die nicht nur global, sondern vor allem regional eine große Rolle spielt. Um diese Veränderungen sowie deren Einfluss besser zu verstehen, wird auf globale Klimamodelle (GCM) sowie regionale Klimamodelle (RCM) zurückgegriffen. Vor diesem Hintergrund befasst sich diese Arbeit mit drei Hauptaspekten der Bodenfeuchte sowie im speziellen deren Auswirkungen auf die maximale Lufttemperatur und die Bodenfeuchte-Lufttemperatur Rückkoppelung im Allgemeinen. Im ersten Schritt wird gezeigt, wie gut die Klimamodelle die Beobachtung im Sommer reproduzieren können. Insbesondere wird auf die Bodenfeuchte-Lufttemperatur-Rückkoppelung sowie die Einteilung der verschiedenen europäischen Regionen, die während der gesamten Arbeit verwendet werden, eingegangen. Zusätzlich wird die Beziehung zwischen den verschiedenen Klimamodelltypen zueinander näher diskutiert. In einem weiteren Schritt betrachten wir die Bodenfeuchte und die maximale Lufttemperatur als mögliche Faktoren für die Reduktion der Unsicherheiten in Modellprojektionen. Die Verwendung sogenannter Emergent Constraints ist hierbei entscheidend. Zusätzlich wird die Stärke der Bodenfeuchte-Lufttemperatur-Rückkoppelung innerhalb Europas für den Sommer ermittelt. Es wird dabei auf die Nettosolarstrahlung sowie die Evapotranspiration zurückgegriffen um ein möglichst genaues jedoch unverfälschtes Ergebnis zu bekommen. Es zeigt sich dabei, dass es zu großen Unterschieden innerhalb Europas während des Sommers kommt. Ebenfalls berücksichtigt werden mögliche Änderungen dieser Rückkoppelungsstärke im Zuge des sich ändernden Klimas.